Functional Analysis of the N-terminal Segment of Agrin
&
Characterisation of the Response of Dendritic Spines to Cholinergic Stimulation

Dissertation
zur
Erlangung der naturwissenschaftlichen Doktorwürde
(Dr. sc. nat.)

vorgelegt der
Mathematisch-naturwissenschaftlichen Fakultät
der
Universität Zürich

von

Philipp Schätzle

aus

Deutschland

Promotionskomitee
Prof. Dr. Peter Sonderegger (Vorsitz)
Prof Dr. Urs Gerber
Prof. Dr. Fritjof Helmchen

Zürich, 2011

Content

Abstract

The synaptically released serine protease neurotrypsin is important for higher cognitive function, since its deficiency results in severe mental retardation. At the present time, the extracellular matrix proteoglycan agrin is the only identified substrate of neurotrypsin. Proteolytic processing of transmembrane agrin releases two fragments from the N-terminal moiety. The released C-terminal agrin-22 fragment promotes the formation of dendritic filopodia and thus contributes to structural plasticity in the brain. In this thesis, I analysed potential functions of the N-terminal agrin region which remains linked to the plasma membrane after cleavage. Microscopical and biochemical analysis revealed three regions within the agrin molecule that are capable of binding neurotrypsin. Two of them consist of glycosaminoglycan chains and are located in the N-terminal region of agrin. The third is a heparin binding site positioned in the C-terminal LG2 domain. Interaction of neurotrypsin with the glycosaminoglycan chains enhances the agrin cleavage process and suggests additional regulatory influence on the protease. N-terminal agrin contains several follistatin domains that have high affinity to bind several members of the TGF-β superfamily. I tested three of these cytokines on possible effects on synaptogenesis in dissociated neuron cultures. For the synapse quantification, I developed a new quantification method that enabled the automated processing of huge datasets. Finally, I studied the fate of the N-terminal segment of agrin after cleavage of full-length agrin by neurotrypsin.

In the second part of my thesis I investigated morphological modifications of dendritic spines after cholinergic stimulation. Remodelling of spines is a key feature of excitatory synapses, which in conjunction with receptor trafficking modifies the efficacy of neurotransmission. Cholinergic activity has important functions in modulating synaptic plasticity that may also be reflected in changes of dendritic spine structure. Using confocal time-lapse microscopy in organotypic slice cultures, we found that brief activation of muscarinic receptors induced the emergence of fine filopodia from spine heads in all CA1 pyramidal cells examined. This response was widespread occurring in 48% of imaged spines, appeared within minutes, was reversible, and was blocked by atropine. Electron microscopic analyses showed that the spine head filopodia extend along the presynaptic bouton but were absent of postsynaptic densities, suggesting that they are not involved in the formation of new synaptic contacts. Instead, structural spine head modifications affected synaptic transmission indicated by a longer decay time of miniature EPSCs. Both morphological and electrophysiological changes were reduced by preventing microtubule polymerisation with nocodazole. The extension of spine head filopodia during cholinergic receptor activation represents a novel structural form of spine plasticity that may promote microtubule invasion in spines and regulate synaptic properties by fine-tuning interactions between presynaptic boutons and dendritic spines.

Zusammenfassung

Es wurde gezeigt dass die synaptisch sekretierte Serinprotease Neurotrypsin von Bedeutung für höhere kognitive Funktionen ist, da ihre Störung zu schwerwiegende geistige Behinderung führt. Das extrazelluläre Matrixprotein Agrin ist gegenwärtig das einzig identifizierte Substrat von Neurotrypsin. Proteolytisches Schneiden von transmembranem Agrin bewirkt die Abspaltung von zwei Fragmenten vom N-terminalen Teil des Moleküls. Das freigesetzte C-terminale agrin-22 Fragment fördert die Entstehung von dendritischen Filopodien und trägt daher zur strukturellen Plastizität innerhalb des Gehirns bei. In der vorliegenden Doktorarbeit untersuche ich potenzielle Funktionen von N-terminalem Agrin, das auch nach Prozessierung weiterhin mit der Plasmamembran verbunden bleibt. Mikroskopische und biochemische Analysen identifizierten drei Regionen innerhalb des Agrinmoleküls, welche in der Lage sind Neurotrypsin zu binden. Zwei dieser Regionen besitzen Glykosaminoglykanketten und befinden sich im N-terminalen Abschnitt von Agrin. Die dritte Bindungsstelle befindet in der C-terminal gelegenen LG2 Domäne und beinhaltet eine Heparinbindungsstelle. Die Interaktion zwischen Neurotrypsin und den Glykosaminoglykanketten verstärkt die proteolytische Prozessierung von Agrin und lässt auf einen zusätzlichen regulatorischen Einfluss auf die Protease schliessen. N-terminales Agrin beinhaltet sieben Follistatindomänen, welche eine hohe Affinität zu mehreren Mitgliedern der TGF-β Superfamilie aufweisen. Drei dieser Cytokinine wurden in dissoziierten Neuronenkulturen auf mögliche Auswirkungen auf die Synaptogenese hin überprüft. Dafür entwickelte ich eine neuartige Synapsenquantifizierungsmethode, die eine automatische Verarbeitung von grossen Datensätzen ermöglicht. Zuletzt untersuchte ich das weitere Schicksal von N-terminalem Agrin nach Prozessierung durch Neurotrypsin.

Im zweiten Teil meiner Arbeit untersuchte ich morphologische Veränderungen von dendritischen Spines nach cholinerger Stimulierung. Die Umstrukturierung von dendritischen Spines ist eine grundlegende Eigenschaft von exzitatorischen Synapsen, welche im Zusammenspiel mit gezieltem Rezeptorentransport, die Effizienz der neuronalen Übertragung reguliert. Cholinerge Aktivität hat bedeutenden Einfluss auf die Modulation der synaptischen Plastizität, was sich in einer Veränderung der dendritischen Struktur äussern könnte. Mit Hilfe von konfokaler Zeitraffermikroskopie untersuchten wir organotypische Gewebekulturen. Nach kurzer Stimulierung muskarinerger Rezeptoren beobachteten wir die Entstehung von Filopodien (dünnen Fortsätzen), die von den Spineköpfchen ausgingen und in allen CA1 Pyramidalzellen gefunden wurden. Der Effekt wurde in 48% aller Spines beobachtet, zeigte sich innerhalb von Minuten, war reversibel und konnte durch Atropin blockiert werden. Elektronenmikroskopische Analysen zeigten, dass die „Spine Head Filopodien“ entlang der präsynaptischen Boutons verlaufen und frei von postsynaptischer Dichte waren, was darauf hindeutete,

dass sie nicht in die Entstehung neuer synaptischer Kontakte involviert sind. Jedoch hatten die strukturelle Veränderungen der Spines einen Einfluss auf die synaptische Übertragung, da wir eine Verlängerung der „decay tau“ von Miniatur-EPSCs beobachteten. Sowohl morphologische als auch elektrophysiologische Veränderungen waren reduziert, sobald die Polymerisation von Mikrotubuli durch Zugabe von Nocodazole verhindert wurde. Die Entstehung von „Spine Head Filopodien“ durch Stimulierung cholinerger Rezeptoren stellt eine neuartige Form der Spineplastizität dar. Diese könnte die Spineinvasion von Mikrotubuli fördern und zur Feinregulierung der Interaktion zwischen präsynaptischen Boutons und dendritischen Spines beitragen.

List of Figures

List of Tables

Abbreviations

3D	three dimensional
AMPA	α-amino-3-hydroxy-5-methyl-4-isoxazolepropionic acid
AP-5	amino-5-phosphonovaleric acid
CA1	cornu ammonis area 1
Ca^{2+}	calcium / calcium ions
CAMKII	calmodulin-dependent protein kinase II
CNQX	6-cyano-7-nitroquinoxaline-2,3-dione
CNS	central nervous system
CREB	cAMP response element binding protein
DHPG	dihydroxyphenylglycine
DIV	days *in vitro*
EB3	end-binding protein 3
ECM	extracellular matrix
EGF	epidermal growth factor
eGFP	enhanced green fluorescent protein
EPSC	excitatory postsynaptic current
EPSP	excitatory postsynaptic potential
FCS,	fetal calf serum
GAG	glycosaminoglycan
HRP	horse radish peroxidase
IC,	immunocytochemistry
IP	immunoprecipitation
kDa	kilodaltons
LN-agrin	long NH(2)-terminal agrin
MCh	methacholin
mRFP	monomeric red fluorescent protein
NMDA	N-Methyl-D-aspartate
NMJ	neuromuscular junction
Nt	neurotrypsin
PFA	paraformaldehyde
PKC	protein kinase C
PLL,	poly-L-lysine
PNNs	perineuronal nets
PS,	Peter Sonderegger
PSD	postsynaptic density
RT	room temperature
SHF	spine head filopodia
WB,	Western blotting
y0	agrin alternative splice insert y0
y4	agrin alternative splice insert y4
ZMB	center for microscopy and image analysis

Publications

The following publications contain experimental results that have been obtained during my thesis:

Original articles:

Philipp Schätzle, Jeanne Ster, David Verbich, R. Anne McKinney, Urs Gerber, Peter Sonderegger, and José María Mateos. Rapid and reversible formation of spine head filopodia in response to muscarinic receptor. J Physiology, in press, published online July 18, 2011.

Philipp Schätzle, Urs Ziegler, René Wuttke, and Peter Sonderegger. Automated quantification of synapses by fluorescence microscopy. J Neurosci Methods, manuscript submitted.

Philipp Schätzle, Claudio Gisler, Daniel Lüscher, Stephanie Dürr and Peter Sonderegger. Studies on the role of the glycan chains of agrin for neurotrypsin-dependent cleavage of agrin. Manuscript in preparation.

Meeting abstracts:

Philipp Schätzle, Jeanne Ster, David Verbich, R. Anne McKinney, Urs Gerber, Peter Sonderegger and José María Mateos. Rapid and reversible formation of spine head filopodia in response to muscarinic receptor activation. ZNZ PhD Retreat 11, Clinic Valens, 12 - 14 May 2011.

Philipp Schätzle, Jeanne Ster, U. Gerber, P. Sonderegger and J. María Mateos. Rapid and reversible spine head filopodia formation in response to muscarinic receptor activation. ZNZ Symposium, ETH Zurich, 17 Sep 2010.

1. Introduction

1.1 General introduction

Neurons are the basic information processing structures in the brain. They communicate with each other through chemical and electrical synapses and form large neural networks. The human brain consists of about 10^{11} neurons and 10^{15} synapses and is considered as the most complex structure on earth (Chklovskii *et al.*, 2004). One day it will be possible to decrypt how terms like intellect and awareness are reflected in the organisation and function of the brain. At present, limitations in knowledge and technique force us to investigate less complex brain functions. Currently, to understand the principles of learning and memory is one of the main investigated topics in neurobiology. In 1949 the Canadian neuropsychologist Donald Hebb postulated a model for cell-based learning (Hebb, 1949). He proposed that after learning both presynaptic and postsynaptic structural changes occur and form the neural substrate of long-term memory. Based on this theoretical framework of synaptic plasticity, neuroscientists tested the Hebbian postulate during the last decades experimentally and today his theory is widely accepted (Lamprecht & LeDoux, 2004).

On the following pages I will illustrate some of the established views about mechanisms and function of synaptic plasticity. The chapter begins with a presentation of the basic anatomy of the hippocampus and its use as an experimental model system. Next, I introduce dendritic spines as the fundamental structure of excitatory synapses in the central nervous system (CNS). The section about synaptic plasticity, presented for this thesis, focuses on relevant glutamergic and cholinergic receptors and continues with the concepts of short- and long-term plasticity. Then, I focus on structural plasticity, primarily changes at dendritic spines, and the implication for learning and memory. The last section illustrates the extracellular matrix and its involvement in neural plasticity. Finally, I summarise recent findings about the role of neurotrypsin in mediating activity-dependent structural plasticity in the hippocampus.

1.2 The Hippocampus

1.2.1 Anatomy, connectivity and functionality

The hippocampus is part of the temporal lobe of the cerebral cortex and belongs to the limbic system. Anatomists divide the hippocampal formation in entorhinal cortex (EC), dentate gyrus (DG), hippocampus proper (HP) or “Ammon’s horn”, and the subicular complex (SC) (Jarrard, 1993). Ontogenetically, the DG and the HP are the earliest structures in the hippocampal formation and thus consist of a three-layered cortex. The principle neurons in the DG are the granule cells, while in the HP they are the pyramidal neurons. The HP is further subdivided in three regions designated “Cornu Ammonis” area 1 (CA1), CA2, and CA3 based on size and appearance of the neurons.

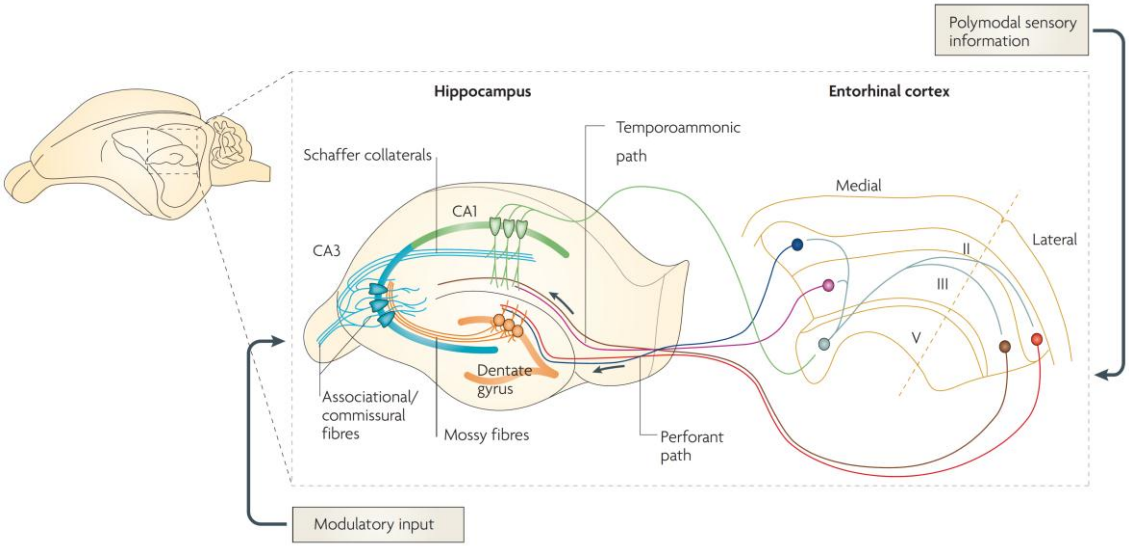

Figure 1. Basic wiring of the hippocampus

The trisynaptic circuit receives input from axons of the perforant path originating in the layer II of the entorhinal cortex. Granule cells of the dentate gyrus integrate the signals and project via mossy fibres to the apical dendrites of CA3 pyramidal cells. Projections of CA3 neurons proceed either ipsilateral via Schaffer collaterals to CA1 neurons or contralateral to CA3 and CA1 pyramidal cells through commissural connections. CA1 axons enter the subiculum and are relayed to the deep layers of the EC providing a feedback loop within the hippocampal formation. Apart from the trisynaptic circuit, CA1 and CA3 neurons receive direct connections from the layer III or layer II of the entorhinal cortex, respectively. Further, a dense associative network interconnects CA3 neurons. (Figure from: Neves *et al.*, 2008)

Connectivity within the hippocampus is characterised by a mostly unidirectional progression of information flow. The principle cells build an afferent glutamatergic circuit, called the “trisynaptic circuit”, which originates and terminates in the EC (Andersen *et al.*, 1966). The EC receives a variety of inputs from different brain areas and projects primarily from layer II to granule cells of the dentate gyrus via the perforant path (PP). Depending on the origin of these fibres the perforant path is subdivided into a lateral (LPP) and a medial (MPP) pathway (Witter *et al.*, 2000). Axons from the granule cells

(mossy fibers) reach the CA3 region and synapse with pyramidal neurons. The pyramidal cells of the CA1 region are included in the trisynaptic circuit by axons arising from CA3 neurons. These axons either project to CA1 cells in the same hippocampus (ipsilateral) forming the Schaffer collaterals (SC) or into the opposite hemisphere (contralateral) forming the associational-commissural path (A/C). Finally, the output from the trisynaptic circuit enters the subiculum and is relayed to the deep layers of the EC providing a feedback loop within the hippocampal formation (Andersen, 2007). The clearly defined routes of synaptic information flow made the hippocampus a very popular model system to investigate synaptic transmission and plasticity. However, it has to be mentioned that the trisynaptic circuit, as presented here, reflects only a very simplified view of the hippocampal functionality. Additional input and output connections within the trisynaptic circuit, as well as associational fibres which connect the hippocampus along the septal-temporal axis and enable an integrated functioning of the hippocampus, tremendously increase the functionality.

The hippocampus is involved in different forms of learning and memory. A well-known example is the patient H.M., who suffered from intractable epilepsy and underwent in 1953 a bilateral surgical resection of his hippocampus (Scoville & Milner, 1957). Ultimately successful in reducing the epileptic seizures, he afterwards suffered from severe anterograde amnesia and was no longer able to commit new events to long-term memories (Schmolck *et al.*, 2002). However, his short-term and working memory were unaffected and he had access to memories encoded before his surgery. Together, these observations suggested that the hippocampus is involved in the retaining of incoming memories but cannot be the place of long-term memory storage.

The hippocampus receives a prominent cholinergic input from projections originating in the medial septum and the diagonal band of Broca (Lewis & Shute, 1967; Mesulam *et al.*, 1983). Anatomical studies provide evidence that cholinergic release appears primarily as volume transmission (Descarries *et al.*, 1997). However, there is an ongoing debate about the mode of cholinergic transmission and both volume and wired release are discussed as possible mechanisms (Sarter *et al.*, 2009). The levels of acetylcholine vary massively during different behaviours (Giovannini *et al.*, 2001) and different stages of waking and sleep (Diekelmann & Born, 2010). Functional properties of the cholinergic system were extensively addressed by computational modelling (Hasselmo & McGaughy, 2004). Low cholinergic concentrations are considered to be important for the process of memory consolidation and appear during waking phase with low activity and much stronger during slow wave sleep. In contrast, high levels of acetylcholine are implicated with enhancement in attention and the encoding of information in memory. This is impressively demonstrated by behavioural tests using either cholinergic drugs of lesions of cholinergic pathways (Hasselmo & McGaughy, 2004; Hasselmo, 2006).

1.2.2 Hippocampal cells used as a model system

1.2.2.1 Dissociated neuronal cultures

Cultures of dissociated primary neurons are a powerful *in vitro* tool to address a wide range of questions in molecular and cellular neurobiology. The cultures are prepared from suspensions of individual cells generated by trypsin digestion and dissociation of neural tissue (Banker & Goslin, 1998). Although the cells have lost their natural environment, they retain their individual identity and develop many properties of mature neurons *in vivo*. Cultured neurons have been found to develop well defined axons (Banker & Cowan, 1979), generate functional synapses between each other (Fletcher *et al.*, 1994), possess characteristic ion channel patterns and release appropriate neurotransmitter, hence they also show spontaneous network bursts typical for neuronal networks (Siebler *et al.*, 1993). The reason why dissociated neurons keep all these characteristic features is presumably due to their post-mitotic identity and the stage of determination they have adopt at the time they are inserted in cell culture.

Cultured neurons offer certain advantages for experimental approaches. Morphological studies have demonstrated that the neurons pass through defined stages of maturation which can be visualised in their entirety, unless the neural network becomes too complicated (Dotti *et al.*, 1988). This makes them a very suited model system to study axonal and dendritic outgrowth and branching (Aoyagi *et al.*, 1994; Dent *et al.*, 2003; Hutchins & Kalil, 2008). In comparison to the three-dimensional arrangement of cells *in situ*, dissociated neuronal cultures offer a broad spectrum of experimental manipulation because they can be accessed much easier. Ectopic protein expression, changes in the ionic composition of the extracellular solution, application of stimulants or growth factors, are just a few examples, cultures have been used for, and demonstrate the experimental potential of this model system. Apart from the cellular questions, dissociated hippocampal cultures were also widely used to study spatiotemporal patterns of neuronal network activity, using planar microelectrode arrays (Morin *et al.*, 2005).

The power of cell culture is at the same time its weakness. The nervous system achieves its impressive qualities by the interaction and communication between different cell types and its complex organisation. The isolation of neuronal populations with certain characteristics facilitates the analysis of neurobiological questions, however, at the same time it requires a considerable caution in interpreting the obtained results.

In general, one can differentiate between two culturing approaches. High density cultures consist of a mixture of neural cells (mainly neurons and astrocytes) that are plated in a cellular monolayer. Coculturing with astrocytes seems to protect the neurons and make them relatively robust against external stress. The generation of these cultures is relatively simple and also high number of cells can be produced within a reasonable expenditure of time. Thus, they are also well suited for biochemical analysis. Because they require large amounts of primary cells they are usually made of cortical neurons of rat or mice. The second approach produces highly pure neuron cultures from

hippocampal cells. Typically, these cultures are used for light microscopy and have very low densities in order to identify single cells. They were developed by Gary Banker and are based on a sandwich coculture system of neurons and glial cells (Kaech & Banker, 2006). Usually, the hippocampal neurons are plated on coverslips and are placed above a layer of astrocytes, separated by small wax feet. At low cellular density astrocytes are essential to supply neurotrophic substances and maintain a stable oxygen atmosphere. Another great advantage of this approach is the homogeneity of the neurons in culture. In the hippocampus, pyramidal cells account for around 85-90% of the total neuronal population (Banker & Goslin, 1998). Possible contaminations by other cell types, like dentate granule cells or glial cells, are reduced to a minimum by the time point of tissue extraction. Pyramidal cells in the hippocampus start to differentiate at around embryonic day 15, while dentate granule and glial cells can be avoided in the cultures because they are primarily generated postnatally (Bayer & Altman, 1974; Bayer, 1980). High density and low density hippocampal cultures were both used in this study for biochemical and microscopical experiments.

1.2.2.2 Organotypic slice cultures

The lamellar cytoarchitecture of the hippocampus makes it easy to examine experimentally since all neurons and projections of the trisynaptic circuit are located within the same plane. This organisation allows cutting the hippocampus in transverse orientation to obtain a better accessibility for imaging or electrophysiology, without destroying the basic neural network. Hippocampal explants are usually cut by a tissue chopper or vibratome and results in so-called acute slices. They retain the original cellular and connective properties of the synaptic circuits and are mostly used for electrophysiology (Skrede & Westgaard, 1971). However, the superficial layers are strongly damaged form the slicing procedure and also deeper layers suffer from the neurotoxic insults which is introduced by mechanical and excitotoxic stress. Another disadvantage of acute slices is that they are relatively short-lived.

For these reasons many attempts were made to introduce hippocampal slices *in vitro* (Gahwiler *et al.*, 1997). Today, two methods are established which results in slightly different slice cultures (Fig.2). They are both called organotypic cultures which refer to the preservation of the basic structural and connective organisation of the tissue. The basic challenge in culturing hippocampal slices is to maintain a constant supply of oxygen and culture medium. The membrane interface type cultures are grown on semiporous membranes which are positioned at the interface between culture medium and atmosphere (Stoppini *et al.*, 1991). The liquid crosses the membrane by capillary force and ensures that the slice is constantly covered by a thin film of medium. In parallel the oxygen supply is secured by the surrounding atmosphere. In the roller-tube method the culture is embedded in a plasma clot on a glass coverslip (Gahwiler, 1981). The slice is placed in a culture tube and combined with some media before positioning in a roller drum. Oxygenation and nutrition is assured because the slow rotation results in an alternating contact with the liquid and gas phase.

Both types of cultures survive for several weeks to months *in vitro* and retain many architectural features of the host tissue. A major difference between the two approaches is that roller tube cultures become clearly thinner than membrane cultures and evoke the appearance of a quasi-monolayer culture (Banker & Goslin, 1998). The increased cellular density makes these cultures less suited for electrophysiological studies, particular those performed at population level, but on the other side is better suited for microscopical applications (Pena, 2010). Regarding morphological and neurochemical features of neurons there are no major differences between organotypic cultures and *in vivo* conditions. The expression of glutamate receptors (Bahr, 1995; Gerfin-Moser & Monyer, 2002) and other neuronal markers like synaptophysin, MAP-2 and GAP-43 resemble adult tissue at comparable developmental stage (Bahr, 1995; Mielke *et al.*, 2005).

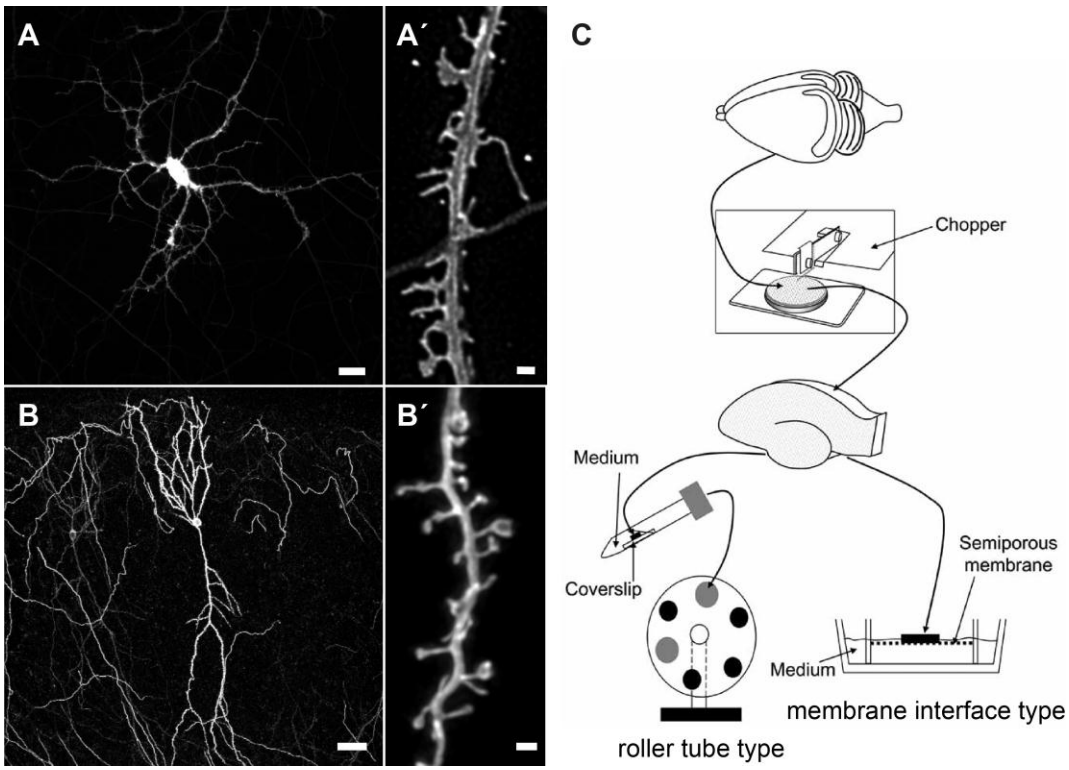

Figure 2. Cell culture systems based on hippocampal cells

(A) Dissociated hippocampal neuron cultured for 14 DIV. These neurons appear in stellate shape and (A´) form spine-like structures from the dendrites. (B) CA1 pyramidal neuron cultured in organotypic slice culture (roller tube type) for 3 weeks. This culturing method maintains the typical neuron shape with a single apical and several basal dendrites. (B´) Also dendritic spines rather resemble spines found *in vivo*. (C) Schematic drawing of the two approaches to generate organotypic slice cultures. The hippocampus is chopped in slices and then either mounted on a coverslip and placed in a roller drum or put on a semiporous membrane positioned at the interface of culture medium and atmosphere. Scale bars: A 30 µm; A´ 1 µm; B 50 µm; B´ 1 µm. Neurons in images express membrane targeted eGFP.

The kinetics of excitatory postsynaptic potentials (EPSPs) are identical between mature organotypic slices and acute slices (Gahwiler *et al.*, 1997). However, the connectivity within cultures strongly varies depending on the time *in vitro*. Immediately after

explantation, the synaptic density decreases due to the chopping of many axons, which inevitably occurs during slice preparation. A comparison between acute slices and organotypic cultures revealed that the slices undergo a dramatic rearrangement of connectivity within the first week in culture. This is reflected by an increased number of dendritic spines, a more complex dendritic tree of CA1 neurons, and a high frequency of excitatory miniature synaptic currents (De Simoni *et al.*, 2003). Interestingly, the *ex vivo* development of organotypic slice cultures gradually resemble the *in vivo* development, with increasing time in culture. Many studies have demonstrated that hippocampal slice cultures display several forms of synaptic plasticity that appear identical to those described in acute slices. This includes short-term and long-term changes in synaptic strength as well as homeostatic synaptic plasticity (Muller *et al.*, 1996; Gahwiler *et al.*, 1997; Pozo & Goda, 2010). Recently, organotypic slice cultures were used to combine electrophysiology with high resolution imaging to demonstrate the linkage between synaptic plasticity and morphological alteration at the level of single spines (Nagerl *et al.*, 2007; Becker *et al.*, 2008).

1.3 Dendritic spines

1.3.1 Spine morphology

The glutamergic synapse can be clearly subdivided in a pre- and postsynaptic element based on electron microscopy data. Postsynaptic sites are characterised by an electron dense thickening, the postsynaptic density (PSD), which arise from a massive accumulation of membrane associated proteins, cytoplasmic scaffolding proteins and cytoskeletal elements. Microscopical data revealed that this structure is mostly localised in a compartment called the dendritic spine. Dendritic spines are small membranous protrusions with length of 0.5 – 2 µm and a volume of 0.01 – 0.8 μm^3 (Fiala *et al.*, 2002 ; Hoogenraad & Akhmanova, 2010). In the 19th century, Santiago Ramón y Cajal was the first to describe spines as dendritic protrusions and suggested that these are contact sites between neurons (Garcia-Lopez *et al.*, 2007). Indeed, dendritic spines are the main site of synaptic input. In the mature CNS more than 90% of all excitatory synapses occur on dendritic spines (Harris & Kater, 1994). The prototypical dendritic spine consists of a bulbous head which is connected to the dendritic shaft by a constricted neck. However, spines are very heterogeneous in their size and shape. Based on the morphological characteristics (relative sizes of spine head and neck) the dendritic spine can be classified into 4 main categories (Bourne & Harris, 2008): 1. Mushroom spines have large heads that exceed 0.6 microns in diameter and a narrow neck. 2. Thin spines have smaller heads and similar neck properties. 3. Stubby spines have a large head but no obvious constriction between the head and the dendritic shaft. 4. Branched spines have multiple heads emerging from a shared neck (Fig. 3 E). There is a continuum of shapes between these categories indicating that these structures do not represent a development endpoint but a plastic stage (Arellano *et al.*, 2007).

In rare cases it is possible to correlate spine shape directly with the source of inputs. For instance, in the lateral nucleus of the amygdala, cortical terminals synapse on thin spines, while thalamic inputs are connected to mushroom spines (Humeau *et al.*, 2005). Within the hippocampus, however, pyramidal neurons appear to have a great variability in spine shape and size. It is believed that the size of a spine head is closely related to the size of its excitatory synapse (von Bohlen und Halbach, 2009; Noguchi *et al.*, 2011). According to this, mushroom spines were found to exhibit larger more complex PSDs (Harris *et al.*, 1992), contain a higher density of glutamate receptors (Matsuzaki *et al.*, 2001), and therefore probably produce larger EPSCs (Kasai *et al.*, 2010). Further, the spine density is directly related to the degree of connectivity of the parent dendrite with the surrounding axons (Fiala *et al.*, 2002).

The variability of spine structures combined with the observation that presynaptic terminal can form synapses with two or more spines of different dimensions (Shepherd & Harris, 1998; Toni *et al.*, 2007), lead to the conclusion that the synaptic structure is not completely determined by either the presynaptic or postsynaptic cell (Harris, 1999). Astrocytes are an additional modulator of synaptic contacts and cover about 57% of all synapses in the hippocampus, thereby building an intercommunicating tripartite complex (Ventura & Harris, 1999). Therefore, the morphological spine structure represents the sum of interactions with the surrounding partners.

1.3.2 Spines facilitate structural compartmentalisation

Synaptic contacts at dendritic spines offer several advantages compared to synapses which are directly located at the dendrite (shaft synapses): spines enlarge the dendritic surface area and allow a higher number of potentially formed synapses along the dendrite. Further, it increases the possible range to interact with nearby axons (Stepanyants *et al.*, 2002).

The narrow spine neck serves an important function by facilitating a microcompartmentalisation, which makes the spine a semi-autonomous signalling unit. It was shown that diffusion through the spine neck is regulated in an activity-dependent manner (Bloodgood & Sabatini, 2005). This enables the local control of ions and other signalling molecules within the spine head and allows responding biochemically to glutamate or other transmembrane signals. Dendritic spines contain recycling endosomes that facilitate an independent regulated membrane trafficking. Thus, the spine actively controls the shuttling of membrane proteins and can easily promote spine growth by fusion of vesicle with the spine membrane (Park *et al.*, 2006). Several spines were also identified to contain organelles for the synthesis of new proteins. Protein synthesis is essential for the establishing of long-term memories (Cajigas *et al.*, 2010) and according to this it is reported that polyribosomes are preferentially transported into spines after induction of long-term plastic changes (Ostroff *et al.*, 2002).

One of the most important signals within spines is the level of cytoplasmic Ca^{2+}. Two-photon imaging showed that Ca^{2+} can be compartmentalised in dendritic spines

(Svoboda *et al.*, 1996). More recently, a report indicated that the Ca^{2+} levels inside spines become dynamically regulated by spine neck plasticity (Grunditz *et al.*, 2008). Intracellular spine dynamics in Ca^{2+} levels are essential for synaptic signalling, induction of short- and long-term plasticity, and regulation of gene transcription (Higley & Sabatini, 2008). Ca^{2+} can enter the spine through glutamate-gated channels, such as NMDA or some subtypes of AMPA receptors, as well as voltage-sensitive Ca^{2+} channels. Further, it can be externalised from internal stores which are the endoplasmic reticulum and the spine apparatus. The rise in Ca^{2+} triggers a variety of signalling cascades including: calmodulin, CaMKII (calmodulin-dependent protein kinase II), PKC (Protein Kinase C), PKA (Protein Kinase A), Fyn tyrosine kinase, among others. Interestingly, the local amounts of Ca^{2+} inside the spines are much higher than in the parent dendrites. These high concentrations are probably required to activate the calcium-dependent kinases (Segal, 2010). The tight control of Ca^{2+} levels plays also a key role in the regulation of actin dynamics, which are mediated by Ca^{2+} responding regulatory proteins (Oertner & Matus, 2005). The development of fluorescent calcium indicators opened the field for functional imaging studies that confirm the importance of Ca^{2+} signalling for electrical and structural plasticity. As another function, spines may also protect the parent dendrite from excitotoxicity (Bourne & Harris, 2008) that would otherwise result in very high concentrations of somatic Ca^{2+} and trigger apoptotic process causing cell death. Evidence for a role in preventing excitotoxicity is concluded from experiments that show an increased vulnerability of neurons which possess reduced amounts of spines following experimental manipulations (Segal, 2010).

The constriction of the spine neck could further serve as a resistive element and generate an electrical compartment. Changes in the spine neck dimensions could then modulate electrical characteristics and synaptic strength. The hypothesis seemed to be disproven when electron microscopy studies indicated that spine necks probably do not significantly reduce the charge transfer to impede synaptic currents (Harris & Stevens, 1989; Koch & Zador, 1993). However, recent studies using two-photon uncaging of glutamate or photoactivatable dyes found evidence that spine necks indeed have the ability to isolate synapses electrically (Bloodgood & Sabatini, 2005; Araya *et al.*, 2006; Grunditz *et al.*, 2008). It is also likely that the impact of spine neck geometry varies across different brain regions (Bourne & Harris, 2007). Taken together, spines have the ability to directly participate in the dendritic computation process.

1.3.3 Spinogenesis: From filopodia to spines?

Dendritic filopodia are long (2-10 µm) and thin (less than 1 µm) protrusions emerging from the dendritic shaft. They are highly dynamic structures and possess a relatively short live span, compared to mature spines. Some research groups categorise them as immature spines because they do not show a well-defined head and neck structure (Harris, 1999; Hering & Sheng, 2001). Ultrastructually, filopodia can be clearly distinguished from spines by the lack of a PSD specialisation and a denser actin matrix

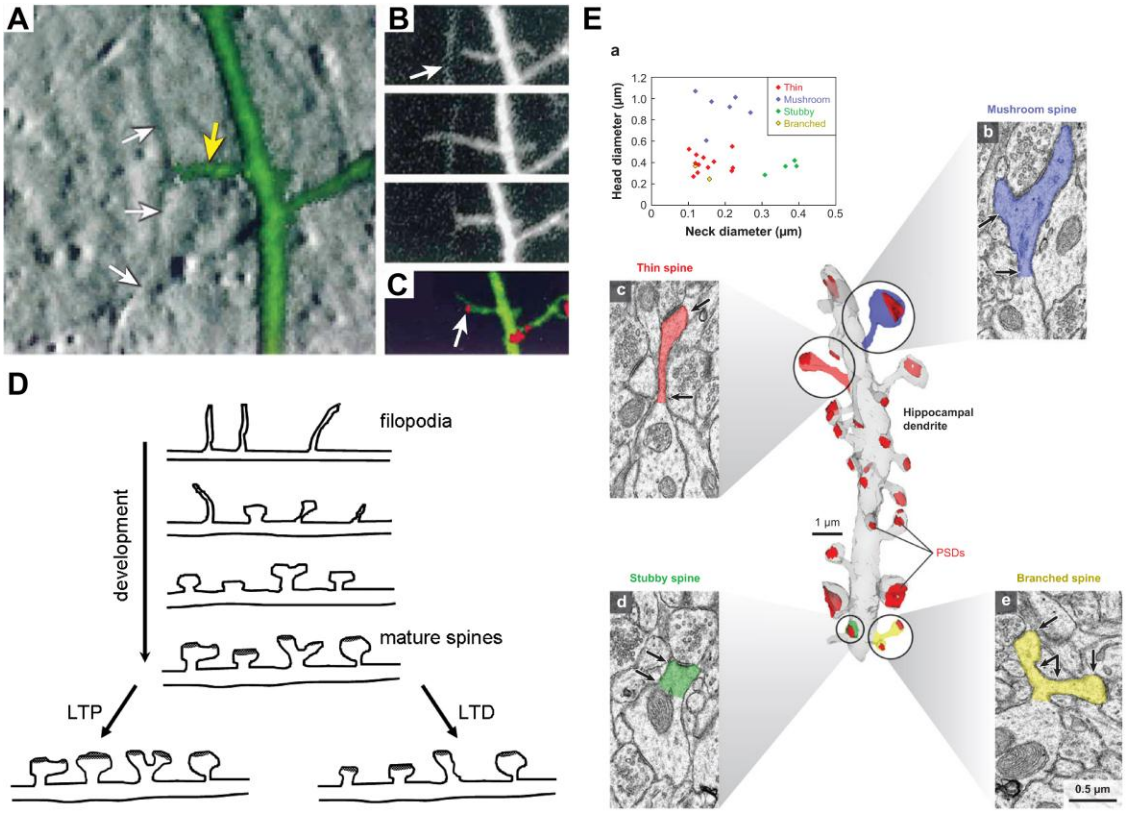

Figure 3. Synaptic involvement of dendritic filopodia and dendritic spines

(A-C) Dendritic filopodia initiate synaptic contacts with neighbouring axons. (A) FAST DiO-labelled dendrite (green) of a cultured hippocampal neuron is overlaid onto the DIC image. White arrows indicate an axon near the dendrite. The yellow arrow indicates a filopodium extending from the dendritic shaft. The filopodium establishes a synaptic contact with the axon, as shown in panels (B) and (C). (B) Time-lapse sequence of the filopodium shown in panel (A) at 0, 18, and 90 min. The white arrow indicates the axon shown in panel (A). (C) Merged image showing FAST DiO-labelled dendrite (green) and FM 4-64-labelled presynaptic boutons (red). The white arrow indicates a bouton that formed at the filopodium contact site. (D) Schematic representation of morphological changes of dendritic spines during development and after LTP and LTD. (E) Dendritic spine varies in shape and size. A three-dimensional reconstruction of a hippocampal dendrite (gray) illustrating different spine shapes including mushroom (b), thin (c), stubby (d), and branched (e). PSDs (red) also vary in size and shape. Arrows indicate where the head and neck diameters were measured for each spine in (b)-(e). (E-a) A graph plotting the ratio of head diameters to neck diameters for the spines on the reconstructed dendrite. Scale bar = 0.5 µm. (Figures and text adapted from: Bourne & Harris, 2008; Sala *et al.*, 2008; Bhatt *et al.*, 2009)

(Fiala *et al.*, 2002). Newly formed dendrites are devoid of synaptic contacts (Petrak *et al.*, 2005; Knott *et al.*, 2006). During the first postnatal week dendrites become highly covered with filopodial protrusions that rapidly extend and retract (Dailey & Smith, 1996; Lendvai *et al.*, 2000). As synaptogenesis proceeds, dendrites begin to exhibit spines and the number of filopodia decline. In 4 week-old mice filopodia represent only ~11% of all dendritic protrusions while in the adult just 2-3% were reported (Zuo *et al.*, 2005). The decreasing number of filopodia which is accompanied by an increasing number of spines led to the hypothesis that a transformation from filopodia to spine occurs (Fig. 3 B). Thus, filopodia would represent an intermediated stage in spine development. This concept was strongly supported by live imaging data demonstrating that contacts between

dendritic filopodia and crossing axons indeed result in functional synapses (Dailey & Smith, 1996; Ziv & Smith, 1996; see also Fig. 3). More recent data show that only a very small percentage of filopodia is transformed into spines, while the majority disappear within a short time interval (Zuo *et al.*, 2005). The majority of developmental filopodia forms synapses on the dendritic shaft that may later form new spines or get eliminated (Bourne & Harris, 2007). Interestingly, even neurons that do not form spines in maturity, like retinal ganglion cells, exhibit dendritic filopodia during the early phase of synaptogenesis (Wong & Wong, 2001; Bonhoeffer & Yuste, 2002).

The mechanism of dendritic spine generation, and the question if they require filopodia as an intermediate stage, is still under debate (Ethell & Pasquale, 2005). It is likely that the mechanism of spine formation during early development substantially differs from spinogenesis in the adult animal. The lifetime of filopodia in both young and adult cortex is on the order of minutes to hours underlining the general transient nature of this structure. Based on the observations during synaptogenesis, it was hypothesised that filopodia could be involved in the localisation and recognition of potential axonal partners. According to this, it is reported that filopodia outgrowth is initiated after inhibition of synaptic transmission. This is interpreted as a neuronal response to compensate for the loss of synaptic activity and suggest that filopodia are generated in order to find new synaptic connections (Kirov & Harris, 1999; Petrak *et al.*, 2005). Further, glutamate was identified to promote the extension of filopodia, suggestion a mechanism to guide filopodia to existing presynaptic terminals (Portera-Cailliau *et al.*, 2003). The extension of filopodia increases Ca^{2+} levels in the filopodia which spread into the adjacent dendrite. Uncaging of Ca^{2+} in the dendrite leads to a stabilisation of these filopodia (Lohmann *et al.*, 2005). Subsequent work by this group demonstrated that the decision about stabilisation or retraction of a filopodium can be predicted on the base of the measured Ca^{2+} concentration. Filopodia, that were later found to be stabilised, possessed a three times higher concentration of Ca^{2+} directly after contact formation compared to filopodia that were later retracted (Lohmann & Bonhoeffer, 2008). This indicates that filopodia are capable of evaluating and discriminating potential synaptic partners before a synapse is established. A cellular base for such a mechanism is signalling via cell adhesion molecules located at the tip of the filopodia. Another model includes adhesion-mediated target recognition and signalling via membrane tensions (Heiman & Shaham, 2010).

1.4 Synaptic plasticity

1.4.1 Adult brain plasticity

Neuroplasticity refers to the ability of the brain to change its structure and/or function as a result of new experiences. Until the end of the last century, neuroscientist believed that the brain's wiring becomes fixed in early life, during the so-called critical period, and that beyond this stage changes are impossible. In this model, adult learning would have depended exclusively on changes in connection strength of existing synapses

(Chklovskii *et al.*, 2004). Today, we have broad evidence that adult neuroplasticity, in addition, involves a huge variety of structural modifications. These were shown to range from the insertion of new born neurons in pre-existing neuronal circuits, to modulation of synaptic connectivity, and morphological alterations of single synapses, in particular their dendritic spines (see e.g. Chklovskii *et al.*, 2004; Fortin *et al.*, 2011; Inokuchi, 2011). In the following, I will focus on structural and functional modifications of dendritic spines and the implications for adult neuroplasticity.

1.4.2 Neurotransmitter receptors involved in synaptic plasticity

1.4.2.1 Ionotropic receptors

Synaptic release of glutamate in the synaptic cleft activates two types of ligand-gated ion channels: AMPA and NMDA receptors. Both are largely located on the surface of dendritic spines.

AMPA receptors are the predominant ionotropic receptors in the CNS and consist of a heterotetrameric complex, composed of four types of subunits (GluR1-4). They mediate fast postsynaptic membrane depolarisation by the influx of K^+ and Na^+ ions. AMPA receptors lacking the GluR2 subunit additionally show a high Ca^{2+} permeability (Burnashev *et al.*, 1992). At the synapse they are anchored in the PSD via cytoskeletal and scaffolding proteins. The number of AMPA receptors located at the cell surface of a spine varies substantially ranging from about 5 to 200 (Newpher & Ehlers, 2008). AMPA receptors are continuously exchanged between synapses and intracellular storage compartments. Defined pattern of synaptic activity cause a shift in the balance between the different compartments and either results in the recruitment or dispersal of synaptic AMPA receptors (Opazo & Choquet, 2011).

NMDA receptors form a heterotetramer composed of three subtypes of subunits: GluN1, GluN2 and GluN3. Functional recombinant NMDA receptors in mammalian cell require the co-expression of at least one GluN1 and one GluN2 subtype (Paoletti & Neyton, 2007). Receptor activation is mediated by the binding of the transmitter glutamate and the coagonist glycine. Glutamate binds to the GluN2 subunit, while glycine interacts with the GluN1 subunit (Rebola *et al.*, 2010). The receptor is blocked by extracellular Mg^{2+} at resting membrane potentials and its activation requires the depolarisation of the postsynaptic membrane that relieves this block. The NMDA receptor activation (50 - 150 ms) is, therefore, relatively slow compared to AMPA receptors (1 - 10 ms) (Bear *et al.*, 2007). The unique opening property makes the NMDA receptor a coincidence detector for the activation of the pre- and postsynaptic site. Channel opening increases the permeability for Ca^{2+}, Na^+ and K^+ ions and is relatively long-lasting. The influx of Ca^{2+} is one of the key regulators of synaptic plasticity. While AMPA receptor number varies greatly from one spine to another, the number of NMDA receptors is small but more constant (Sheng, 2001).

1.4.2.2 Metabotropic receptors

Metabotropic receptors do not conduct ions, but mediate intracellular signalling via G-protein coupled second messenger pathways. The brain possesses a huge number of different metabotropic receptor types. Here, I will only focus on metabotropic glutamate and muscarinic acetylcholine receptors.

Metabotropic glutamate receptors (mGluRs) comprise a family of eight subtypes that are categorised into three groups based on sequence homology, pharmacological properties, and associated second messenger pathways. Group I mGluRs (mGluR1 and mGluR5) couple to $G_{q\,/\,11}$ second messenger pathway, whereas group II (mGluR2 and mGluR3), and group III (mGluR4, mGluR6, mGluR7, and mGluR8) signal via $G_{i\,/\,o}$ pathways (Gerber *et al.*, 2007). They are broadly distributed throughout the brain and concentrated at synaptic or extrasynaptic sites in both neurons and glia. Group I mGluRs are primarily found postsynaptically. The signalling cascade of this receptor group involves inositol trisphosphate (IP_3), PKC and the mobilisation of Ca^{2+} from internal stores. The receptor activity adjusts and fine-tunes synaptic transmission and plays important roles in the induction of long-lasting forms of synaptic activity, including LTD and LTP (Niswender & Conn, 2010). In contrast, group II and group III receptors are often localised on presynaptic terminals where they inhibit neurotransmitter release and act as a negative-feedback loop to prevent runaway excitation at glutamergic synapses (Scanziani *et al.*, 1997).

Muscarinic acetylcholine receptors (mAChRs) comprise five molecular distinct subtypes M_1-M_5. They are subdivided into two major functional classes according to their G-protein signalling pathways. Receptors M_1, M_3 and M_5 activate G-proteins of the $G_{q\,/\,11}$ family, whereas M_2 and M_5 receptors couple to $G_{i\,/\,o}$-type pathways. In the brain, the five subtypes are expressed in a distinct pattern in neurons and glial cell (Wess *et al.*, 2007). Thus, activation of mAChRs induces different effects in various brain regions that can be excitatory or inhibitory. Here, I focus on the functional roles of the subtypes M_1 and M_2. The M_1 mAChR is the predominant subtype expressed in brain areas involved in cognitive functions (Volpicelli & Levey, 2004). In the hippocampus it is highly expressed on dendrites and dendritic spines of CA1 cells (Yamasaki *et al.*, 2010) and its activation potentiates NMDA receptor currents (Marino *et al.*, 1998). Activation of M_1 receptors can also induce LTP in hippocampal slice cultures (Shinoe *et al.*, 2005). Studies in M_1 receptor knock-out mice demonstrated an involvement of the MAP kinase pathway in the receptor signalling. Although the MAP kinase pathway is an important modulator of synaptic plasticity, the mice showed impairments only for a few selective behavioural tasks (Wess *et al.*, 2007). M_2 receptors are found both pre- and postsynaptic (Volpicelli & Levey, 2004). At presynapses it acts as an autoreceptor and mediates the inhibition of hippocampal and cortical Ach release (Zhang *et al.*, 2002). Further studies in M_2 knock-out mice demonstrated an involvement in hippocampal synaptic plasticity by impairing short-term potentiation and reducing LTP in CA1 pyramidal neurons. Accordingly, these mice were impaired in several behavioural test indicating significant deficits in working

memory and behavioural flexibility (Seeger *et al.*, 2004). Likewise, pharmacological studies in humans conclusively demonstrated a function for muscarinic receptors in the encoding of new memories (Hasselmo, 2006).

1.4.3 Short-term and long-term plasticity in the hippocampus

The excitatory synapses in the hippocampus display several forms of activity-dependent synaptic plasticity. This is reflected by changes in the amplitude of postsynaptic potentials which are correlated to the recent history of received activity patterns. Based on the persistence of the induced change they are classified in short-term and long-term plasticity (Citri & Malenka, 2008).

Short-term plasticity includes synaptic changes that range from the tens or hundreds of milliseconds to several seconds or minutes. Generally, they depend on presynaptic mechanisms and increase or decrease the probability that an incoming presynaptic action potential triggers the release of neurotransmitter into the synaptic cleft. Depending on the mode of modulation and involved time course the changes are termed paired-pulse facilitation (~10-100 msec), augmentation (sec), post-tetanic potentiation (min) or depression (50 msec to min) (Zucker & Regehr, 2002). Facilitation occurs when two stimuli reach the presynaptic element in rapid succession. In this case, the second postsynaptic potential can be up to five times higher than the first. The effect is caused by an elevated intracellular Ca^{2+} concentration that remains from the first stimulus (residual Ca^{2+}) and increases the probability of a synaptic vesicle release (Kamiya & Zucker, 1994). If presynaptic activity is sustained, facilitation is followed at most synapses by a slower phase of increased efficacy called augmentation (Squire, 2009). Augmentation is also Ca^{2+}-dependent and decays more slowly than facilitation. The mechanism probably depends on Na^{+} accumulations that decrease the Ca^{2+} extrusion out of the presynapse (Thomson, 2000). Post-tetanic potentiation shows decays from tens of seconds to minutes and requires high frequency or tetanic firing to be induced. Although the mechanism is not completely clear it is thought to result from Ca^{2+}-dependent mobilisation of reserve pools of synaptic vesicles (Thomson, 2000). Synaptic depression is induced after a period of sustained activity and is believed to result from a depletion of synaptic vesicles. Taken together, because of short-term synaptic plasticity, the amount of externalised neurotransmitter can vary between each presynaptic action potential.

Long-term plasticity refers to synaptic changes that clearly exceeds the time scale of short-term plasticity. The best studied experimental paradigms that mimics many aspects of long-term plasticity, are long-term potentiation (LTP) and long-term depression (LTD). They are characterised by a long-lasting increase or decrease of synaptic strength and were extensively studied in the hippocampus. The classical LTP induction depends on a mechanism that detects coincident pre- and postsynaptic activity (Citri & Malenka, 2008). NMDA receptors at the postsynapse bind glutamate that is released from the presynapse. However, this does not necessarily open the channel because the pore is

blocked by magnesium ions at resting membrane potential. Only when the postsynapse receives sufficient depolarisation the magnesium ion is expelled from the channel and allows the influx of Ca^{2+} ions (Nowak *et al.*, 1984). The increased Ca^{2+} levels trigger several intracellular signalling cascades including PKC and CaMKII. Once activated, they can phosphorylate AMPA receptors which change its biophysical properties to a more active stage (Barria *et al.*, 1997; Malenka & Bear, 2004). Additionally, AMPA receptor trafficking is modified in favour of an increased insertion of receptors in the plasma membrane (Bredt & Nicoll, 2003). In the hippocampus LTP lasts for hours *in vitro* and can persist for weeks or months *in vivo*. While the early phase of LTP is independent of protein synthesis, long persistence requires gene transcription and protein synthesis (Frey *et al.*, 1988; Ahmed & Frey, 2005; Abraham & Williams, 2008). This can be mediated e.g. by the transcription factor CREB that governs the expression of a variety of immediate early genes (Segal & Murphy, 1998).

LTD is the opposing process to LTP and leads to a persistent decrease in synaptic strength. It is found in many brain regions and varies between these in the mechanisms of induction. In the hippocampus it can be induced at synapses of CA1 pyramidal cells by low-frequency stimulation. Interestingly, LTD is also mediated by postsynaptic Ca^{2+} entry through NMDA receptors (Kullmann *et al.*, 2000). However, the concentrations of postsynaptic Ca^{2+} are smaller and slower rising compared to LTP induction and therefore activate Ca^{2+}-dependent phosphatases that dephosphorylate AMPA receptors and other target proteins. This leads to the decrease in AMPA receptor activity and causes internalisation of the receptor by clathrin-dependent endocytosis (Luscher *et al.*, 1999; Man *et al.*, 2000).

1.4.4 Structural synaptic plasticity

1.4.4.1 Structural plasticity serves for long-term storage of information

Synaptic plasticity in the form of LTP and LTD, also termed synaptic weight changes, enable the storage of information in a neural network. However, several pieces of evidence indicate that synaptic weight changes are not the exclusive mechanism of long-term memory formation. A critical factor for memory storage by weight changes is the maintenance of individual synapse properties over long time periods. This is difficult to achieve because synapses operate with only small numbers (~10) of receptors (Nimchinsky *et al.*, 2004) and synaptic weight changes hence modulate only a few proteins that additionally exhibit short lifetimes (Ehlers, 2003; Kasai *et al.*, 2010). The regulation of receptors on the level of single-molecules possesses a high susceptibility and seems to be less suited for long-term storage of information. Long lasting memory formation is believed to rely on modifications of the connection pattern between neural circuits. This model serves some advantages compared to a scenario that only consists of synaptic weight changes. First, wiring changes involve structural plasticity that is long-lasting and underlies well established control mechanisms. Second, it provides a

substantial boost in storage capacity and can be combined with the properties of synaptic weight changes (Stepanyants *et al.*, 2002; Chklovskii *et al.*, 2004).

1.4.4.2 Turnover of synaptic elements in the adult animal

Structural plasticity is a well characterised process during brain development (Portera-Cailliau *et al.*, 2005; Calabrese *et al.*, 2006; Sala *et al.*, 2008). To prove the link between structural plasticity and learning it was essential to demonstrate experience-dependent structural modifications in adult animals. The adult brain was intensively analysed for large-scale structural plasticity of axons and dendrites. Evidence for axonal dynamics was primarily observed in experiments involving lesions of the sensory periphery (Holtmaat & Svoboda, 2009). Spatial learning induces structural remodelling in the hippocampal mossy fibres (Holahan *et al.*, 2006), and long-term imaging revealed length changes in short branches and distal axonal endings that are accompanied by the turnover of boutons (De Paola *et al.*, 2006; Holtmaat *et al.*, 2008). Overall, reports for axonal remodelling in the adult brain are rather rare. Dendrite plasticity was extensively studied by the classic Golgi method and suggested structural changes following experimental manipulations (Chklovskii *et al.*, 2004). More recent live imaging studies failed to reproduce this data and rather indicate that the large-scale organisation of dendrites is relatively stable and alterations of the dendritic tree are mainly restricted to adult-born neurons (Holtmaat & Svoboda, 2009; Barnes & Finnerty, 2010). Although long-range structural plasticity would strongly increase the number of potential interaction partners of an individual neuron (Stepanyants *et al.*, 2002; Chklovskii *et al.*, 2004), the data of axonal and dendritic dynamics in adult animals does not suggest such a process as an elementary mechanism of learning and memory.

Another strategy for cortical rewiring comprises short-range structural plasticity including axonal boutons and dendritic spines. Early evidence for structural plasticity of these structures came from studies using electron microscopy and 3D reconstructions of axonal and dendritic segments (Sorra & Harris, 2000; Toni *et al.*, 2001). During the last decade, improvements in optical techniques, like fast two-photon microscopy, in conjunction with advanced fluorescent probes have opened the door to investigate structural plasticity of axonal boutons and dendritic spines in the living animal. Mice kept under normal laboratory conditions show a low but permanent bouton turnover, while the overall density remains stable (De Paola *et al.*, 2006; Majewska *et al.*, 2006).The rate of plasticity is dependent on the regional origin of the axon and the type of bouton (*terminaux* boutons are more plastic than *en passant* boutons; see Barnes & Finnerty, 2010 for definition). Dendritic spine plasticity is extensively investigated under baseline conditions in adult mice. Spine populations are very inhomogeneous in their turnover rates. Some spines appear and disappear over days, whereas a big proportion remains stable and persist for months, eventually for the entire life of the mouse (Grutzendler *et al.*, 2002; Trachtenberg *et al.*, 2002; Holtmaat *et al.*, 2005). Similar as for the bouton turnover, also spine turnover shows variations between different cell types and brain regions. In general, spine plasticity strongly correlates with the stage of brain maturation

and continuously decreases during the first six month of the rodent's life (Zuo *et al.*, 2005; Holtmaat & Svoboda, 2009). Interestingly, the average lifetime of individual spines can be well predicted based on two criteria: spine size and prior history of turnover. Spines that recently appeared are likely to disappear again and small spines are rather eliminated than large spines (Grutzendler *et al.*, 2002; Holtmaat *et al.*, 2005; Zuo *et al.*, 2005).

The high turnover rate of newly established spines raises the question if these, in fact, can mature into functional synaptic contacts. Early work on this topic was performed using dissociated hippocampal cultures and suggested the establishment of functional glutamergic synapses within 1-2 hours (Friedman *et al.*, 2000; Okabe *et al.*, 2001). First *in vivo* data obtained in the mouse barrel cortex demonstrated that newly formed spines establish functional synapses and proposed around 1 day for this transformation (Knott *et al.*, 2006). The time course of synaptogenesis was explicitly addressed in a study using two-photon imaging after theta-burst stimulation in organotypic slice cultures (Nagerl *et al.*, 2007). Subsequent analysis by serial section electron microscopy revealed synaptic structures in new spines after ~15 hours. A recent study investigated spontaneously appearing spines by a similar technical approach but additionally used glutamate uncaging to determine functional properties of the nascent spines (Zito *et al.*, 2009). Intriguingly, they found that the new established spines respond to glutamate shortly after their formation, indicating a close coupling between spine growth and glutamate receptor recruiting. Further, they reported that the newly formed spines are contacted by presynaptic boutons within a couple of hours. Such a short time scale of synapse formation is well in agreement with the proposed model of information transfer from short-lived synaptic weight changes to long-lasting structural rearrangement of synapses (Chklovskii *et al.*, 2004).

1.4.4.3 Experience-dependent spine plasticity

Animal rearing or training in enriched environments are well known to increase spine and synapse densities (Greenough *et al.*, 1985; Beaulieu & Colonnier, 1987). Similarly, different learning paradigm induced brain region-specific changes in spine density in rodents and chicken (Lowndes & Stewart, 1994; Moser *et al.*, 1994; O'Malley *et al.*, 2000). To prove causality between the acquiring of new information through selective generation and elimination of synapses, however, it requires more specific experimental approaches. LTP induction in organotypic slice cultures is followed by the generation of new filopodia and spines (Engert & Bonhoeffer, 1999; Maletic-Savatic *et al.*, 1999). Subsequent work demonstrated that the initial increase of dendritic protrusion is followed by a phase of increased destabilisation and loss of spines. Hence, LTP induction rather promotes protrusion turnover than affecting total spine number. Interestingly, spine elimination predominantly affects nonactivated spines suggesting LTP to function as a selection mechanism to stabilise potentiated synapses that may result in a refinement of the synaptic network (De Roo *et al.*, 2008). An *in vivo* study analysed the mouse barrel

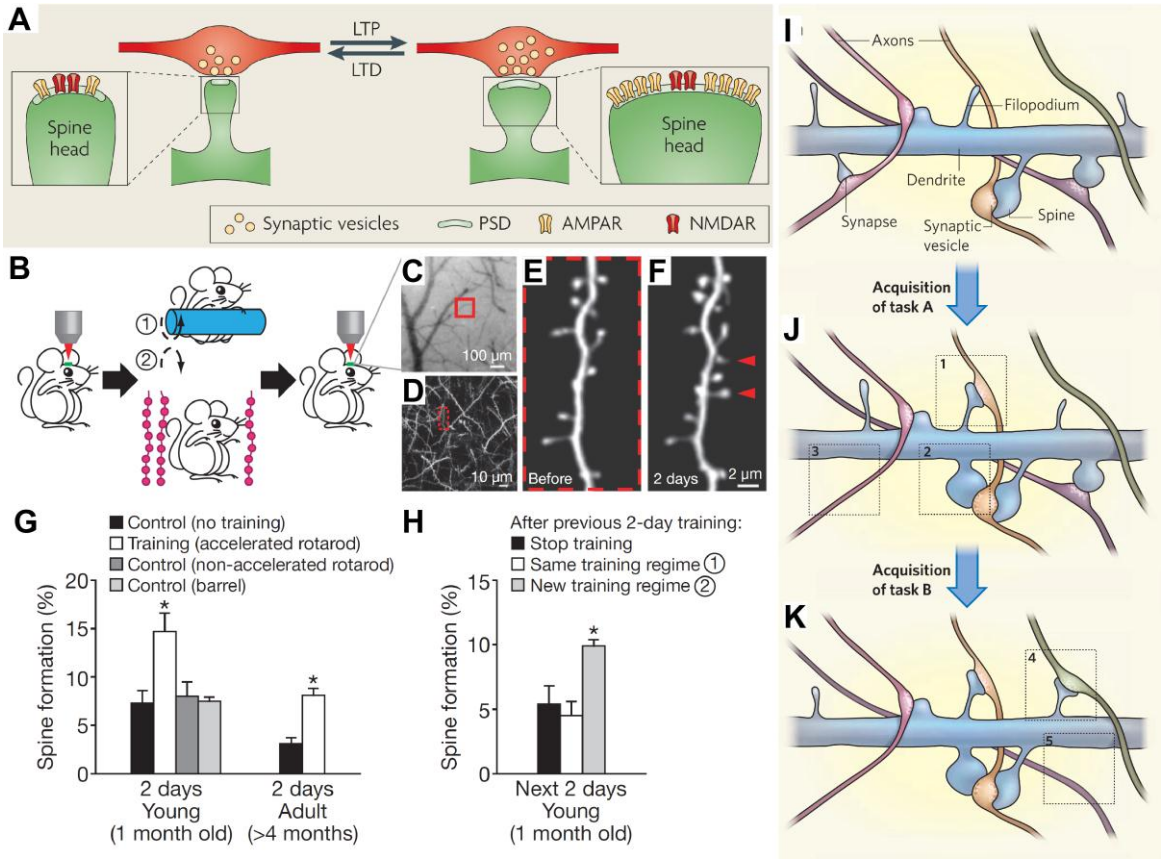

Figure 4. Experience-dependent spine head plasticity

(A) Spine volume is proportional to the area of PSD, which in turn is proportional to synapitc AMPA receptors. At the same time these quantities co-vary with presynaptic parameters such as synaptic vesicle concentration. LTP induces spine volume increase, while LTD causes spine head shrinkage. (B) Transcranial two-photon imaging of spines before and after rotarod training or sensory enrichment. (C) CCD camera view of the vasculature of the motor cortex. (D) Two-photon image of apical dendrites from the boxed region in (C). A higher magnification view of a dendritic segment in (D) is shown in (E). (E-F) Repeated imaging of a dendritic branch before (E) and after rotarod training (F). Arrowheads indicate new spines formed over 2 days. (G) The percentage of new spines formed within 2 days in the motor cortex was significantly higher in young or adult mice after training as compared with controls with no training or running on a non-accelerated rotarod. No increase in spine formation was found in the barrel cortex after training. (H) After previous 2-day training, only a new training regime (reverse running) caused a significant increase in spine formation. (I) Several axons can form en passant synapses (synapses formed along axons rather than at their tips) with dendritic spines extended from a nearby dendrite. Synaptic vesicles contain neurotransmitters secreted at these synapses. (J) The acquisition of new motor task A is associated with the formation of new spines. This can occur by the selective stabilisation of a dendritic filopodium that had contacted a nearby axon beforehand (spine 1) or by the direct emergence of a new spine that extends towards a nearby axon (spine 2). Motor task acquisition is then followed by the elimination of other spines (3). (K) Acquisition of a second motor task (task B) is followed by the formation of an additional set of new spines (4) and the elimination of others (5), without significantly affecting the spines formed during the acquisition of task A.

(Figures and text adapted from: Holtmaat & Svoboda, 2009; Yang *et al.*, 2009; Ziv & Ahissar, 2009)

cortex after whiskers were trimmed in a chessboard pattern (Holtmaat *et al.*, 2006). The authors reported an enhanced stabilisation of new spines (~15%) compared to controls under baseline conditions (~5%). Recently, two imaging studies in the mouse cortex presented strong evidence for the direct relationship between spine remodelling and learning (Xu *et al.*, 2009; Yang *et al.*, 2009; see also Fig4 B-H). Learning of new motor tasks or exposure to an enriched environment significantly increased the number of newly formed spines after a training period (1-2 days). Continuous training was accompanied by increased rates of spine elimination resulting in an equalised total number of spines between trained and control mice, within 1-2 weeks. Remarkably, the general sequence of events is identical to the results obtained in LTP stimulated slice cultures (De Roo *et al.*, 2008). Two additional observations strengthen the correlation between learning and spine remodelling in these studies: First, animals that failed to learn the task for certain circumstances, did not show the training-associated spine remodelling. Second, re-exposure of the trained mice to the original training tasks did not induce spine remodelling, whereas training of novel motor tasks did (Ziv & Ahissar, 2009). Altogether, these experiments clearly demonstrated that stable contacts can be eliminated or created *de novo* through experience.

1.4.4.4 Morphological plasticity of spine heads

Beside increased spine turnover rates, synaptic activity also causes structural modifications at individual spine heads. Spine volumes increase after LTP induction (Matsuzaki *et al.*, 2004; Kopec *et al.*, 2006; Yang *et al.*, 2008) and this change is attended by an intensified postsynaptic sensitivity demonstrated by glutamate uncaging experiments (Harvey & Svoboda, 2007). Similarly, LTD induces spine head shrinkage (Nagerl *et al.*, 2004; Okamoto *et al.*, 2004; Zhou *et al.*, 2004). Spine expansion is rapid in its onset (~1 min) and long lasting (up to 2 h) (Yang & Zhou, 2009). Interestingly, large and small spines undergo the same absolute increase in spine head volume (Lang *et al.*, 2004; Kopec *et al.*, 2006). The morphological change is depend on an increase in F-actin (Okamoto *et al.*, 2004; Lin *et al.*, 2005; Kramar *et al.*, 2006) and further requires membrane recruitment by mobilisation of recycling endosomes, vesicles, and amorphous vesicular clumps (Park *et al.*, 2006). The tight correlation of the PSD size with the size of the presynaptic bouton and the containing number of vesicles (Harris *et al.*, 1992), implies similar plastic changes for the presynapse. The direct functional consequences of the spine enlargement remain elusive. Spine heads generate expansive forces via F-actin (Honkura *et al.*, 2008) and it was hypothesised that this mechanical force may affect presynaptic structure, thereby increasing the release probability of presynaptic terminals (Kasai *et al.*, 2010).

Time-lapse imaging acquired at intervals of seconds revealed a considerable motility of spine heads (Fischer *et al.*, 1998; Dunaevsky *et al.*, 1999). There is evidence that this actin-based motility is controlled by synaptic activity because activation of AMPA or NMDA receptors inhibits these spine dynamics and leads to rounded and regular spine shapes (Fischer *et al.*, 2000). This inhibition in spine motility relies on postsynaptic

depolarisation and voltage-dependent Ca^{2+} channels and can be also induced by anaesthetics like chloroform or isoflurane (Kaech *et al.*, 1999; Fischer *et al.*, 2000). Spine motility was also described *in vivo* in the developing cortex (Lendvai *et al.*, 2000) (Majewska & Sur, 2003) (Majewska *et al.*, 2006). It remains to be elucidate if spine motility contributes to the process of intrinsic spine fluctuations that were recently reported (Yasumatsu *et al.*, 2008).

1.4.4.5 Cytoskeletal elements involved in plastic spine changes

Dendritic spine morphology is governed by the actin cytoskeleton and structural changes depend largely on actin dynamics. Both the monomeric form of actin (G-actin) and filamentous actin polymers (F-actin) are present in spines and the degree of actin polymerisation (G-actin/F-actin ratio) has, therefore, fundamental effects on spine morphology. Induction of LTP shifts this ratio towards F-actin and facilitates the growth of spine volume, whereas LTD shifts the ratio towards G-actin resulting in spine head shrinkage (Okamoto *et al.*, 2004). Mature spines consist of a mixture of branched and linear actin filaments and the most branched filaments are found at the distal regions of the spine head (Korobova & Svitkina, 2010). Regarding dynamics, there exist three pools of actin which are differently involved in spine modulation (Honkura *et al.*, 2008). Highly dynamic filaments, which undergo permanent treadmilling motility, are localised at the tip of the spine and generate expansive force. The spine base comprises a pool of relatively stable actin filaments. The third pool, termed the “enlargement pool”, can be induced on individual spines by postsynaptic activity (uncaging glutamate in the study) and reacts relatively slowly. The increase in this pool was necessary but not sufficient for the long-term increase in spine size. Interestingly, the structural organisation of actin in dendritic filopodia differs in many aspects from conventional filopodia (Hotulainen & Hoogenraad, 2010; see also Fig. 5). The molecular mechanism involved in the initiation of dendritic filopodia remains unexplained yet. Small GTPases of the Rho and Ras families are the major signalling molecules for actin dynamics in dendritic spines. Activation of RhoA and Cdc42 is induced after LTP stimulation and mediates spine head enlargement (Hotulainen *et al.*, 2009; Murakoshi *et al.*, 2011). Rac and Cdc42 also regulate spine head morphology by activation of the Arp2/3 complex. This complex binds to existing actin filaments and nucleates a new filament resulting in branched actin filaments. The Arp2/3 complex is concentrated in spines and functional alterations affect number and morphology of spine heads (Haeckel *et al.*, 2008; Nakamura *et al.*, 2011). The importance of controlling actin dynamics in dendritic spines is demonstrated by several examples of mutations of Rho and Ras family members that were implicated with mental retardation (Newey *et al.*, 2005).

Only until recently, microtubules were believed to be distributed only along the dendritic shaft in mature neurons but absent from dendritic spines. New data from several groups conclusively demonstrate that microtubules enter spines under physiological conditions (Gu *et al.*, 2008; Hu *et al.*, 2008; Jaworski *et al.*, 2009). Microtubule invasion into dendritic spines and filopodia occurs in only a small percentage of protrusions at a given

time point (~1% of all spines) and is highly transient with an average of about three minutes per invasion. Time-lapse recordings showed that within one hour about 10% of dendritic protrusions were targeted by microtubules. Microtubules can repeatedly enter the same spine and target mushroom spines more frequently than filopodia (Hu *et al.*, 2008; Jaworski *et al.*, 2009). Interestingly, all studies report that increased synaptic activity promotes spine invasion by microtubules. The functional role of this effect is currently not understood. Given the important function of microtubules in cellular trafficking, it is likely that the short entry in spines facilitate the transport of essential proteins into the spine head. In this context, it is interesting that pharmacological blockage of microtubule dynamics inhibit the maintenance of LTP in hippocampal slice cultures (Jaworski *et al.*, 2009). However, the blockage also affected trafficking from the soma and should be interpreted with caution. Another effect associated with microtubule entry is a transient morphological change of spine heads, such as spine growth and the formation of spine head protrusions (Hoogenraad & Akhmanova, 2010).

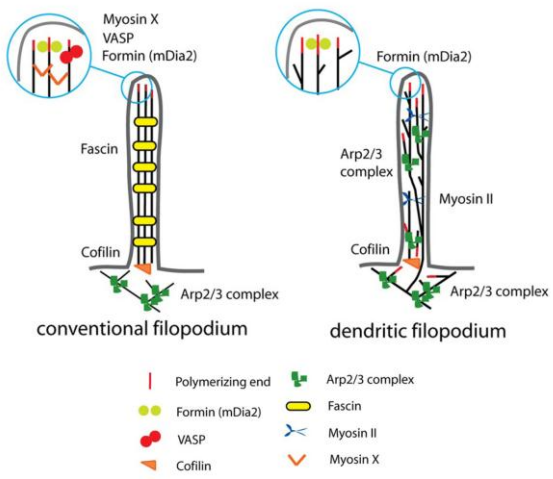

Figure 5. Comparison of actin organisation in conventional filopodia and dendritic filopodia

In conventional filopodia from fibroblast cells, actin filaments are elongated from the tip of filopodia by mDia2, Ena/VASP, and myosin X. Polymerised actin filaments are bundled by fascin and show no branched filaments. In dendritic filopodia, mDia2 elongates actin filaments from the tip of filopodia. The functions of Ena/VASP and myosin X have not yet been studied in dendritic protrusions. In addition to tip polymerisation, actin filaments of dendritic filopodia also elongate from the filopodium base. Fascin is absent from dendritic filopodia.

(Figure and text adapted from: Hotulainen & Hoogenraad, 2010)

1.5 Extracellular matrix molecules and synaptic function

1.5.1 The extracellular matrix of neural cells

Cells in animal tissue are surrounded by an extracellular matrix (ECM) consisting of collagens, proteoglycans and glycoproteins. Besides providing structural support to the cell, the ECM is required to determine functional interaction between the cell and its environment in a wide range of functions, such as development, migration, differentiation, cell maturation, cell survival and tissue homeostasis. In the context of this thesis, the main focus is put on proteoglycans which are briefly introduced in the following section.

Proteoglycans consist of a core protein to which at least one glycosaminoglycan (GAG) chain is covalently attached via a tetrasaccharide bridge. They differ from other glycoproteins by the arrangement and nature of their sugar side chains. Functionally, they are defined by the core protein and the associated GAG chains. GAGs are attached to serine residues of the core protein and consist of repeating disaccharide units incorporating an aminosugar and an uronic acid. According to their sugar composition, GAGs can be classified as keratin sulphates (KS), chondroitin sulphates (CS), dermatan sulphates (DS) and heparan sulphates (HS) (Bulow & Hobert, 2006). Additional modifications of the sugar residues inside the Golgi complex generate an enormous molecular diversity within the groups (see Fig. 6).

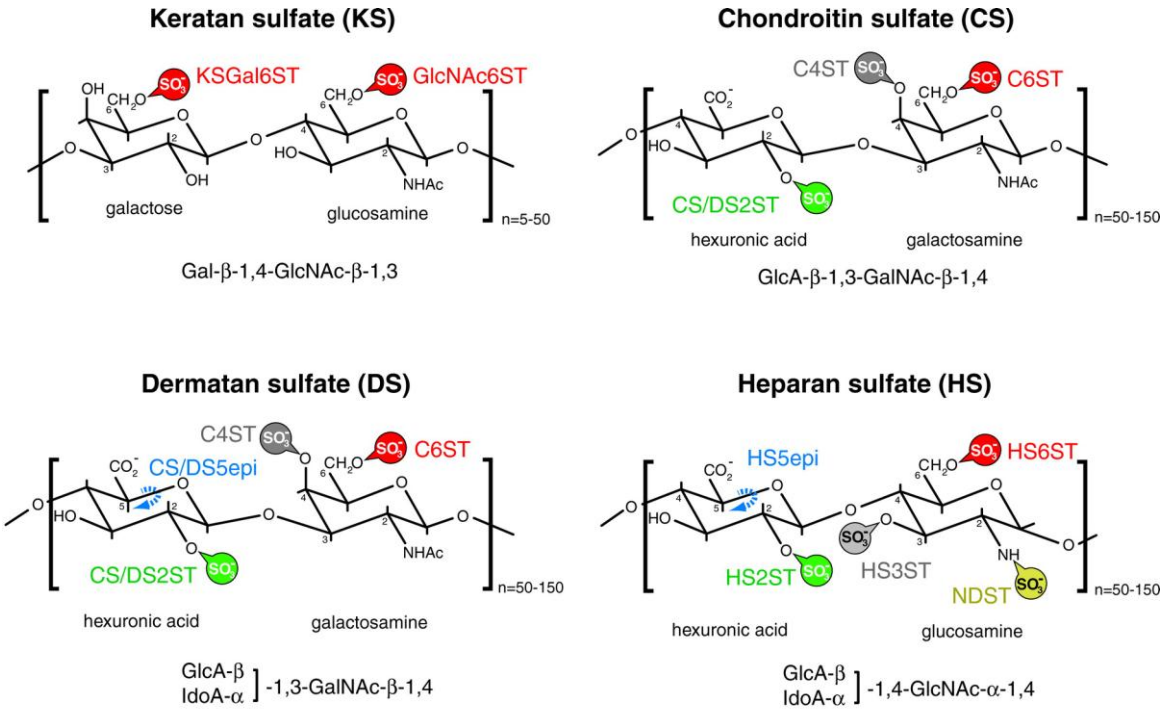

Figure 6. Classes of GAG disaccharide repeat units

KS, CS, DS, and HS can carry two, three, four, and five modifications on their disaccharide repeat units, respectively. Potential sites for modifications are shown in different colours and with the catalysing enzyme. Abbreviations used: C4ST, CS-4O-sulfotransferase; C6ST, CS-6O-sulfotransferase; CS/DS2ST, CS/DS-2O-sulfotransferase; Gal, galactose; GalNAc, N-acetyl-galactosamine; GlcA, glucuronic acid; GlcNAc, N-acetyl-glucosamine; GlcNAc6ST, N-acetyl-glucosamine-6O-sulfotransferase; HS2ST, HS-2O-sulfotransferase; HS3ST, HS-3O-sulfotransferase; HS6ST, HS-6O-sulfotransferase; IdoA, iduronic acid; KSGal6ST, KS-galactose-6O-sulfotransferase; NDST: N-deacetylase-N-sulfotransferase. (Figure and text adapted from: Bulow & Hobert, 2006)

GAG chains bind different neurotrophic substances: growth promoting factors such as midkine, pleiotrophin and FGFs, as well as growth inhibitory factors such as semaphorins (Galtrey & Fawcett, 2007). The binding serves different function. Growth factors can be targeted at defined sites to mediate distinct spatiotemporal functions. Furthermore, binding can regulate the activity of the molecules, as for example demonstrated for semaphoring 5A where GAG binding converts the protein from a permissive to an

inhibitory molecule (Kantor *et al.*, 2004). Association with GAGs may also promote ligand-receptor binding and protects the growth factors from degradation.

Proteoglycans are a major component of perineuronal nets (PNNs). These structures surround cell bodies and proximal dendrites in a mesh-like structure and display a specialised organisation of the ECM (Dityatev & Schachner, 2003). Biochemical investigations have shown that the composition of proteoglycans associated with PNNs differs from those in the ECM (Galtrey & Fawcett, 2007). PNNs can be observed in virtually all regions of the CNS but are restricted to only a subset of neurons. Interestingly, the formation of PNNs relies on neuronal activity (Reimers *et al.*, 2007). In tissue both neurons and glia express specific subsets of proteoglycans that form PNs. Dense extracellular meshwork that resembles PNNs were also reported from dissociated cortical and hippocampal cultures that were free of glial cells (Miyata *et al.*, 2007; Frischknecht *et al.*, 2009). Many ECM molecules at PNNs are replaced by others of the same family during nervous system maturation, reflecting the high degree of structural organisation (Rauch, 2004). PNNs are believed to play an important role in synaptic stabilisation and plasticity, ion homeostasis, intracellular linkage of cytoskeletal element of neighbouring cells, and neuroprotection (Gogolla *et al.*, 2009; Karetko & Skangiel-Kramska, 2009; Faissner *et al.*, 2010).

1.5.2 Involvement of the ECM in synaptic plasticity

Individual ECM components are highly expressed before the temporal peak of postnatal synaptogenesis and might be involved in synapse formation. For instance, aggrecan accumulations appear on the surface of cortical cultures before the formation of presynaptic specialisations and suggest that this may control the localisation of future synapses (Dino *et al.*, 2006). Another example are the thrombospondins, a group of astrocyte-derived extracellular matrix proteins, that promote synaptogenesis *in vitro* and *in vivo* (Christopherson *et al.*, 2005).

In the developing brain ECM proteins have growth-promoting and growth-inhibitory effects on axons and are strongly involved in axon guidance (Margolis & Margolis, 1997; Van Vactor *et al.*, 2006). During postnatal maturation chondroitin proteoglycans play an important role as inhibitors of axon growth, thereby creating a barrier against the formation of new synapses. Intriguingly, the appearance of these boundaries coincides with the end of some critical periods in development (Karetko & Skangiel-Kramska, 2009). This can be well illustrated on the model of ocular dominance plasticity that is only observed in young animals, which exhibit immature ECM structures, but is absent in adults. Enzymatic degradation of chondroitin proteoglycans reactivates ocular dominance plasticity in adult animals and demonstrates that the mature ECM is an important regulator of experience-dependent plasticity (Pizzorusso *et al.*, 2002). In another study, chondroitin sulphate proteoglycans containing PNNs were associated with the protection of erasure-resistant fear memories (Gogolla *et al.*, 2009). Similar as for the

previous example, the establishment of PNNs represents a cellular mechanism to close a postnatal critical period in the animal.

On the level of single synapses, the ECM and especially the PNN may provide a diffusion barrier for extracellular signalling molecules, thereby also affecting the degree of transmitter spillover out of the synaptic cleft (Faissner *et al.*, 2010). Several ECM molecules were identified to contribute to synaptic plasticity via interaction with postsynaptic receptors and ion channels. L-type voltage-dependent Ca^{2+} channels are regulated by at least two ECM components: hyaluronic acid and the glycoprotein tenascin-C (Evers *et al.*, 2002; Kochlamazashvili *et al.*, 2010). Disturbance of these molecules affects Ca^{2+} transients in dendritic spines of hippocampal pyramidal neurons and impairs the induction of LTP. The ECM can further influence postsynaptic Ca^{2+} levels by regulation of NMDA receptors. Binding of the extracellular glycoprotein reelin to its postsynaptic receptors induces a signalling cascade that results in phosphorylation of the GluN2 subunit of NMDA receptors and potentiates Ca^{2+} influx through the receptor (Herz & Chen, 2006). ECM signalling also regulates AMPA receptor dynamics and thus directly affects synaptic transmission. Increased β3 integrin signalling reduces the endocytosis of AMPA receptor and intensifies synaptic strength (Dityatev *et al.*, 2010). In dissociated neurons, PNN-like structures prevent lateral movement of AMPA receptors on the surface of dendritic spines. Experimental degradation of the ECM network releases the neuronal compartmentalisation and is followed by changes in synaptic short-term plasticity (Frischknecht *et al.*, 2009).

Structural modifications at the spine level also require interaction with the extracellular matrix. Mice deficient for α3, α5, and α8 integrins are impaired in short-term plasticity (paired-pulse facilitation), LTP and spatial memory (Chan *et al.*, 2003). Subsequent investigations identified α5 integrin as a regulator of spine morphology in hippocampal neuronal cultures (Webb *et al.*, 2007). LTP consolidation depends on reorganisation of the spine actin cytoskeleton and can be blocked by inhibition of β1 integrin signalling (Kramar *et al.*, 2006). Additionally, structural spine head plasticity and maintenance of LTP is also dependent on activity-induced remodelling of the ECM. Spine head enlargement and LTP induced by theta-burst pairing is not persistent when activity of metalloproteinase-9 (MMP-9) is prevented (Bozdagi *et al.*, 2007; Wang *et al.*, 2008). Accordingly, MMP-9 null mutant mice show impairments in hippocampal-dependent associative learning (Nagy *et al.*, 2006). ECM degradation by serine proteases was also reported to be involved in various functions in the brain (Shiosaka, 2004; Almonte & Sweatt, 2011; Wlodarczyk *et al.*, 2011). Interaction between the serine protease neurotrypsin and the proteoglycan agrin induces another form of ECM-derived structural plasticity, which is described in detail in the following chapters. Taken together, synaptic plasticity requires bidirectional signalling between the involved neurons and their surrounding extracellular matrix.

1.5.3 Agrin

Agrin is an extracellular matrix protein that was first purified from the synapse-rich electric organ of the pacific electric ray *Torpedo californica* (Nitkin *et al.*, 1987). It attracted attention after demonstrating that agrin is sufficient to induce postsynaptic differentiation at the neuromuscular junction (NMJ). The core protein is build-up of 21 domains and has a predicted molecular weight of 220 kDa (Fig. 7). The N-terminal part of agrin possess several attachment sites for heparin sulphate and chondroitin sulphate glycan chains, as well as additional N- and O-linked glycosylations, which increase the molecular weight to 400-600 kDa in the mature protein and classifies it as a proteoglycan (Tsen *et al.*, 1995; Winzen *et al.*, 2003). Different splice sites within the molecule induce structural and functional modifications of the protein. The splice variants are expressed in a tissue-dependent manner (Ruegg & Bixby, 1998; Bezakova & Ruegg, 2003). The second laminin-globular domain (LG2) comprises the y-splice site and contains zero (y0) or four (y4) amino acids. The y4 insertion gives rise to a heparin binding site and modulates the binding of α-dystroglycan (Gesemann *et al.*, 1996; O'Toole *et al.*, 1996). The z-splice site is located within the LG3 domain and contains 0, 8, 11 or 19 (8+11) amino acids. Insertion at the z-site is essential for AChR clustering at the NMJ. These "active" isoforms are expressed by neuronal and Schwann cells, while the z0 variant is expressed in non-neuronal cells (Bezakova & Ruegg, 2003). Alternative splicing at the N-terminus results in the expression of either a secreted (LN-agrin) or a type II transmembrane (TM-agrin) isoform (Burgess *et al.*, 1999; Neumann *et al.*, 2001). LN-agrin is integral part of the basal lamina in many tissues and binds to laminins via the N-terminal NtA domain (Denzer *et al.*, 1997). TM-agrin is expressed by all populations of neurons in the CNS (O'Connor *et al.*, 1994). Interestingly, glia cells were reported to express both LN- and TM-agrin

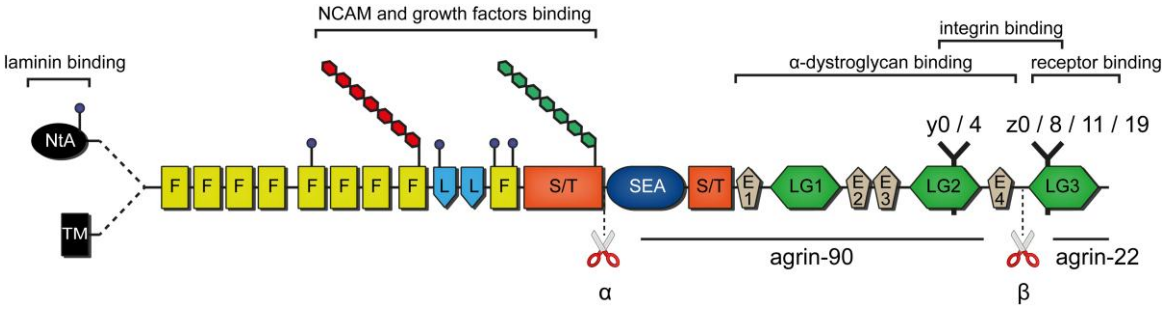

Figure 7. Domain structure and interaction sites of the agrin protein

Alternative splicing either generates transmembrane or secreted agrin variants, containing inserts of variable length at the y and z splice sites. Two multiple SG clusters attach heparan sulphate (red) and chondroitin sulphate chains (green) to the protein backbone. Neurotrypsin cleavage at the α- and β-cleavage site releases two agrin fragments (agrin-90 and agrin-22) from the N-terminal moiety. Identified binding sites of agrin are indicated. NtA - N-terminal agrin domain; TM - transmembrane domain; F - follistatin-like domains; L - laminin-epidermal growth factor (EGF)-like domains; S/T - serine-threonine-rich region; SEA - sperm protein, enterokinase and agrin domain; E - EGF-like domains; LG - laminin-globular domains (adapted from: Bezakova & Ruegg, 2003).

The best characterised function of agrin is its role as a synaptic organiser at the NMJ (Bezakova & Ruegg, 2003). Synaptogenesis requires interaction between motor neurons and muscle fibres to form the postsynaptic specialisation. Briefly, agrin is secreted by presynaptic terminals and becomes part of the basal lamina via binding to laminin. The recently identified coreceptor Lrp4 (lipoprotein receptor-related protein 4) forms a complex with MuSK (Muscle Specific Kinase) and becomes activated by agrin (Kim *et al.*, 2008; Zhang *et al.*, 2008). The receptor tyrosine kinase induces a signalling cascade that affects the protein rapsyn (receptor-associated protein at the synapse) that mediates AChR aggregation. This pathway is conclusively demonstrated by knock-out mice for agrin, MuSK or rapsyn that all show impaired AChR clustering (Gautam *et al.*, 1999).

The role of transmembrane agrin in the brain is less well-understood. Agrin expression is developmentally regulated and mRNA levels peak around the first postnatal week except for the z8 splice variants which steady rise until adulthood (Li *et al.*, 1997). *In-situ* hybridisation showed high agrin levels in hippocampus and cortex (Cohen *et al.*, 1997). In brain homogenates, strong agrin expression is observed during late embryonic stages until around two weeks postnatal. Immunoelectron microscopy revealed a subcellular localisation at perisynaptic and extrasynaptic regions in the hippocampus (Stephan *et al.*, 2008).

The course of agrin expression in the CNS and the accumulation of agrin in the synaptic cleft of interneuronal synapses suggest an involvement in synaptogenesis or synapse maturation (Kroger & Schroder, 2002). The literature provides contradictive findings for this hypothesis. Studies on dissociated hippocampal neurons generated from agrin-deficient mice showed normal morphological development and synapse formation (Li *et al.*, 1999; Serpinskaya *et al.*, 1999). In contrast, agrin depletion by antisense oligonucleotides or lentivirus in wild-type neurons strongly reduced synaptic densities and alters dendritic development (Ferreira, 1999; Bose *et al.*, 2000; McCroskery *et al.*, 2009). Expression of functionally redundant molecules that compensate for the loss of agrin may explain the discrepancy between genetic and *in vitro* silencing of agrin. *In vivo* data of agrin-deficient mice confirmed a synaptic effect. These mice were prevented from perinatal death by transgenic expression of agrin in motor neurons and exhibit a reduction of presynaptic and postsynaptic elements in the cortex (Ksiazek *et al.*, 2007).

Agrin expression affects axonal and dendritic elongation during development of cultured hippocampal neurons (Mantych & Ferreira, 2001) and induces changes in axonal growth cones (Bergstrom *et al.*, 2007). Interestingly, agrin depletion in dendrites was twice as effective in reducing synapse density as suppression in axons (McCroskery *et al.*, 2009). This suggests an involvement of agrin in an important mechanism of postsynaptic development. Agrin promotes the formation of dendritic filopodia either by its overexpression or by cell surface clustering of endogenous agrin with antibodies (Annies *et al.*, 2006; McCroskery *et al.*, 2006; McCroskery *et al.*, 2009). Considering the important role of dendritic filopodia in spine formation, this function may account for the reported changes in synaptic densities. Further, it was reported that the extracellular N-

terminal part of agrin is responsible for the process-inducing properties of the protein (Annies *et al.*, 2006; McCroskery *et al.*, 2006). There is dissent between the two laboratories regarding the involvement of individual agrin domains in this process. Glycosaminoglycan chains as well as the seventh follistatin-like domain were reported to be the exclusive structure that induce filopodia formation (Lin *et al.*, 2010; Porten *et al.*, 2010). In addition it was demonstrated that agrin signalling to the cytoskeleton requires activity of Fyn (Src-family) and MAP kinases and include activation of the small GTPases Cdc42, Rac1, and RhoA (Ramseger *et al.*, 2009; Lin *et al.*, 2010).

1.5.4 Neurotrypsin

Neurotrypsin is a secreted trypsin-like serine protease. It is composed of a proline-rich basic domain, a kringle domain, three (rodents) or four (humans) scavenger receptor cysteine-rich (SRCR) domains, and the C-terminal located serine protease domain (Gschwend *et al.*, 1997). The protease is secreted as inactive precursor and requires proteolytic processing (Reif *et al.*, 2008). The zymogen activation site is located between noncatalytic part and protease domain and can be cleaved by proprotein convertases. Activated neurotrypsin maintain its structural integrity because the protease domain is connected to the rest of the protein by a disulphide bridge (Reif *et al.*, 2007).

Neurotrypsin is expressed in a wide range of tissues including lung, kidney, blood vessels and the nervous system (Gschwend *et al.*, 1997; Aimes *et al.*, 2003; Reif *et al.*, 2007). *In situ* hybridisation revealed a distinct pattern of neurotrypsin expression in the adult murine brain. High concentration of neurotrypsin mRNA was found in hippocampus, amygdala, cortex and motor neurons of the spinal cord (Gschwend *et al.*, 1997). In the hippocampus neurotrypsin was found in granule cells of the dentate gyrus, pyramidal cells of CA3 and CA1 and neurons of the subiculum. In the cortex the amount of positive neurons is prominent in layers V and VI and sparse in layers II and III. In layers I and IV neurotrypsin-expressing cells are absent. A follow-up study analysed the spatio-temporal expression of neurotrypsin in the brain of mice during pre- and postnatal development (see Fig. 8 E from Wolfer *et al.*, 2001). The results demonstrate a developmental regulation that peaks around the first postnatal week within the cerebral cortex. The same pattern is confirmed on the protein level by Western Blot of brain homogenates (Stephan *et al.*, 2008).

Neurotrypsin was found to be enriched in synaptosomes that were generated by subcellular fractionation of mouse brain tissue (Stephan *et al.*, 2008). The synaptic localisation was confirmed by immunoelectron microscopy and shows a presynaptic enrichment of neurotrypsin at excitatory synapses in human and mice (Molinari *et al.*, 2002; Stephan *et al.*, 2008). Gold particles were accumulated at vesicular structures close to the synaptic cleft and suggest a controlled release of the protease. Externalisation of neurotrypsin was analysed by live imaging of hippocampal neuron cultures. Neurotrypsin release is triggered by presynaptic activation (Frischknecht *et al.*, 2008; see also Fig. 9 C). The protein could be detected for several minutes at the place

of externalisation which indicates its interaction with an extracellular located structure. The study further revealed that also the synaptic localisation of the protein is regulated by neuronal activity. The activity-dependent recruitment and externalisation combined with the prominent expression in regions involved in higher brain functions, suggest an important role for neurotrypsin in cognitive processes.

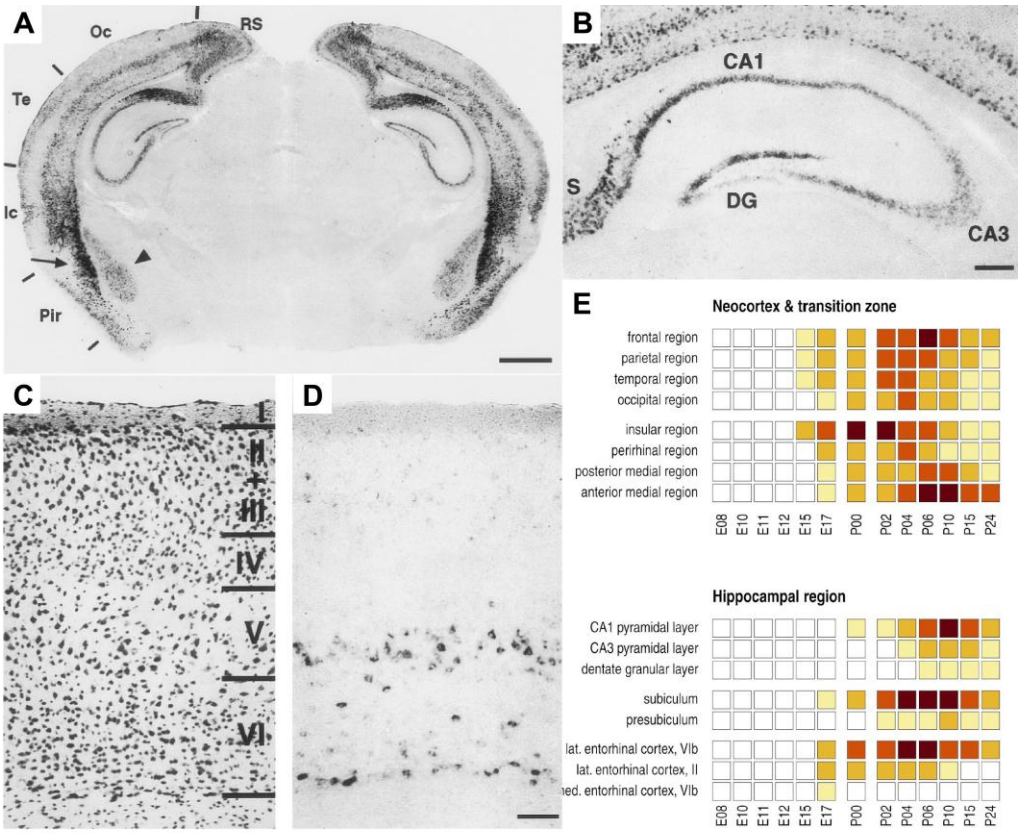

Figure 8. Neurotrypsin expression patterns revealed by in-situ hybridisation

(A) Brain section cut in dorsocaudal-rostroventral plane (~30° angle to the coronal plane) and incubated with neurotrypsin antisense riboprobe. Cells are labeled in distinct layers throughout the neocortex, the transition zones between iso- and allocortex (Ic and RS) and in the hippocampus. (B) Coronal section of the hippocampus shows neurotrypsin expression in the subiculum, pyramidal cells of CA1 and CA3, and in granule cells of the dentate gyrus. (C+D) Consecutive coronal sections of the parietal cortex, either stained with cresyl violet (C) or hybridised with neurotrypsin riboprobe. Comparison between (C) and (D) shows neurotrypsin expression in the lower half of layer V and in layer VI. Only sparse labelling is detected in layers II and III. (E) Time course of neurotrypin mRNA expression in the neocortex and hippocampus from early embryonic to late postnatal development. Intense colours represent high levels of neurotrypsin expression. Scale bars: A 1 mm; B 300 µm; D 100 µm (Figures from: Gschwend *et al.*, 1997; Wolfer *et al.*, 2001)

1.5.5 Interaction between neurotrypsin and agrin contribute to synaptic plasticity

Evidence for an outstanding role in brain function came from a study which analysed the consequences of a neurotrypsin loss-of-function mutation in a consanguineous family (Molinari *et al.*, 2002). Here, nonsyndromic autosomal recessive mental retardation was

attributed to a mutation in the neurotrypsin gene that resulted in the expression of a truncated protein lacking the protease domain. The affected individuals exhibit severe cognitive impairments with an IQ below 50, after prior normal psychomotor development during the first 18 month. The relatively late age of onset combined with the absence of major neurodevelopmental abnormalities suggests a role for neurotrypsin in adaptive synaptic function, such as reorganisation of neural networks by synaptic plasticity that is essential to establish higher cognitive functions (Molinari *et al.*, 2003). Further evidence for this implication comes from an evolutionary study in primates (Xu & Su, 2005). Considering higher cognitive function as an important selective advantage for primates it is conclusive that the neurotrypsin gene remained highly conserved during primate evolution.

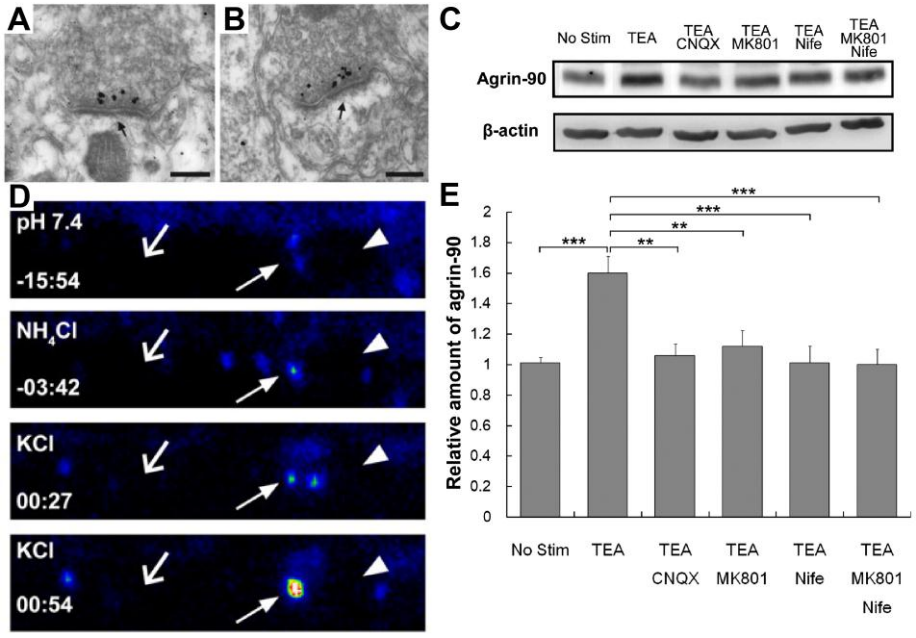

Figure 9. Activity-dependent externalisation of neurotrypsin from presynaptic terminals

(A+B) Subcellular localisation of neurotrypsin visualised by immuno-electron microscopy in the hippocampus (A) and cerebral cortex (B) of mice. (C) Overexpression of neurotrypsin-pHluorin in neuron culture. Storage of Nt-pH in synaptic vesicles with low pH reduces the fluorescence signal (-15:54). Perfusion with NH4Cl containing buffer temporarily increases vesicle pH and uncovers Nt-pH signal at a synaptic terminal (arrow at -03:42). Depolarisation by high extracellular KCl cause an increase in Nt-pH fluorescence induced by the externalisation of the protease from the presynaptic site. (D) Chemical LTP induced by TEA results in increased agrin cleavage demonstrated by Western blot detection of the agrin-90 fragment. Efficient agrin cleavage requires activity of AMPA, NMDA receptors, and L-type voltage-dependent Ca2+ channels. (E) Summary of the Western blot results. Scale bars: 0.2 µm (Figures from: Frischknecht *et al.*, 2008; Stephan *et al.*, 2008; Matsumoto-Miyai *et al.*, 2009)

At the present time, the extracellular matrix protein agrin is the only identified substrate of neurotrypsin. First evidence for a potential interaction between the two proteins came from investigations of the neuromuscular junction in neurotrypsin-overexpressing mice which strongly resembled the well-known phenotype of agrin-deficient mice (Gautam *et*

al., 1996; Reif *et al.*, 2007; Bolliger *et al.*, 2010). Ectopic expression of neurotrypsin and transmembrane agrin in cell lines allows the detection of three agrin fragments (agrin-110, agrin-90 and agrin-22 kDa) in the cell supernatant. Biochemical studies revealed the existence of two highly conserved cleavage sites, which are termed α- (PIER$^{\downarrow}$ASCY) and β-cleavage site (LVEK$^{\downarrow}$SVGD). Characteristic for both cleavage sites is a basic amino acid at the P1 and a strictly conserved Glu at the P2 position. Substrate recognition is further enhanced by surrounding amino acids and exosite interactions, together creating a substantial barrier for nonselective hydrolysis (Reif *et al.*, 2007). Beside *in vitro* digestion, neurotrypsin-mediated agrin cleavage was also demonstrated in wild-type and neurotrypsin overexpression mice (Stephan *et al.*, 2008; Matsumoto-Miyai *et al.*, 2009). Brain homogenates of neurotrypsin-deficient mice were absent for any of the agrin cleavage products indicating that agrin is exclusively processed by neurotrypsin. In the murine brain, agrin cleavage occurs preferentially at synapses and exhibits a strong preference for heavily glycanated agrin variants (Stephan *et al.*, 2008). Chemical stimulation on dissected whole hippocampi revealed that efficient *in vivo* cleavage requires not only presynaptic activity for neurotrypsin release but also simultaneous postsynaptic activation (Matsumoto-Miyai *et al.*, 2009). Blockage of both AMPA and NMDA receptors significantly reduced the amount of agrin-90 fragment (Fig 9 E). This indicates an involvement of LTP in the synaptic cleavage of agrin. Our current model assumes that neurotrypsin is released in the inactive form. The activity-dependent release of a postsynaptic located proprotein convertase would provide a mechanism for the extracellular activation of neurotrypsin after coincident activation of pre- and postsynapse.

The highly sophisticated regulation of agrin cleavage at the synapse suggests an important signalling function within the nervous system. Loss of neurotrypsin function is linked to severe mental retardation in humans and implies a role in adaptive cognitive processes. Thus, it was conclusive when demonstrated that the agrin-22 cleavage product promotes dendritic structural plasticity (Matsumoto-Miyai *et al.*, 2009). Induction of LTP is well-known to increase the number of dendritic filopodia (Bourne & Harris, 2011). However, this activity-dependent growth of filopodia is absent in neurotrypsin-deficient mice (Matsumoto-Miyai *et al.*, 2009). In these mice the formation of filopodia can be rescued by exogenous administration of agrin-22 which demonstrates that the interaction between neurotrypsin and agrin is crucial for this form of structural plasticity. The underlying signalling cascade has not been identified yet. A neuronal receptor for the C-terminal agrin fragment was first identified in cortical neuron cultures and activates CaMKII and MAP kinase pathways (Hoover *et al.*, 2003; Hilgenberg & Smith, 2004). Subsequent investigations revealed that agrin-22 binds to the α3 subunit of the Na^+/K^+-ATPase and inhibits its activity, resulting in membrane depolarisation and increased frequency of action potentials (Hilgenberg *et al.*, 2006). Additional studies are required to verify whether dendritic filopodia plasticity is mediated by the Na^+/K^+-ATPase or another so far unidentified receptor.

1.6 Aim of the study

The aim of this study was to reveal further functional properties of the neurotrypsin-agrin interaction and its relevance for synaptic plasticity. Experimentally, this was addressed by fluorescence light microscopy and to a lesser extent by biochemical approaches.

In search for a chemical LTP protocol to induce structural plasticity in organotypic slice cultures we discovered a muscarinic effect on dendritic spine structure. This plastic change occurs in all examined CA1 neurons of the hippocampus. Thus, we decided to study and characterise such strong effect of the cholinergic system and analyse its potential functional relevance

.

2. Material and Methods

2.1.1 Antibodies

The majority of antibodies used in this thesis were generated in the laboratory of Prof. Peter Sonderegger. Antigen was produced in *E.coli* or HEK293T cells and purified by affinity chromatography. Animal injection and serum collection was routinely performed by Dr. Beat Kunz.

Table 1. Primary antibodies

Epitope	Antibody Name	Species	Type	Dilution	Application	Provider
Agrin-C-22	R139	rabbit	serum		WB	PS laboratory
Agrin-C-90	R132 2nd boost	rabbit	serum	1:3000	WB	PS laboratory
Agrin-C-90	R132 aff.	rabbit	aff.purified	1:400	IC	PS laboratory
Agrin-N-110	R169 2nd boost	rabbit	serum	1:90	IP	PS laboratory
HA-tag	12CA5	mouse	IgG	1:5000	WB	Roche
HA-tag	anti-HA high affinity (3F10)	rat		1:2000	IC	Roche
Homer-1	Homer-1 (160002)	rabbit	Serum	1:500	IC	Synaptic Systems
MAP-2	MAB3418	mouse	IgG	1:1000	IC	Chemicon
MAP-2	NB-300-213	chicken	serum	1:5000	IC	Novus
mNt protease domain	G87 aff.	goat	aff.purified	1:3000	WB	PS laboratory
mNtfl (myeloma)	G93 3rd boost	goat	serum	1:2000	WB	PS laboratory
mNtfl (myeloma)	G93 4th boost	goat	serum	1:500	IC	PS laboratory
mNt	SZ177	rabbit	serum	1:200 1:1000	IC/WB	PS laboratory
Strep-Tag (WSHPQFEK)	Strep-MAB-classic	mouse	IgG	1:500	IC	IBA
Synaptophysine	MAB5258	mouse	IgG	1:1000	IC	Chemicon

Fluorescently labelled secondary antibodies (FITC, Cy3, Cy5 and DyLight649) were purchased from *Jackson ImmunoResearch Laboratories*. Horseradish peroxidase (HRP)-conjugated antibodies (*Sigma-Aldrich or Chemicon*) were used at following concentrations: α-goat, 1:40000; α-rabbit, 1:30000 and α-mouse, 1:20000.

2.1.2 Neurotrypsin protein

Neurotrypsin protein was produced in myeloma cells and then purified from the culture medium by several chromatography steps, as described previously (Reif *et al.*, 2008). For all performed experiments, I used neurotrypsin from the purification of 23.08.06 (0.07 mg/ml in PS7 / Rack 39 / Box R297, blue label) that has been generated by Reymond Reif.

2.2 Molecular biology techniques

2.2.1 Cloning

2.2.1.1 Primers

MARCKS-mRPF (pCMV-transfer)

mRFP-5'-BamHI_sens: 5'-AAGGATCCGCCTCCTCCGAGGAC-3' (P1)
mRFP-3'XhoI_antis: 5'-AACTCGAGTTAGGCGCCGGTGGA-3' (P2)

PCR-program: 1x (3', 95 °C), 10x (30'', 95 °C; 30'' 55 °C; 1', 72 °C), 15x (30'', 95 °C; 30'' 60 °C; 1', 72 °C) 1x (10' 72 °C)

agrin-eGFP (pCMV-transfer)

5'Bgl-agrin-eGFP: 5'-GCCAGATCTTCCGGAGGTAGCGGT-3' (P10)
3'agrin-eGFP-XbaI: 5'-TCTCTAGAAGCTTTACTTGTACAGCTC-3' (P11)

PCR-program: 1x (3', 95 °C), 30x (30'', 95 °C; 30'' 55 °C; 45'', 72 °C), 1x (10' 72 °C)

Mini-agrin-8-minus (pcDNA3.1(+))

dl172+: 5'-GAGCGCGGCCGCGGGAGACCATCCGTGCTTACCT-3'
dl173-: 5'- GCTCGCGGCCGCAAAAGGTGAGACATCTACTGC-3'

PCR-program: 1x (3', 95 °C), 30x (30'', 95 °C; 30'' 55 °C; 45'', 72 °C), 1x (10' 72 °C)

mNt-mCherry / mNt-S/A-mCherry (pcDNA3.1 (+))

5'-mNTBspElmCherry: 5'GATCCGGATCAGGTGTGAGCAAGGGCGAGGAGG-3'
3'Nt-Cherry-AflII: 5'-GACTTAAGACTTACTTGTACAGCTCGTCCATGC-3'

PCR-program: 1x (3', 95 °C), 30x (30'', 95 °C; 30'' 53 °C; 60'', 72 °C), 1x (10' 72 °C)

2.2.1.2 Generated DNA constructs

Table 2. Cloned expression constructs

Construct name	Vector backbone	Restriction sites	Notes
MARCKS-mRFP	pcDNA3.1(+)	EcoRI+XhoI (BamHI)	based on MARCKS-eGFP, MARCKS and mRFP are linked by a BamHI site
pcT-MARCKS-mRFP	pCMV-transfer	EcoRI+ApaI	virus vector based on pcDNA3.1 construct
mNt-S/A-pHluorin	pcDNA3.1(+)	Acc65I+NotI	subcloning from pcTransfer
pcT-rSN-HA-agrin-mRFP (y4z8)	pCMV-transfer	NotI+BspEI	based on pcDNA construct from Claudia Fortes, HA-containing region was inserted in pcT-agrin-mRFP
mNt-mCherry	pcDNA3.1(+)	BspEI+AflII	based on mNt-eGFP, eGFP was cut out and replaced by mCherry
mNt-S/A-mCherry	pcDNA3.1(+)	BspEI+AflII	based on mNt-S/A-eGFP, eGFP was cut out and replaced by mCherry
Mini-agrin-8-y0	pcDNA3.1(+)	NotI	as other Mini-agrins from D. Lüscher
pcT-agrin-eGFP (y4z8)	pCMV-transfer	NotI+XbaI (BglII)	based on pcT-agrin-mRFP, BglII links eGFP to agrin (there are 2 BglII sites inside the construct!)
pcT-agrin-D37-eGFP	pCMV-transfer	NotI+XbaI	uncleavable agrin, based on agrin-D37-eGFP
agrin-eGFP	pcDNA3.1(+)	NotI+XbaI	based on pcT-agrin-eGFP
agrin-D37-eGFP	pcDNA3.1(+)	NotI+XbaI (Bsu36I+BmgBI)	uncleavable agrin, α+β cleavage sites were cut out with Bsu36I+BmgBI from D37-construct and insert in agrin-eGFP

2.2.1.3 Restriction digest

Digests have been carried out using enzymes from *New England BioLabs* or *Promega*. It was generally assumed that 1 U of restriction enzyme cuts 1 µg DNA in one hour at 37°C. Samples were incubated for 60 – 90 minutes at 37°C.

Restriction Digest	
10 x enzyme buffer	2 µl
DNA	up to 1 µg
Enzyme	10 U
ddH_2O	to final 20 µl volume

2.2.1.4 Ligation

The digested pcDNA3.1 vector (*Invitrogen)* was dephosphorylated with 2 µl alkaline phosphatase (1-2 h). DNA was purified by gel extraction or PCR-purification kit (*Machinery-Nagel*). Purified vector and insert quantities were estimated on an agarose gel. Ligation was incubated for 30 min in a shaker at 16°C.

Ligation	
Vector : Insert ratio	1:3 - 1:10
TaKaRa ligation kit	5 µl
ddH_2O	to final 10 µl volume

2.2.1.5 Transformation of chemically competent *E.coli*

XL-1 blue or DH5-α cells were thawed on ice. 5 µl of ligation sample was given to 60 µl competent cell, following incubation for 15 min on ice. Cells were heat pulsed at 42°C for 45 sec and then placed on ice for 5 min. LB medium (10 g Bacto-Tryptone, 5 g Bactor-Yeast extract, 10 g NaCl in 1 l distilled H_2O) was added (100 µl) and samples were shake at 37°C for a minimum of 30 min. Cells were plated on antibiotic containing LB-agar plates (1 l LB, 15 g Bacto-Agar) and incubated over night at 37°C. When Zeomycin was used for selection, salt concentration in the LB medium was reduced to 5 g NaCl per litre.

2.2.1.6 Antibiotics for molecular biology

Following antibiotics (*Invitrogen*) were used according to the inserted plasmid: ampicillin (100 µg/ml; 60 µg/ml when combined with 30 µg/ml Zeomycin), Zeomycin (30 µg/ml), Kanamycin (25 µg/ml).

2.2.2 Genotyping of transgenic animals

2.2.2.1 Genomic DNA preparation & PCR reaction

DNA was extracted from tail or toe biopsies by alkaline lysis. Tissue was frozen at -20°C for ~1h and then incubated for 45 min in 300 µl lysis solution (25 mM NaOH, 0.2 mM Na_2-EDTA, pH 12) on a rocking platform at 96°C. Lysis was stopped by adding 300 µl neutralising agent (40 mM Tris-HCl, pH 5.0).

Genotyping PCR master mix was combined with 0.15 µl of forward and reverse primer (100 µM) for each sample, and finally with 1.5 µl of genomic DNA.

Genotyping PCR master mix	
10 x *Taq* buffer	3 µl
dNTPs (2.5 mM)	3 µl
$MgCl_2$ (25 mM)	1.8 µl
ddH_2O	20.25 µl
Taq polymerase	0.15 µl (5U/µl)

2.2.2.2 Primers for genotyping

L15 mice (De Paola et al., 2003)

GFPLfor: 5'-GCGGGGATCCGTGAGCAAGGGCGAGGAGC-3'
GFPLrev: 5'-GCGCCCTCGAGGCGGCCGCTTTACTTGTAC-3'
TAG83for: 5'-GGAGGAGAGAGACCCCGTGAAA-3'
TAG82back: 5'ACACGAAGTGACGCCCATCCGT-3'

PCR-program: 1x (3', 94 °C), 40x (45'', 95 °C; 45'' 62 °C; 60'', 72 °C), 1x (5' 72 °C)

Neurotrypsin-deficient mice (Reif et al., 2007)

mNT3F: 5'-GCTGACATAGCTTGCTTGCATTTG-3'
mNTendF: 5'-CTCCTGGAGTTTATACCAGAGTCC-3'
mNT2R: 5'-GTCAGGTTAGTCTCAGGAGATCTG-3'

PCR-program: 1x (3', 94 °C), 40x (45'', 95 °C; 45'' 62 °C; 60'', 72 °C), 1x (5' 72 °C)

Agrin-deficient mice (Lin et al., 2001)

Ex 31: 5'-CAGGGGATAGTTGAGAAG-3'
Ex 32 rev: 5'-GCTGGGATCTCATTGGTC-3'
77730: 5'-TCGCAAGTTCTAATTCCA-3'
30234: 5'-GGGCAGGGCTAACACCAA-3'

PCR-program: 1x (3', 94 °C), 40x (45'', 95 °C; 45'' 58 °C; 45'', 72 °C), 1x (5' 72 °C)

2.3 Adenovirus H5

Fluorescence-tagged proteins are essential for live imaging studies. The ectopic expression of such fusion proteins in primary neuron cultures is difficult because of a high resistance against conventional transfection techniques in this model system. We achieved sufficient expression by infecting neurons with recombinant adenovirus derived from human adenovirus 5 (Acc. Nr. M73260). This virus offers following experimental advantages over other systems: low toxicity, high transduction efficiency, acceptance of large DNA fragments (up to 8 kb), infection of replicating and post-mitotic cells, simple generation and amplification. In addition, the used virus is of low safety hazard because

its vector lacks the ER1 and ER3 regions that are responsible for DNA replication and cell lysis of infected cells. For that reason, the virus is considered as being replication deficient in conventional cells. Virus amplification requires a special packaging cell line (HEK-293wt), which expresses the viral transactivators of the ER1 region.

2.3.1 Generation, production and purification of adenovirus H5

Virus generation and production was based on the method previously described (Mohanty *et al.*, 2005). All tools for virus production were kindly provided by T. Trüb, Uni. Zurich. The constructs of interest were cloned into the pCMVtransfer vector. Functional viral vectors were achieved by Cre-mediated recombination of the transfer vector with a vector containing the adenovirus genome (pReceiver). Cre recombination was carried out in electroporated *E.coli* BM25.8 cells and resulted in the pAdlox vector which carries the construct of interest and required parts of the adenoviral genome. The vector had to be retransformed into DH5α bacteria to obtain clean vector DNA. Virus production was started by Lipofectamine2000 transfection of linearized pAdlox vector (PacI digested) in HEK 293wt cells. Transfected 6-well plates were analysed for fluorescence and then applied to successive rounds of virus enrichment. Virus titer was enriched in at least two rounds using cells on 10 cm dishes and two rounds on 15 cm dishes.

The virus production and purification varied in several aspects from the original protocol of T.Trüb. Large scale virus production was performed with 30 x 15 cm dishes. Strongly infected cells round up its shape and finally detach from the culture dish. We used this characteristic as an indicator for the stage of infection and harvested the virus when at least 50% of the cells were displaced. Virus containing cells were resuspended in collection buffer (10 mM Tris-HCl, 150 mM NaCl, 1 mM $MgCl_2$, pH8.1) before virus was released by three cycles of freezing and thawing, followed by a short sonication. Two centrifugation steps at 4500g and 8000 g (each for 15 min) were applied to remove most of the cellular debris. Remaining debris was excluded by filtering with a 0.22 µm PES filter (*Milipore*). The volume of the crude virus solution was reduced by tangential flow filtration (*Milipore*, Amicon Ultra-15 tubes, 100,000 MWCO). Viral particles were purified by a discontinuous CsCl density gradient centrifugation (1.25 g/cm^3 and 1.40 g/cm^3), which isolated the virus in a sharp opalescent band. The high density of viral particles is the most essential factor for virus stability in the -80°C. Therefore, special attention was paid to the collection of virus from the CsCl gradient to enable long term storage of the virus. Subsequently, the concentrated virus solution was dialysed using a “slide-a-lyzer cassette” (*Pierce*, 10,000 MWCO) to exclude the CsCl. Finally, glycerol was added to a final concentration of 10% and virus was snap frozen in liquid nitrogen.

2.3.2 Application of adenovirus

Dissociated neuron cultures were infected with 1-5 µl adenovirus prediluted in 100 µl of neurobasal (+B27, Glu, P/S) medium. Usually, cells were infected two days prior experimental procedures.

Table 3. Produced adenovirus

Adenovirus	Label	Source	Notes
ADAM10-eGFP	Adenovirus ADAM10-eGFP 09/06/11	newly generated	~20 µl aliquots
ADAM10-mCherry	Adenovirus ADAM10-mCherry 09/06/11	newly generated	~20 µl aliquots
agrin-eGFP	Adenovirus agrin-eGFP 10/11/10	newly generated	~15 µl aliquots
agrin-mRFP	Adenovirus rSN-agrin-mRFP 13/02/08	cloned and first generation by A. Stephan	~25 µl aliquots, produced by infection with old virus
agrin-D37-eGFP	Adenovirus agrin-D37-eGFP 10/11/10	newly generated	~15 µl aliquots
agrin-D37-mRFP	Adenovirus D37 rSN-agrin-mRFP (D37) 18/03/08	cloned and first generation by A. Stephan	~25 µl aliquots, produced by infection with old virus
APP-mCherry	Adenovirus APP-mCherry 11/02/11	cloned by M. Steuble	~28 µl aliquots
Bace-eGFP	Adenovirus Bace-eGFP 11/02/11	cloned by M. Steuble	~20 µl aliquots
rSN-HA-agrin-mRFP	Adenovirus HA-agrin-mRFP 15/09/09	newly generated	~15 µl aliquots, HA-tag is inserted extracellular following the TM-domain
MARCKS-eGFP	Adenovirus M9_2 MARCKS-eGFP 18/03/08	cloned and first generation by A. Stephan	~25 µl aliquots
	Adenovirus MARCKS-eGFP 17/07/08		
MARCKS-mRFP	Adenovirus MARCKS-mRFP 17/07/08	newly generated	~25 µl aliquots
mNt-eGFP	Adenovirus mNt Neurotrypsin-eGFP 09/04/08	cloned and first generation by M. Irschara	~25 µl aliquots
mNt-S/A-eGFP	Adenovirus S/A mNt (S/A)-eGFP 09/04/08	cloned and first generation by M. Irschara	~25 µl aliquots
mNt-pHluorin	AV mNt-pHluorin-eGFP (ecliptic) 07/05/08	cloned and first generation by M. Irschara	~25 µl aliquots
mNt-S/A-pHluorin	AV mNt-(S/A)-pHluorin-eGFP 29/05/08	cloned and first generation by M. Irschara	~25 µl aliquots
eGFP-Cst1 (N81)	Adenovirus m-eGFP-Cst1 16/06/09	cloned by M. Steuble	~20 µl aliquots
mRFP-Cst1 (N72)	Adenovirus mRFP-Cst1 16/06/09	cloned by M. Steuble	~20 µl aliquots

2.4 Cell culture techniques

2.4.1 Culturing of immortal cell lines

2.4.1.1 Cos7 and HEK 293T

Both cell lines were cultured in DMEM (*Gibco* 41966; 4.5 g/l glucose, 5 mM glutamine, 1mM sodium pyruvate) supplemented with 10% fetal calf serum (FCS). Cells were plated on uncoated cell culture dishes or PLL-coated coverslips and kept at 37°C in a humidified incubator containing 10% CO_2. Cellular density was controlled by regular passaging (1/20) into fresh culture dishes, using trypsin to detach cells.

2.4.1.2 Transient transfections with Lipofectamine 2000

Transfections were carried out according to the manufacturer's protocol (*Invitrogen*).

	Immunocytochemistry	Western blot
Culture vessel	12-well plate (1 ml)	6-well plate (2ml)
Cell density	20-30% confluent	90% confluent
DNA	1 µg	2 µg
Lipofectamine	2 µl	6 µl

2.4.2 Preparation of dissociated neuron cultures

2.4.2.1 Low density cultures (for immunocytochemistry)

Cultures of dissociated hippocampal neurons were prepared from embryonic day 18 NMRI mice based upon the method developed by G. Banker (Kaech & Banker, 2006). Briefly, hippocampi were dissected, trypsinized for 7 min and then titurated with a 1 ml *Eppendorf* tip. Cells were plated on poly-L-lysine-coated (0.5 mg/ml) glass coverslips (~4,000 cells/cm^2) and cultured in neurobasal medium supplemented with B27, 5 mM glutamine, and antibiotics (penicillin/streptomycin), above a monolayer of astrocytes. Cells were maintained in 12-well plates in a humidified incubator with 5% CO_2 at 37°C. Two days after plating, cytosine arabinoside (AraC) was added to a final concentration of 15 µM to prevent proliferation of astrocytes. All substances for cell culturing were purchased from *Invitrogen*.

2.4.2.2 High density cultures (for Western blotting)

Cultures were prepared from whole cortices of E18 NMRI mice. Cells were dissociated as described above and passed through a 40 µm nylon cell strainer (Falcon) to remove clumps and tissue debris. Cells were plated at a density of 100,000-150,000 cells/cm^2 on poly-L-lysine-coated 6- or 12-well plates (*Nunc*). High density cultures were maintained under the same culturing conditions and media as for low density cultures.

2.4.2.3 Agrin knock-out cultures

Neuron cultures from genetically modified mice are usually generated from P0 mice because it enables the genotyping straight after birth which simplifies the selection for the right genotype. However, this is not possible for agrin-deficient mice (Lin *et al.*, 2001) because they die perinatally due to a breathing defect. For that reason, preselecting mice for agrin knock-out cultures is not possible and cultures had to be generated from individual E18 embryos, while the genotype was verified afterwards. Usually, we prepared cultures from 6 to 8 animals in order to obtain at least one knock-out culture.

2.4.3 Generation of organotypic slice cultures

Cultures were generated according to the method established by Beat Gähwiler (Gahwiler, 1981). Brains of 6 day old L15 mice were explanted and hippocampi dissected. Slices were cut to a thickness of 300-400 µm using a McIllwain tissue chopper (*Mickle Laboratory Engineering Co*). Individual cultures are placed in a drop of chicken plasma on 12 x 24 mm glass coverslips coated with PLL. The tissue is kept in place by another drop of thrombin solution (0.2 mg/ml) which induces coagulation of the plasma. Coverslips are placed in plastic tubes (*Falcon* No. 3033) and fed with 1 ml of culture medium (25% horse serum, 50% basal medium (Eagle) and 25% Hanks BSS supplemented with 6.5 mg/ml glucose). Cultures were maintained in a roller drum incubator at 37°C for a minimum of three weeks before imaging. In weekly intervals old medium was replaced by 1 ml of fresh medium. Organotypic slice cultures were kindly prepared by Dubravka Göckeritz-Dujmovic from the Brain Research Institute, Uni. Zurich.

2.5 Protein analysis

2.5.1 “Wessel-Fluegge” protein precipitation

This protocol was used to concentrate protein samples for Western blotting (Wessel & Flugge, 1984). Usually, 300 µl samples were combined with 900 µl methanol and 150 µl chloroform and vortexed. 600 µl ddH_2O were added and then centrifuged at RT for 5 min at 16000g. Resulting upper layer was removed and sample was mixed with 900 µl methanol. During a second centrifugation step all proteins were pelleted. All liquid was removed and pellet was resolved in 1x Laemli buffer (15.6 mM Tris/HCl, 2.5% glycerine, 0.5% SDS, 0.3 mg/ml bromophenol blue, 250 mM DTT, pH 6.8).

2.5.2 Immunoblotting

Proteins were separate according to their molecular weight by sodium dodecyl sulphate polyacrylamide gel electrophoresis (SDS-PAGE). Two different gel systems were used: Self-made gels were prepared using a *Bio-Rad* gel system. Stacking and resolving gels were prepared as described in “Molecular Cloning - A Laboratory Manual”, A8.40-8.45 (Sambrook & Russell, 2001). The gel running buffer was composed of 25 mM Tris, 192

mM glycine and 0.1% SDS and gels were run at constant voltage of 90 V. Alternatively, pre-cast NuPAGE Novex 4-12% Bis-Tris gels (*Invitrogen*) were used when a wide range of protein sizes had to be separated. Gels were run in MOPS buffer (*Invitrogen*) at 120-200 V using a water cooled chamber.

Proteins from both gel types were transferred to polyvinylidene difluoride (PVDF) membranes (*Milipore*) by Western blotting. PVDF membranes were activated by incubation in methanol (1 min) and then assembled in a semi-dry blotter (Trans-Blo SD Cell, *Bio-Rad*), to a stack consisting of filter paper, membrane, gel and filter paper (anode beneath). Filter papers were soaked in blotting buffer (25 mM Tris, 192 mM glycine, 20% (v/v) methanol) before assembly. Proteins were transferred during 1 h at a voltage of 20 V. Subsequently, the membrane was placed in methanol and then air-dried for at least 30 min to block unspecific binding sites. That followed the immunological detection of the proteins of interest. Primary antibodies were applied for 2 h at RT, or over-night at 4°C in TBST (10 mM Tris/HCl, 150 mM NaCl, pH 8.0, 0.1% Tween20) supplemented with 2.5% blocking reagent (*Roche*). HRP-coupled secondary antibodies were applied for 45 min at RT. Blots were developed using ChemiGlow (*Alpha Innotech*) and the luminescence signals were measured in the Luminescent Image Analyzer LAS-3000 (*Fujifilm*). The digital images of the Western blot results were quantified with AIDA software 3.52 (*Raytest*).

2.5.3 Immunoprecipitation (IP) of neurotrypsin

Lipofectamine transfection of HEK 293 cells was carried out 48 hours prior the IP experiment. Cell culture medium was replaced by prewarmed DMEM (FCS-free), 6 hours after application of the transfection reagent. Supernatant was supplemented with Tris/HCl (final concentration 50 mM) to adjust pH 7.4 and then centrifuged for 10 min at 800 rpm to remove floating cells and subsequently for 10 min at 4000g to remove cellular debris. 450 µl supernatant were transferred to small *Eppendorf* tubes (0.5 ml), mixed with 5 µl R169 AB (2°boost) and incubated for 2h fixed to a rotator at 4°C. Sepharose-G beads (*GE Healthcare*) were washed 5 times with 1.0 ml IP-buffer (150 mM NaCl, 5 mM EDTA, 1 mM Na_3VO_4, 5 mM NaF in 50 mM Tris, pH 7.4) and then aliquoted (15-20 µl) to 0.5 ml *Eppendorf* “Protein LoBind Tubes”. Supernatant was combined with beads and incubated for 1h rotating at 4°C. Then supernatant was removed and beads were washed 3 times with IP-buffer to remove non-bound agrin protein. Beads were resuspended in 450 µl IP-buffer before purified freshly thawed neurotrypsin was added (~500 ng) and incubated for 1h. Subsequently, supernatant was collected and combined with 4x Lämeli buffer. Beads were washed once with IP-buffer. Then the complete supernatant was removed by especially thin pipette tips (*Sorenson BioScience* 17310) and beads were boiled in 1x Lämeli buffer (70 µl). The amount of bound neurotrypsin was analysed by Western Blot using G87 antibody.

2.5.4 Agrin uptake assay (Western blotting analysis)

High density cortical neuron cultures were plated on PLL coated 6-well dishes and infected at DIV 3 with adenovirus rSN-HA-agrin-mRFP. At DIV 5 neurons dedicated for lysosomal blockage were incubated with 10 µM Leupeptin and 5 µM Pepstatin A for 1 h. Then 50 µl neurotrypsin (2.2 µM) was added and incubated for 30 min. Subsequently, supernatant was collected and wells of control and neurotrypsin-only samples were lysed with 300 µl lysate buffer (20 mM Tris/HCl, 150 mM NaCl, 5 mM EDTA, 1% Triton X-100, pH 7.5, supplemented with 1:100 P-8340 protease inhibitors (*Sigma-Aldrich*)). Trypsin samples were incubated (30 sec) with 1x trypsin solution (*Invitrogen*) and then washed with PBS + 5 mM EDTA before cell lysis. All samples (300 µl) were precipitated by the Wessel Flügge protocol and dissolved in 100 µl 1x Laemli buffer.

2.6 Microscopy & data analysis

2.6.1 Immunocytochemistry

2.6.1.1 Conventional stainings of fixed cells

Cells were fixed on coverslips by application of 4% paraformaldehyde in PBS, pH 7.4 for 7 min at room temperature. Coverslips were incubated for 1 h in blocking solution (10% FCS, 0.1% glycine, 0.05 NaN3 in PBS). Primary antibodies were applied in PBS in the presence of 0.1% saponin that permeabilised the cell membrane. Primary antibodies were usually incubated at room temperature for two hours. Fluorescently labeled secondary antibodies were applied after extensive washing with PBS. Secondary antibodies were centrifuged at maximum speed to exclude precipitates and then incubated for one hour at room temperature.

Coverslips were mounted in vectashield solution (Vector Laboratories) and sealed with nail polish.

2.6.1.2 Live staining for neurotrypsin binding study

All following steps until fixation of the cells were performed in the cold-room at 4°C. Cos-7 cells were washed in Tyrod's buffer (119 mM NaCl, 2.5 mM KCl, 2 mM $CaCl_2$, 2 mM $MgCl_2$, 30 mM glucose, 25 mM HEPES, pH 7.4) to remove serum and dead cells. Afterwards, they were placed upside down on a metal plate that was covered with parafilm. Primary antibodies for neurotrypsin (G93) and agrin (either R132 aff., for full length agrin or anti Strep-tag, for Mini-agrin) were applied in 80 µl of Tyrod's buffer for each coverslip. After two hours of incubation, coverslips were washed 3x in PBS and then transferred in 12-well plates containing 4% paraformaldehyde. Plates were moved to RT and incubated, while rewarming, for 10 min. Coverslips were dislocated into blocking solution for 30 min. Secondary antibodies were applied and staining was finished following the same protocol as for conventional stainings (see chapter 2.6.1.1).

2.6.1.3 Live staining for agrin uptake assay

Low density dissociated neuron cultures were infected with adenovirus rSN-HA-agrin-mRFP at DIV 3 and cultured for additional 36 h. The experiment started with blockage of lysosomes by 1h incubation with 10 µM Leupeptin and 5 µM Pepstatin A. Coverslips were then placed upside down on an ice cold parafilm coated metal plate. Neurons were covered with 100 µl neurobasal medium containing 10 µl neurotrypsin (2.2 µM) and 0.5 µl α-HA antibody (3F10) and remained on ice for 30 min. Coverslips were repositioned in the 12-well plate and put for 45 min in the incubator. That followed fixation in 4% PFA and immunocytochemical detection of the α-HA antibody.

2.6.2 Light Microscopy

2.6.2.1 Live imaging of Cos-7 cells

Cells were plated on 18mm coverslips and transfected or infected one day prior imaging, as described before. Coverslips were transferred into a Ludin chamber (*Live Imaging Services*) and placed under the microscope (*Olympus* IX81) that was surrounded by a Plexiglas box to maintain a stable atmosphere. Cells were perfused with Tyrod's buffer (119 mM NaCl, 2.5 mM KCl, 2 mM CaCl2, 2 mM MgCl2, 30 mM glucose, 25 mM HEPES, pH 7.4) in regular intervals. Dual channel imaging for GFP/mRFP was enabled by a Lambda DG-4 light source (*Sutter Instrument*) in combination with a beam splitter and a custom made "Flickerbox" (*Live Imaging Services*). Images were taken with a SensiCAM QE camera (*Cooke Corporation*; 1376x1040 pixels) controlled by Metamorph Imaging software (*Molecular Devices*).

2.6.2.2 Live imaging of organotypic slice cultures

Hippocampal slice cultures were analysed in a custom-made observation chamber with a volume of ~150 µl. Imaging was performed on an inverted confocal microscope (SP5 *Leica Microsystem*) equipped with a temperature control system (Cube and Box, *Live Imaging Services*) set at 37°C. The cultures were superperfused continuously at a rate of 330 µl/min with artificial cerebrospinal fluid (ACSF, 120 mM NaCl, 3 mM KCl, 1.2 mM NaH_2PO4, 23 mM $NaHCO_3$, 11 mM glucose, 2.4 mM $CaCl_2$, 1.2 mM $MgCl_2$) and continuously oxygenated with oxycarbon.

Time-lapse confocal stacks were acquired with a 63 × objective (NA 1.3) and an additional 6x or 8x confocal scanner zoom (*Leica*). We used an Argon laser 488 nm set to minimum power (~ 6 µW) to minimize phototoxicity and with voxel dimensions of 46 x 46 x 200 nm. To increase the number of dendritic spines imaged per experiment, two to four dendritic segments were recorded consecutively for each time series (*Leica* "Live Data Mode"). In general, we observed only secondary or tertiary dendrites of CA1 pyramidal cells.

2.6.3 Image processing & analysis

2.6.3.1 Deconvolution

Three dimensional image stacks of confocal or widefield data were generally deconvolved to improve image resolution and signal to noise ratio. We used the Huygens Remote Manager (Huygens v1.2.3, *Scientific Volume Imaging*) provided by the "Center for Microscopy and Image Analysis" (ZMB, Zurich). Settings were applied according to the quality of data. Images were subsequently analysed with one of the following programs: Imaris 7 (*Bitplane*), Leica LAS AF Lite (*Leica*), Metamorph (*Molecular Devices*) or ImageJ (http://rsb.info.nih.gov/ij/).

2.6.3.2 Quantification of neurotrypsin bound to cell surface agrin

Cos-7 cells were Lipofectamine transfected with Nt-S/A-eGFP and either a Mini-agrin or full-length agrin construct. Two days after transfection "live stainings" were performed as described before. Confocal stacks with 5 sections (0.13 µm step size) were acquired in sequential mode at a Leica-SP5 microscope for the eGFP, cy3 and cy5 channels. All images were deconvolved to improve signal quality. Image analysis was performed with Imaris. The agrin signal was quantified by transformation in an Imaris surface object and read out of the intensity sum values. Neurotrypsin signals were counted in the same way. To ensure that only cell surface Nt signals were counted I additionally applied a filter that restricted the analysis to Nt signals that were in close proximity to the agrin signal. Values for Nt were normalised against the respective agrin surface to consider cell size differences. Each experiment contained data of at least 20 cells for a single agrin construct. The complete image acquisition as well as data analysis was performed blindly. Statistical significance was analysed using the 2-sample Kolmogorov-Smirnov test for non-parametrical distributed values and inhomogeneous variances. Results were Bonferroni corrected to enable multiple comparisons.

2.6.3.3 Automated synapse quantification in dissociated neuron cultures

The technique for synapse quantification is subject of a detailed method paper (Schätzle et al., 2011 submitted to J. Neuroscience Methods). Briefly, neuron cultures were immunological stained for synaptophysine, Homer-1 and MAP-2 as described in 2.6.1.1. The protocol for the synapse quantification is based on Imaris 7 software (*Bitplane*). In collaboration with Dr. Urs Ziegler (Center for Microscopy and Image Analysis, Zurich) we programmed a Matlab (*MathWorks*) script which sequentially executes all Imaris functions required for synapse quantification. The routine started with the identification of pre- and postsynaptic elements. To identify these synaptic structures, the Imaris spot function localised fluorescent objects based on size and fluorescence intensity via a threshold-based segmentation algorithm. The function ran for the synaptophysin and Homer-1 channel, and resulted in a detection of green and red spots which represent pre- and postsynaptic structures, plus background signals (Fig.10 F). The appearance of high background signals is a general feature of dissociated neuron cultures. In order to

prevent quantification of false positive background signals, we defined that pre- and postsynaptic elements had to be localised close to the dendrite, which was calculated from the MAP-2 signal using an isosurface. All previously defined spots were then tested for their spatial proximity with that isosurface. In this way only spots located within the defined distance to the dendrite were counted as synaptic structures. All quantifications included in this thesis used an inclusion limit of 2 µm. Spots which exceed the limiting value were labelled by a colour shift (cyan/magenta, see also Fig.10 G) and were excluded from the final result.

Pre- and postsynaptic elements have to be localised in spatial proximity to form a functional synapse. Therefore, the synapse quantification algorithm defined a synapse as a pair of spots, one pre- and the other postsynaptic, that were located within a certain distance. The dimension of this inclusion window was the most critical parameter of this quantification method. I tested several distances and found that 700 nm produced results that were in accordance with manually performed quantifications. Spot pairs that fulfil the criteria for a synapse were indicated by a yellow spot positioned between the associated pre- and postsynaptic signals (Fig.10 H).

Additionally, we implemented a graphical user interface, which enables the automated quantification of a series of images. This allowed me to process high numbers of images with little time requirements. All results were finally exported automatically into an excel sheet. The MAP-2 signal served as a reference for dendritic volume and had been used to normalise the synapse number of each image. Therefore, the presented numbers for synaptic elements and synapses represent relative values in relation to the dendritic volume.

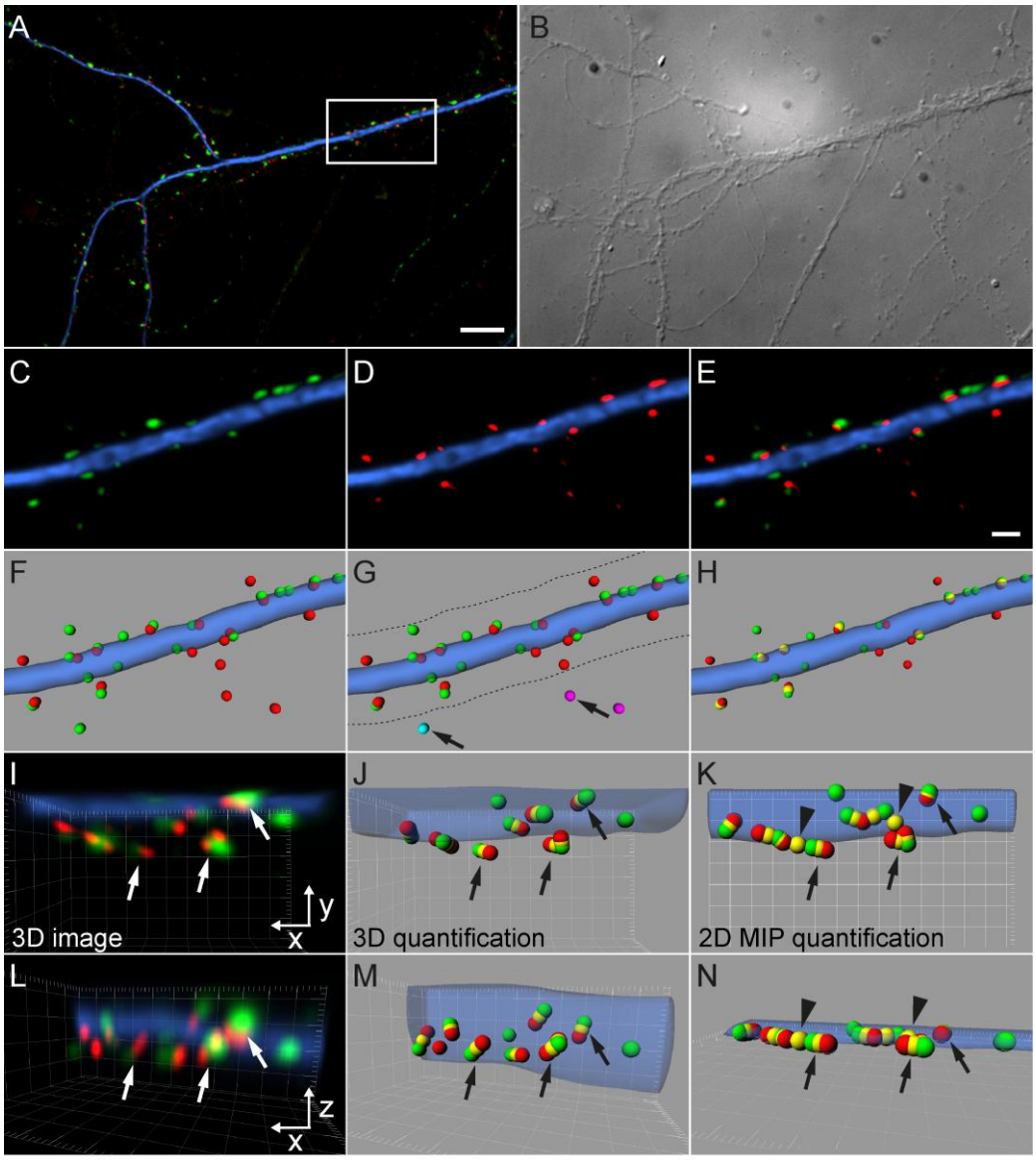

Figure 10. Synapse quantification of dissociated neuron cultures visualised by immunocytochemistry

(A) Example of a dendrite stained with MAP-2 (blue) and synaptic markers. (B) Differential interference contrast (DIC) image of the same section. (C) Presynaptic terminals are labelled in green by synaptophysin; (D) postsynaptic structures in red by Homer-1 antibodies. (E) Merge of both channels indicates synapses at the overlap between green and red labelling. (F) Fluorescent signals of the 3D image stacks have to be integrated into Imaris in order to perform automated synapse quantification. The dendrite is represented by an Imaris "isosurface" generated from the dendritic signal. Pre- and postsynaptic structures are defined by the Imaris "spot function" based on size and fluorescence intensity. (G) Background signals (spots in cyan and magenta) are excluded from the quantification by their distance to the dendritic surface. (H) Synapses are identified by the close proximity of pre- and postsynaptic elements and highlighted by a yellow spot.

A three dimensional synapse analysis results in a more precise quantification compared to maximum intensity projection. (I) Fluorescent signals of a dendritic segment with high synaptic density. Arrows point on exemplary synapses (J) Automated synapse quantification of that region with regard to 3D information. (K) A conversion of the same dataset to a maximum intensity projection and subsequent quantification with the same settings resulted in the identification of artificial synapses (arrowheads) due to missing spatial information. (L), (M) and (N) Lateral projection of the corresponding images (I), (J) and (K). Scale bar (A) = 10µm; (E) = 2µm

2.6.3.4 Spine head filopodia quantification in organotypic slice cultures

Dendrites are very heterogeneous in their content of spines. Therefore, we selected dendrites with a similar spine density to avoid interference in the results from changes in spine densities. We established two quantification methods to demonstrate the quality of spine head changes that follows muscarinic receptor stimulation. The first approach consisted in identifying all dendritic spines in the confocal stacks and then, compared the changes in spine heads which occurred between two time points, first without stimulation and second during muscarinic receptor stimulation. Spine head filopodia (SHF) were identified as new protrusions from the head of the spines. Additionally, we quantified changes in shape, number of spines, and filopodia formation. However, these changes were not significantly different in any condition. Thus, the data contains only percentage changes of SHF. The second approach was designed to demonstrate the structural change during MCh application in more detail. Single spine heads were identified and the sphericity of each spine head volume was quantified over different time points on the time-lapse confocal stack. These measurements were done mainly on mushroom spines because their bigger sizes allowed a clear observation of the changes. The analysis for both approaches was done in Imaris.

3. Results

3.1 Visualisation of agrin cleavage by live imaging

The cleavage of agrin by neurotrypsin (Nt) has been the topic of several recent publications of our laboratory. Beside of *in vitro* results (Reif *et al.*, 2007; Reif *et al.*, 2008) we could further show that the neurotrypsin mediated cleavage of agrin takes place at the synapse (Stephan *et al.*, 2008). However, this study was exclusively based on Western blot data and did not provide information about the spatial restriction of neurotrypsin activity. In order to address this particular question we analysed the neurotrypsin-agrin interaction using light microscopy.

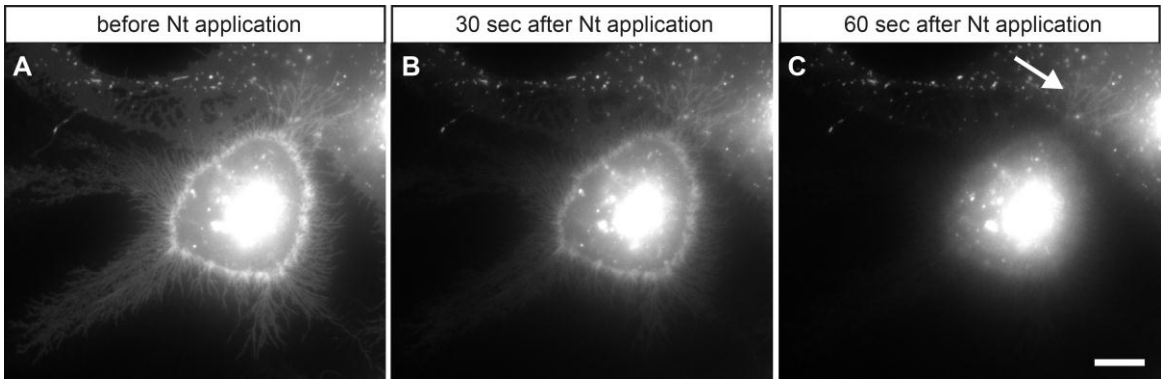

Figure 11. Cleavage of agrin by neurotrypsin at the plasma membrane of living cells

(A) Cos-7 cell overexpressing transmembrane agrin-mRFP. The cell shows typical agrin morphology with many filopodia-like extensions. (B) Brief application of purified neurotrypsin protein by a puff application system clearly reduced the fluorescence at the cell surface after 30 seconds. (C) After 60 seconds neurotrypsin depleted the complete agrin signal from the plasma membrane. Some filopodia remained positive for agrin-mRFP (arrow) because they were covered by a neighbouring cell and therefore not accessible for Nt application. This and the stable intracellular signals indicate that the reduction of membrane fluorescence was based on extracellular proteolytic activity and not on photobleaching of the signals. Scale bar: 10 µm.

I performed live fluorescent microscopy on Cos-7 cells to determine the resolution and viability of the method. Cells were transfected with a transmembrane agrin construct that carries a monomeric red fluorescent protein (mRFP) tag at the C-terminus. Purified neurotrypsin protein was applied on single cells using a thin glass pipette (tip diameter ~1µm) connected to a puff application system. Proteolytic cleavage at the α- and β-site within the agrin molecule resulted in the loss of fluorescence signal from the plasma

membrane (Fig. 11). Intracellular vesicular agrin signals were not affected by neurotrypsin application (negative control) and ensured that loss of the membrane signal is not due to bleaching of the mRFP protein.

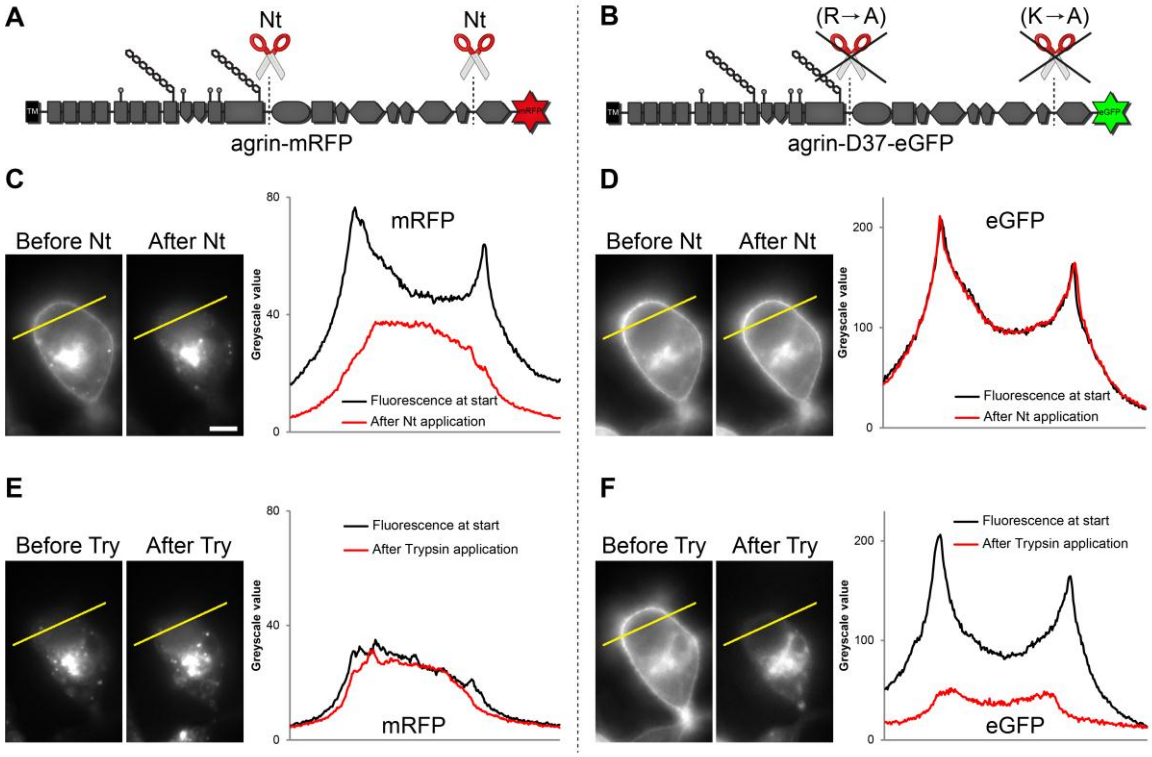

Figure 12. Visualisation of agrin cleavage from the surface of living Cos-7 cells

(A) Schematic drawing of transmembrane agrin-mRFP and (B) of uncleavable agrin-D37-eGFP, which contains mutations in the neurotrypsin cleavage site (α-site: Arg to Ala; β-site: Lys to Ala). (C-F) Widefield images of the same Cos-7 cell co-expressing both agrin constructs. Local applications of neurotrypsin and trypsin were performed by a puff application system. (C) Fluorescence images of agrin-mRFP before and after application of neurotrypsin. The diagram represents the measured greyscale values of a line scan (along the yellow line). Membrane signals were clearly reduced due to proteolytic cleavage of agrin and release of mRFP from the cell surface. (D) Neurotrypsin application did not affect the signal intensity of uncleavable agrin-D37-eGFP, indicating the high substrate specificity of the neurotrypsin protease. (E) A second application with trypsin did not show an additional effect on agrin-mRFP signal. (F) Fluorescence signal of uncleavable agrin-D37-eGFP was completely erased by trypsin application and demonstrated the extracellular localisation of the protein. Scale: 5 µm.

Next, I co-transfected agrin-mRFP with the agrin variant D37-eGFP which contains inactivated cleavage sites (by mutations in the P1 positions from basic amino acids to alanine) and hence cannot be processed by neurotrypsin. This approach allowed a quantification of the agrin cleavage signal. Both fluorophors were imaged in parallel and could be clearly separated from each other by a beam splitter. Fluorescent membrane signals were quantified by line scan (yellow lines in Fig. 12). Application of neurotrypsin slowly reduced the membrane signal of agrin-mRFP, while at the same time the fluorescence intensity of uncleavable agrin-D37-eGFP remained unaffected. The depletion of cell surface agrin-mRFP was usually completed within 1-2 min and could be

significantly accelerated by additional applications of Nt. As a positive control I applied trypsin that nonspecifically cleaves all cell surface proteins. Agrin-D37-eGFP fluorescence immediately disappeared after trypsin treatment. The faster response to trypsin compared to neurotrypsin was based on two factors: Trypsin was higher concentrated and additionally degraded GFP protein, while neurotrypsin only released the fluorescent protein from the cell surface.

These results demonstrated that it is generally possible to visualise neurotrypsin-mediated agrin cleavage by live fluorescence microscopy. In order to study the operation radius of endogenous neurotrypsin, released from synaptic contacts, I collaborated with Dr. José María Mateos, Biochemistry Institute, Uni. Zurich to transfer this technique to organotypic slice cultures. We designed and preformed two approaches, biolistic gene gun transfection and adenoviral infection to overexpress agrin-mRFP in hippocampal slice cultures. Both methods failed for different reasons. First, biolistic gene gun transfection resulted in insufficient expression levels and did not allow the localisation of agrin at the plasma membrane of transfected neurons. Second, adenoviral infection almost entirely targeted astrocytes, but not neurons, and was therefore not suitable for this project. As an alternative approach our laboratory planned to generate mice which express fluorescently tagged transmembrane agrin. However, this project could not be finished up to now.

3.2 Fate of N-terminal agrin after cleavage by neurotrypsin

3.2.1 Uptake of N-terminal agrin after proteolytic processing by Nt?

Cleavage of transmembrane agrin by neurotrypsin releases two fragments from the cell surface. While there are several functions published for the detached agrin-90 (Gesemann *et al.*, 1996) and agrin-22 fragments (Hilgenberg *et al.*, 2006; Matsumoto-Miyai *et al.*, 2009), the role of the remaining N-terminal agrin moiety has not been identified yet. The N-terminal part was linked to the formation of dendritic filopodia (Annies *et al.*, 2006; McCroskery *et al.*, 2006) and it could be shown that this fragment binds several growth factors e.g. FGF-2, thrombospondin, and TGF-β (Cotman *et al.*, 1999; Burgess *et al.*, 2002; Banyai *et al.*, 2010). These findings positioned N-terminal agrin as a potential regulator of extracellular cell signalling.

In the brain, agrin is predominantly expressed in the transmembrane splice variant (Burgess *et al.*, 1999). The transmembrane anchoring of agrin enables a tight cellular control on the spatial and temporal localisation of the molecule. We hypothesised that agrin cleavage by neurotrypsin might trigger a cellular process that finally removes N-terminal agrin from the cell surface. This could occur either by targeted endocytosis or proteolytic ectodomain shedding. The following experiment was designed to demonstrate the uptake of N-terminal agrin following neurotrypsin-mediated cleavage of the full-length protein.

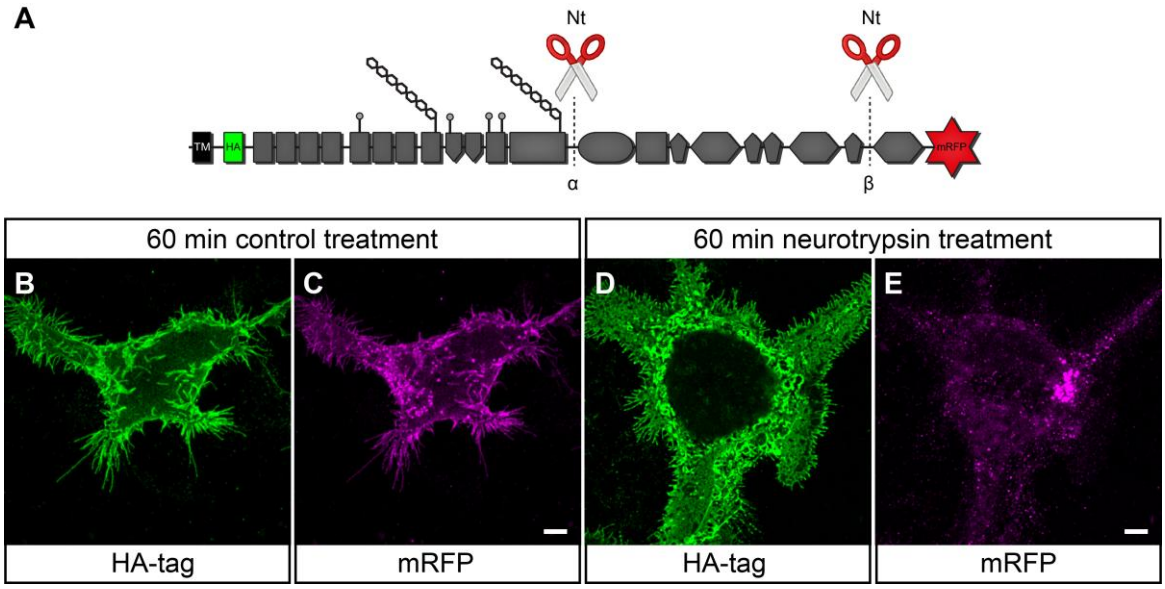

Figure 13. The rSN-HA-agrin-mRFP construct is suitable for an agrin uptake assay

(A) Full-length agrin can be identified by a C-terminal located mRFP protein. Neurotrypsin cleaves agrin at the α- and β-site and release the mRFP protein from its transmembrane anchorage. The N-terminal agrin fragment can be detected by a HA-tag which is inserted between the transmembrane and the first follistatin domain. As a proof of concept Cos-7 cells were transfected with this construct and treated with neurotrypsin or control buffer. (B+C) Agrin was well detectable by both labelling approaches using confocal microscopy. Incubation with control solution did not alter mRFP signal compared to the HA-signal. (D) N-terminal agrin can still be visualised by the HA-tag after incubation with neurotrypsin for 60 min. (E) The mRFP signal of full-length agrin is deleted from the plasma membrane after neurotrypsin treatment. Remaining mRFP signal results from intracellular vesicles which are not accessible for extracellular applied neurotrypsin. Scale bars: 5 µm.

Because of the absence of a specific antibody against N-terminal agrin I used an agrin construct including an extracellular HA tag positioned between the transmembrane and the first follistatin domain (Fig. 13 A). In addition, this variant contained a C-terminally located mRFP protein. The construct integrity was tested by expression in Cos-7 cells. Images were taken by confocal microscopy and showed typical features of agrin over-expressing cells possessing strong membrane fluorescence, and many lamellipodia/filopodia-like extensions. The agrin signal was consistent, apart from intracellular vesicle signals, which were only labelled by mRFP, since cells were incubated with α-HA antibody under non-permeabilised conditions (Fig. 13 B+C). Application of neurotrypsin for 60 min completely changed the ratio between HA and mRFP fluorescence. N-terminal HA signal remained unchanged by the treatment, while proteolytic cleavage removed mRFP fluorescence from the cell surface, so that it could be only detected in intracellular compartments of the cell (Fig. 13 D+E).

Protein recycling pathways differ between cell types. Therefore, to study a potential cellular uptake of processed N-terminal agrin I decided to investigate it in its natural cellular environment. I generated an adenovirus to express rSN-HA-agrin-mRFP in cultures of dissociated neurons. The uptake assay based on the idea to possibly track internalised N-terminal agrin that was prior labelled with antibodies (Fig. 14 B+C).

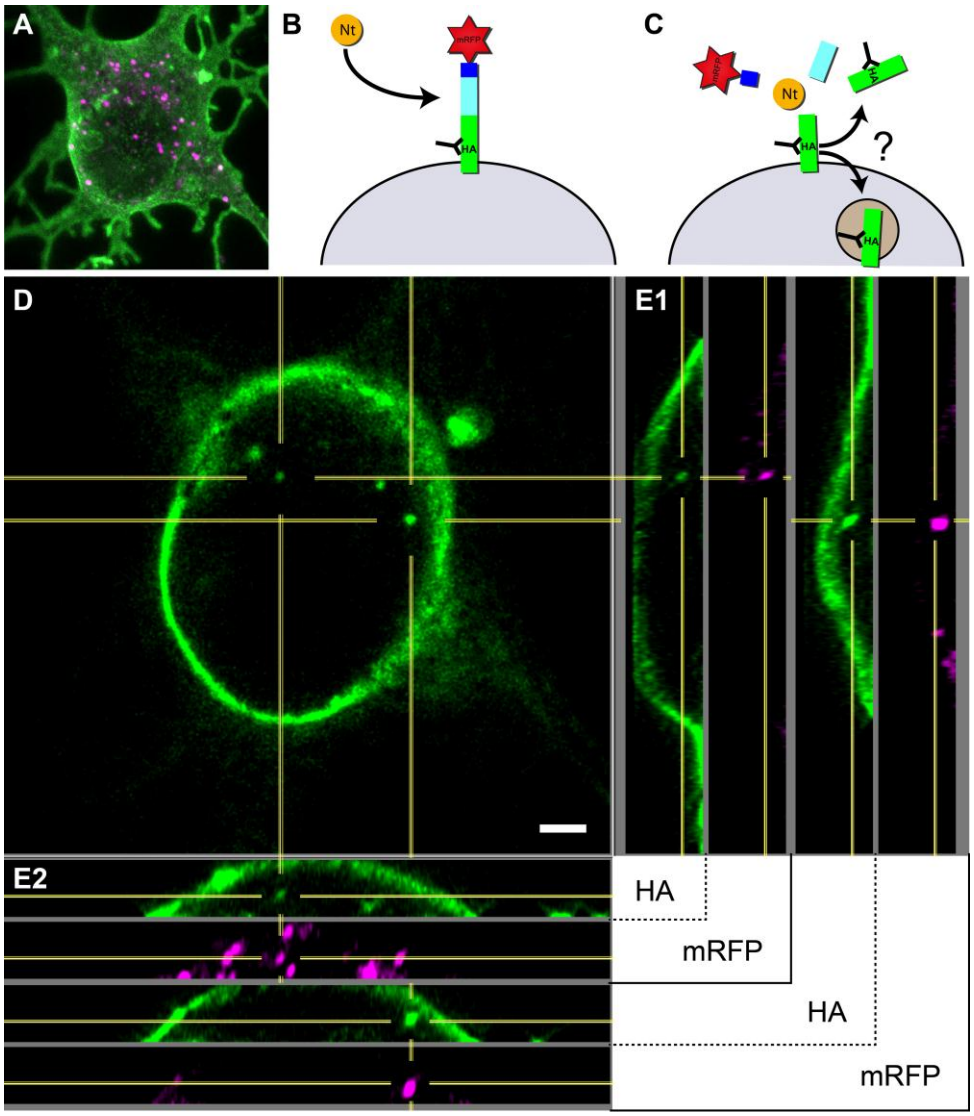

Figure 14. Immunocytochemistry based agrin uptake assay

(A) Maximum intensity projection of an analysed hippocampal neuron (4 DIV). mRFP signal was exclusively found to be intracellular due to extracellular treatment with neurotrypsin. (B+C) Schematic representation of the uptake experiment. (B) Transmembrane agrin was N-terminally labelled by anti HA antibodies before incubated with Nt. (C) The cleaved N-terminal agrin stump could be either uptaken by endocytosis or released from the plasma membrane by additional proteolytic degradation. (D) Single section of the confocal stack showing the HA signal. Several intracellular spots are visible which might result from endocytosis of the N-terminal agrin stump. Two of the spots were selected for 3D analysis (centre of the yellow cross hairs). (E1+E2) Longitudinal and transverse axis along the selected spots in yz and xz orientation. All detected HA vesicles were found to be also positive for mRFP and therefore did not represent cleaved N-terminal agrin. Scale bar: 5 µm.

Infected neurons were labelled with α-HA antibody and then proteolytically digested by neurotrypsin. Lysosomal degradation was inhibited during the uptake incubation time, in order to increase intracellular signals of endocytosed agrin. In summary, this approach showed relatively few spots of internalised HA-agrin positive signals. The best example was presented in figure 14 D. Four HA-agrin positive vesicles were visible in the interior of the neuron. Two of them, which were labelled by the yellow cross hair, were additionally presented in yz and xz orientation. However, the colocalisation with the

mRFP signal clearly indicated that the signal did not arise from cleaved N-terminal fragment but full-length agrin. Together, 15 cells were analysed for agrin uptake, but none was found to be positive for internalised N-terminal agrin.

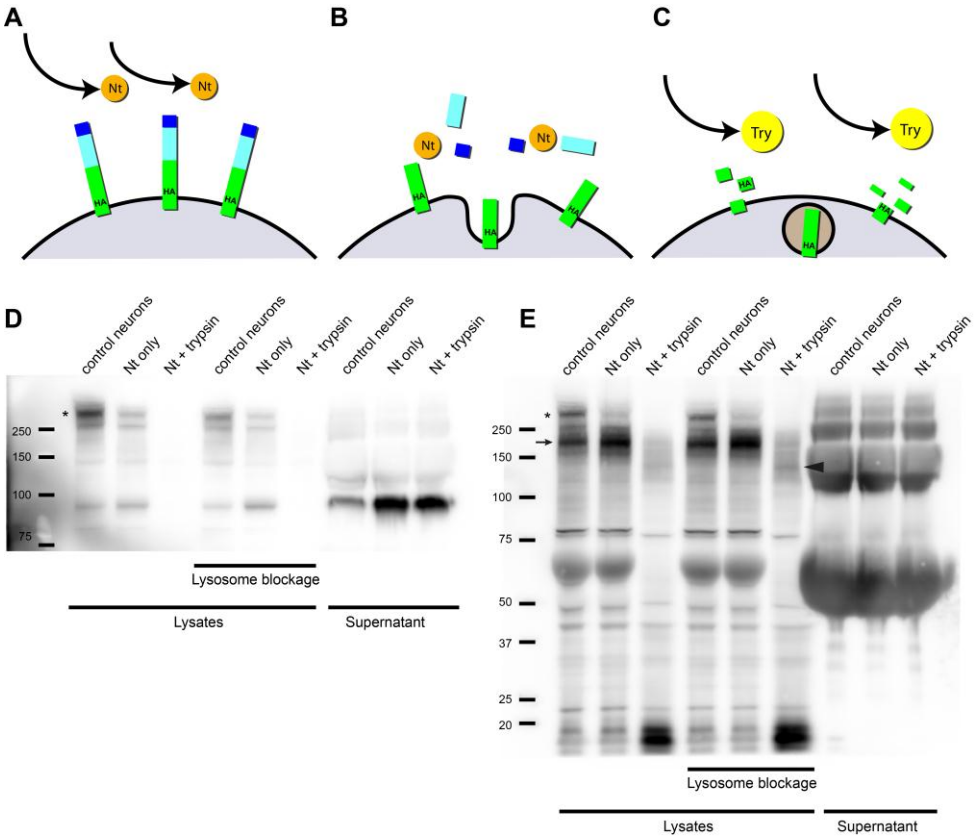

Figure 15. Agrin uptake assay based on Western blot analysis

(A+B) Cell surface agrin was digested by Nt, followed by incubation for 30 min to enable uptake of N-terminal agrin. (C) Analysis of cell lysates by WB do not allow a differentiation between internalised or cell surface N-terminal agrin. For that reason, extracellular trypsin was applied to deplete the remaining N-terminal agrin from the cell surface. (D) Western blot of high density cortical neuron cultures (DIV 5), overexpressing rSN-HA-agrin-mRFP. Agrin protein was detected with R132 antibody that was raised against the agrin-90 kDa fragment. Control neurons were not treated with Nt and represent the experimental baseline. Most of the agrin protein detected by R132 was present as full-length agrin (asterisk). Little amounts of 90 kDa fragment were found in the control samples due to endogenous Nt expression. Next lane contained lysate of neurons treated with Nt. Application of Nt clearly reduced the signal of full-length agrin. In the following lane additional treatment with trypsin completely depleted all agrin signal. The cell supernatant contained increased amounts of 90 kDa fragment in the lanes of Nt-treated cells.

(E) WB of the same experiment analysed with anti-HA antibody. Beside full-lenght agrin (asterisk) this antibody detected a strong band running between 250 and 150 kDa (arrow). This band represented N-terminal agrin remaining after cleavage by endogenous Nt. Extracellular application of Nt increased this band at the expense of full-length agrin. Trypsin treatment strongly reduced the amount of N-terminal agrin and only a blurry signal remained at this position. In a parallel experiment, lyososomal activity was additionally blocked, in order to protect internalised agrin from proteolytic degradation. This approach slightly increased the amount of N-terminal agrin in the sample where only Nt was added. The blurry signal of Nt + trypsin-treated cells also increased and a very faint band appeared at the size of N-terminal agrin. Additionally, a weak band appeared at the size of around 150 kDa (arrowhead) which had not been clearly assigned yet. The supernatant samples could not been analysed by the HA-antibody because of the high background signals.

I used a second agrin uptake assay, based on Western blot analysis, to verify the results of the previous approach. Cell lysates from neurotrypsin-treated neurons contained two theoretical pools of N-terminal agrin: cleaved but not endocytosed cell surface agrin and internalised agrin. Unfortunately, it is not possible to differentiate between the two agrin sources in cell lysates by Western blot. This discrepancy could be avoided by complete removal of all remaining surface agrin through short incubation with trypsin.

Immunological detection of agrin protein by the R132 antibody (raised against the 90 kDa fragment) showed strong expression of full-length agrin in the control neurons (Fig. 15 D). Incubation with neurotrypsin strongly reduced the amount of full-length agrin and at the same time clearly increased the 90 kDa cleavage product in the supernatant. Interestingly, also the supernatant of control neurons contained the 90 kDa fragment. This indicated that endogenous neurotrypsin protein was already activated in dissociated neuron cultures at DIV 5. N-terminal agrin was detected in the mass range 150-250 kDa using α-HA antibody (Fig. 15 E). Control neurons showed a distinct band of N-terminal agrin, which is in accordance with the detected 90 kDa fragment in the supernatant. This band was strongly increased when neurons were exclusively treated with neurotrypsin. The analysis of the trypsin incubated samples, however, did not reveal a clear proof of the uptake of cleaved N-terminal fragment. The procedure resulted in a blurry signal, in which the band of N-terminal agrin was barely detectable. Similar to the first uptake approach, I blocked lysosomal degradation in order to stabilise the internalised N-terminal fragment. Blockage of cellular degradation slightly increased the band of N-terminal agrin fragment and further visualised a so far unidentified band, running below the 150 kDa marker (arrowhead). Ectodomain shedding would be an alternative mechanism to release the cleaved agrin moiety from the cell surface. I aimed on screening cell supernatants for the appearance of N-terminal agrin fragments. Because proteins of the cell culture medium were recognised by the α-HA antibody such an analysis was impossible. This problem could be solved by replacing the cell culture medium with a protein-free buffer (Tyrod's). However, it was not possible to detect N-terminal fragment in the cell supernatant which would have been an indication for ectodomain shedding.

Taken together, the results of both agrin uptake experiments did not allow a clear statement about the fate of N-terminal agrin. Neither was it possible to convincingly demonstrate the uptake of cleaved agrin, nor the ectodomain shedding of agrin protein. However, the fact that we could not detect internalised agrin after strong viral overexpression, speaks against existence of a regulated major pathway for degradation of cleaved agrin protein. It rather suggests that N-terminal agrin is removed from the cell surface by slow constitutive endocytosis. This would also explain the low levels of N-terminal agrin found by the Western Blot experiments.

3.3 Neurotrypsin binds to agrin via glycosaminoglycan chains

3.3.1 Screening for potential neurotrypsin binding sites within the agrin molecule

Live imaging data from our laboratory showed that neurotrypsin is released from synaptic terminals in an activity-dependent manner (Frischknecht *et al.*, 2008). The protein remains at the site of release for several minutes, which was a first indication that neurotrypsin might bind to proteins located at the synapse. Further evidence came from the observation that neurotrypsin preferentially cleaved glycosylated agrin variants (Stephan *et al.*, 2008). Unpublished data from our laboratory also showed that co-expression of transmembrane agrin with neurotrypsin resulted in a redistribution of neurotrypsin to the cell surface of agrin positive cells (PhD thesis D. Lüscher). Taken together, these results suggested that neurotrypsin may bind to its cleavage substrate agrin, possibly mediated by agrin's glycosaminoglycan chains.

This project was based on preliminary observations of Dr. Daniel Lüscher, Institute of Biochemistry, Uni. Zurich. Additionally, I collaborated with my master student Stephanie Dürr, Institute of Biochemistry, Uni. Zurich, who was involved in method development and analysis of the Mini-agrin constructs. We established an immunocytochemistry based approach that allowed the quantification of membrane-bound neurotrypsin protein (Fig. 16). To map all agrin regions involved in binding of neurotrypsin, we used several "Mini-agrin" constructs, which contained the agrin transmembrane domain, different internal agrin fragments, and a C-terminal one-strep tag (Fig. 17 A).

Three Mini-agrin constructs were found to bind neurotrypsin with significantly increased quantities ($P < 0.001$). All constructs have in common that they have a directly connection to glycosaminoglycan chains. Construct HS was composed of two laminin EGF-like domains and a follistatin domain which contained several attachment sites for heparin sulphate chains. Construct CS consisted of a follistatin domain and a serine/threonine domain which anchors chondroitin sulphate chains. The LG2-y4 construct comprised two epidermal growth factor (EGF)-like domains and a laminin globular domain. The latter contains a heparin binding site and is interestingly part of an alternative splice site that is only present in the agrin-y4 variant. The HS and CS constructs showed at least three times as much cell surface-bound neurotrypsin compared to the control construct, which is composed of the transmembrane domain and the one-strep tag only (Fig. 17 B). The highest affinity to neurotrypsin was found for the LG2-y4 construct, and bound around eight times more neurotrypsin than the control. These values were the result of three independent experiments. For each experiment, we quantified at least 20 cells per construct.

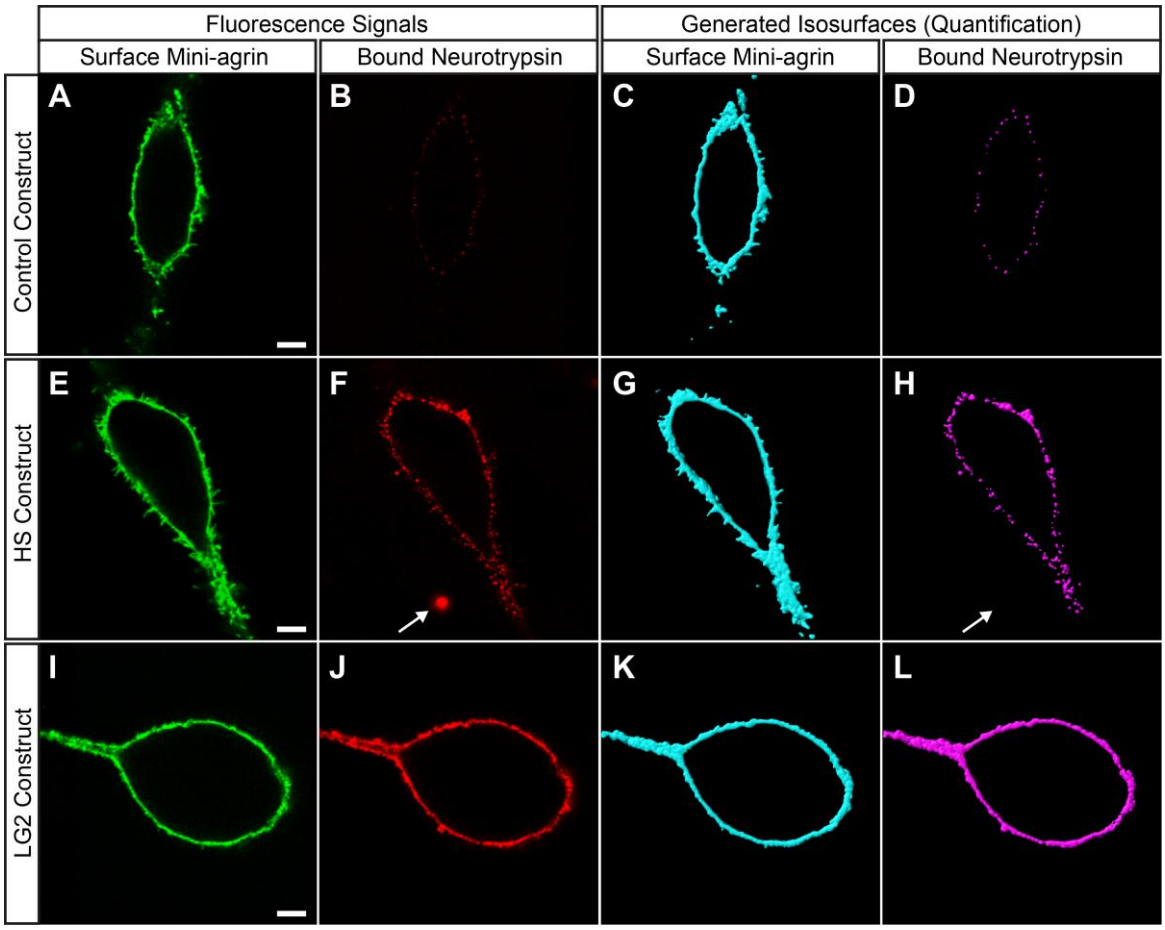

Figure 16. Quantification of agrin and neurotrypsin fluorescence signals at the cell surface of three different Mini-agrin constructs

(A+E+I) Confocal fluorescence signals of different Mini-agrin construct detected by a one-strep-tag located at the N-terminus. (B+F+J) Corresponding Nt signals detected by G93 antibody at the cell surface. Antibodies were applied to living cells (live staining) and thus cannot bind to intracellular agrin/Nt protein. (C+G+K) Imaris software was used to convert the fluorescence signals into „isosurfaces“. To account for differences in cell size, the area covered by isosurface was used to normalize the quantified Nt values. (D+H+L) Nt fluorescence was converted into an isosurface in a similar way as for the agrin signal. Additionally, I applied a filter that depleted all Nt signals that did not show a corresponding agrin signal in the same position. This avoid quantification of false positives from background signals which appear from Nt bound to cell debris (see arrow in F and H). Finally, the greyscale intensities of all pixels lying within the Nt isosurface were added, corresponding to the amount of total bound Nt at the cell surface. Scale bars: 5 µm.

We then generated three control constructs to verify the involvement of glycosaminoglycan chains in the binding of neurotrypsin. The HSΔ and CSΔ constructs contained S→A point mutations for all potential GAG attachment sites. The LG2-y0 construct was made of the agrin-y0 splice variant and lacks the heparin binding site. All three control constructs showed significantly reduced neurotrypsin binding abilities compared to its sibling construct (Fig. 17 D). The deletion of GAG attachment sites in HSΔ and CSΔ completely abolished neurotrypsin binding, thus constructs were equal to the control construct. LG2-y0 showed a slight increase in neurotrypsin binding compared to the control, but was clearly below the HS and CS constructs.

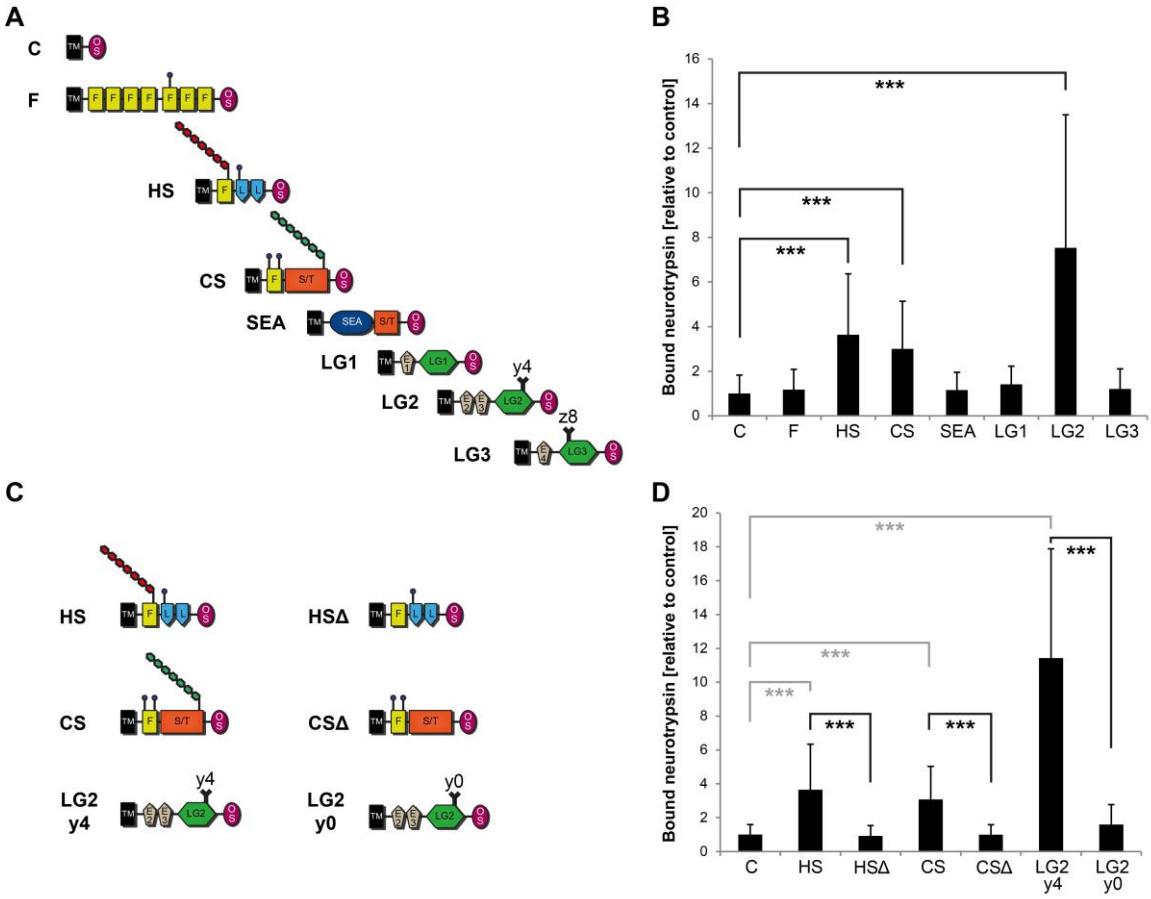

Figure 17. Mapping the neurotrypsin binding site within the agrin molecule

(A) Overview of all agrin-mini constructs used for the mapping of potential neurotrypsin binding sites along the agrin molecule. All constructs were coexpressed with Nt-S/A (inactive neurotrypsin) and analysed by immunological staining and subsequent confocal microscopy. (B) Three constructs were identified as potential Nt binding sites. Construct HS is composed of two laminin EGF-like domains and a follistatin domain which contains attachment sites for heparin sulphate. Construct CS consists of a follistatin domain and the serine/threonine domain which anchors chondroitin sulphate chains. The LG2 constructs is built up of two epidermal growth factor (EGF)-like domains and a laminin globular domain that includes a heparin binding site. The heparin binding site is inserted in an alternative splice site which is only present in the y4 variant. (C) The modified sibling constructs lack all potential sources of glycosaminoglycan, either by mutation of the GAG attachment sites or change to the splice insert y0. (D) Quantification of bound Nt confirmed that GAGs are essential to mediate the binding of neurotrypsin to agrin. The deletion of GAG interaction sites within the agrin molecule completely abolished agrin's binding capacity for Nt. Statistical significance was evaluated by a two-sample Kolmogorov-Smirnov test followed by a Bonferroni correction to enable multiple comparisons. Error bars represent standard deviation. *** $P < 0.001$.

In summary, we identified three intramolecular regions of the agrin molecule that are capable of binding neurotrypsin protein. Within these regions the neurotrypsin binding abilities are mediated by GAG chains, which are either an integral part of the core protein (HS and CS constructs) or connected to this region by a heparin binding site (LG2-y4).

3.3.2 GAG chains are essential for binding of neurotrypsin in full-length agrin

Based on the results of the Mini-agrin experiments we wanted to investigate to which extent the found interaction sites were involved in the binding of neurotrypsin in the agrin full-length molecule. In particular, we were interested if the heparin binding site possessed the same dominance as in the Mini-agrin constructs. Using the same quantification assay I tested four agrin full-length constructs. Agrin wild-type constructs y4 and y0 only differ in the y-splice inserts. The mutated constructs y4 ΔGAG and y0 ΔGAG additionally carry S→A mutations of the GAG attachment sites.

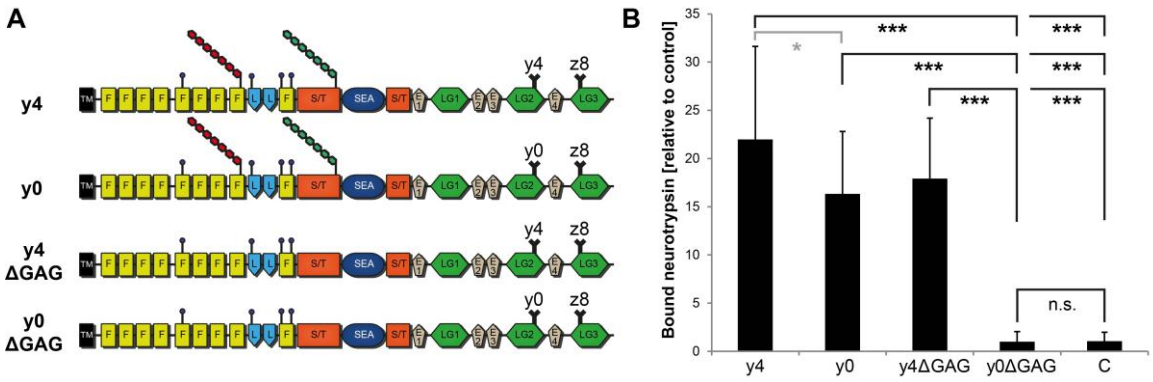

Figure 18. Relevance of identified neurotrypsin binding sites within the agrin full-length molecule

(A) To validate the results found in the Mini-agrin constructs we designed four full-length agrin constructs with different characteristics in the GAG properties. (B) Neurotrypsin was bound most efficiently when all GAG interaction sites were present in the agrin molecule. Changing the splice site to y0 resulted in a slightly decreased neurotrypsin binding that was, however, significantly reduced compared to y4. Deleting the GAG attachment sites in the y4 variant (y4 ΔGAG) showed less reduction compared to y0. All GAG containing agrin variants showed significantly increased neurotrypsin binding compared to the only GAG-free variant y0 ΔGAG and the Mini-agrin control construct. Statistical significance was evaluated by a two-sample Kolmogorov-Smirnov test followed by a Bonferroni correction to enable multiple comparisons. Error bars represent standard deviation. * $P < 0.05$, *** $P < 0.001$.

Construct y0 ΔGAG bound very little amounts of neurotrypsin and did not exceed the level found for the control construct (Fig. 18 B). This confirmed the importance of the GAG chains and indicated that no potential neurotrypsin binding site was abolished by splitting the agrin molecule into the Mini-agrin constructs. Most neurotrypsin was bound by the y4 construct which contained all of the neurotrypsin binding sites identified by the Mini-agrins. Construct y0 bound approximately one quarter less neurotrypsin than the y4 construct and was significantly different from this construct ($p<0.05$). Slightly more neurotrypsin was found to be attached at the y4 ΔGAG construct which lacks the heparin sulphate and chondroitin sulphate chains and contains only the heparin binding site as possible neurotrypsin interaction site. However, the y4 ΔGAG construct was not found to be significantly different from the y4 construct, underlining the importance of the heparin binding site for neurotrypsin binding. All GAG chain containing constructs showed clear

statistical differences from the y0 ΔGAG construct which lacks all potential GAG sources ($P < 0.001$).

3.3.3 Immunoprecipitation of neurotrypsin bound to agrin

A pulldown-assay was used as an alternative approach to confirm the results found for the binding of neurotrypsin to the agrin molecule. First attempts using lysates of neurotrypsin/agrin overexpressing cells as input of the immunoprecipitation did not yield reproducible results (thesis of and communications with Daniel Lüscher). This was probably due to the fact that neurotrypsin protein is very “sticky”. The secreted protease can be detected in cell supernatants of neurotrypsin overexpressing cells by Western blotting. However, a substantial proportion of the expressed protein was found to be attached to the surface of the cell culture plastic. The resulting low levels of soluble neurotrypsin in the supernatant might explain why I was not able to detect neurotrypsin by a classical agrin pulldown. Therefore, I used a different approach for the following immunoprecipitation experiment. HEK 293T cells were transfected with secreted variants of the four agrin full-length constructs, analysed in the previous experiment. Agrin containing cell supernatants were combined with antibody (α-agrin) coated sepharose-G beads that bound the molecule at its surface. Neurotrypsin protein was applied from a large scale purification (Reif *et al.*, 2008) and used in excess. The amounts of bound neurotrypsin were detected by Western blotting. Altogether, Western blots of four independent experiments were included in the analysis. Statistical significance was tested by ANOVA with a Tukey post-hoc test.

The quantification by Western blotting allowed the discrimination of full-length versus activated neurotrypsin (protease domain), which co-exist at undetermined quantities in the purified neurotrypsin stock solution (Reif *et al.*, 2008). Comparing the results of both neurotrypsin variants for the same full-length construct (Fig. 19 C1 vs. C2), we could not conclude a preferential binding of one of these forms. The neurotrypsin signal of each constructs was normalised against the “no antibody” (no AB) control band which originated from agrin-independent binding of neurotrypsin to the beads (background signal). In agreement with the previous experiment we found the agrin-y4 construct binding most neurotrypsin. Construct y0 bound slightly less neurotrypsin but was not significantly decreased from y4. Both GAG chain containing constructs showed significantly increased neurotrypsin binding capacity compared to the negative control. The presence of constructs y4 ΔGAG or y0 ΔGAG did not show increased binding of neurotrypsin compared to the negative control. While this was an obvious result for the y0 ΔGAG construct, at first view it questioned the result of the previous experiment for y4 ΔGAG where similar amounts were detected by the cellular assay. However, the observed discrepancy might be explained by differences in the experimental design. In the previous cell staining based approach all agrin variants were expressed in the transmembrane variant. The major interacting partners for the heparin binding site in the transmembrane y4 variants are most likely nearby positioned, GAG chain carrying, cell

surface proteins. These proteins are unlikely to bind in the same manner to the secreted forms of agrin-y4 used in the IP approach. Therefore, the results suggested that the y4 insertion is of less use for neurotrypsin binding when the protein is not linked to the cell membrane. The relatively small differences observed between the y4 and y0 variants in the IP approach, might point in the same direction.

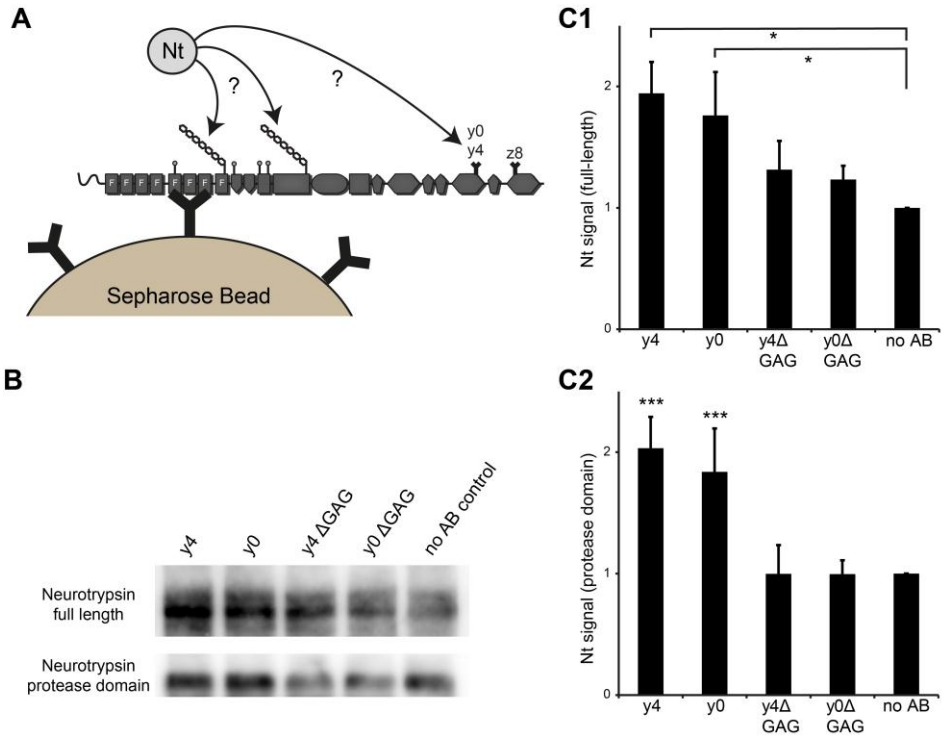

Figure 19. Immunoprecipitation of neurotrypsin

(A) Schematic drawing of the immunoprecipitation experiment. Agrin antibodies raised against the follistatin domains (R169) were coupled to sepharose beads. Secreted agrin variants were expressed in HEK293 cells and cell supernatants were incubated with the antibody coupled sepharose beads. Purified neurotrypsin protein was applied to the system to analyse binding capacities of the different agrin variants. Nt that was bound to beads was quantified by Western blotting. (B) Representative Western blot example. We used two antibodies (G87 and G93) to analyse full length Nt and activated Nt (protease domain), respectively. (C1) Quantification of full length Nt. Signals were significantly increased in agrin y4 and y0 compared to the negative control. (C2) Quantification of activated neurotrypsin. Agrin y4 and y0 also significantly increased Nt binding compared to both ΔGAG variants and the control. Western blots of 4 independent experiments were analysed for both quantifications. * $P < 0.05$, *** $P < 0.001$.

3.4 Agrin binds TGF-β: Influence on synaptogenesis?

3.4.1 Development of a novel synapse quantification method

Dissociated hippocampal neuronal cultures are a well characterised model system for the investigation of synaptogenesis (Grabrucker *et al.*, 2009). The identification of synaptic proteins with a defined subcellular localisation in the pre- or postsynaptic compartment enabled an immunocytochemical approach for the quantification of

synapses. In immunocytochemical terms, a synapse is defined by the apposition of a pre- and a postsynaptic marker signal in a double-immunofluorescent staining (Glynn & McAllister, 2006). I developed a novel way of synapse quantification in dissociated neuron cultures to analyse a potential influence of TGF-β family members on synaptogenesis. For technical details of the quantification method, please see chapter 2.6.3.3.

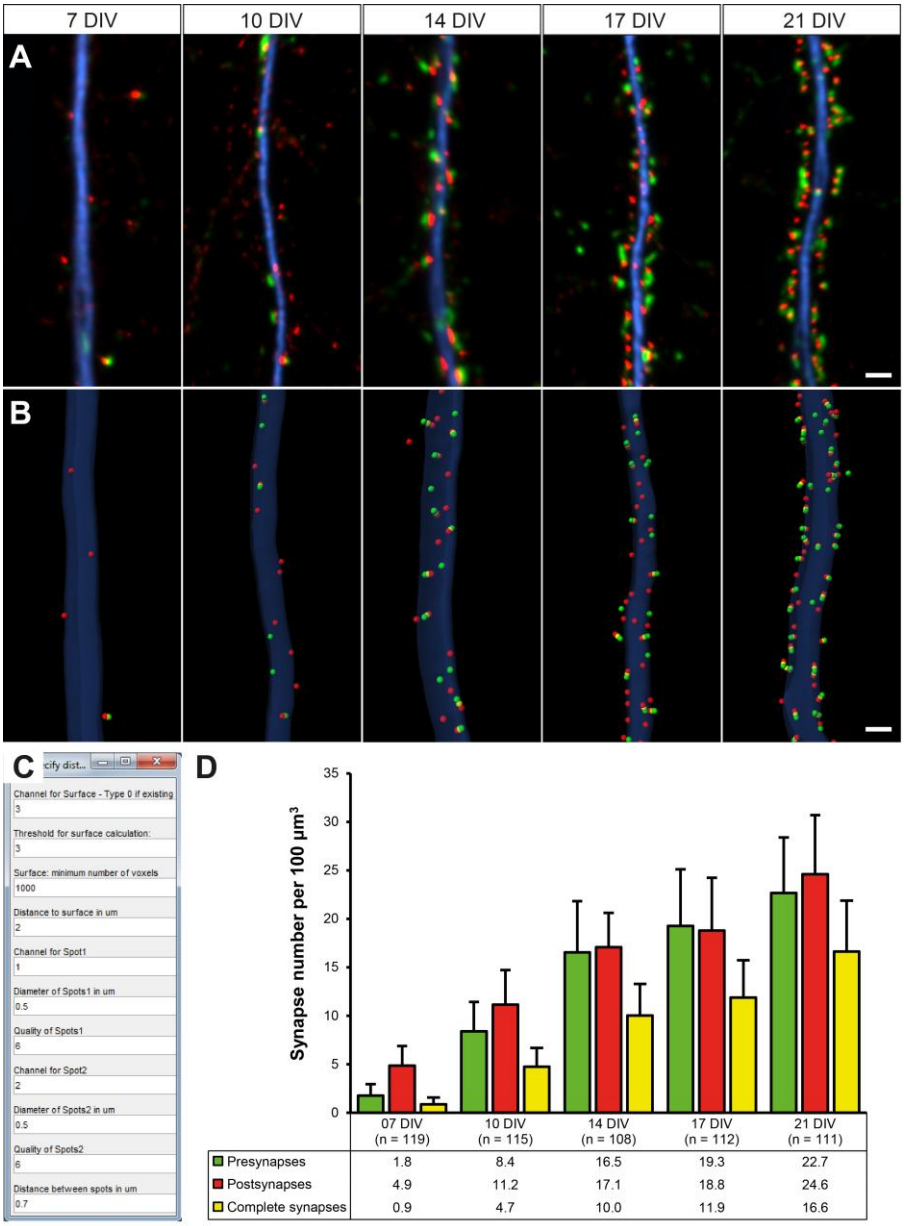

Figure 20. Synaptogenesis in hippocampal neuron cultures measured over time

(A) Representative images of dendrites fixed between 7 – 21 days in vitro (DIV) and processed for quantification. (B) The quantification method provides a graphical user interface, which allows a simple variation of all relevant quantification parameters, as well as the batch processing of multiple files without any additional user interaction. (C) Results of synapse quantification over time. Values presented here were normalized against the dendritic volume in order to discard size differences between the imaged dendrites. Error bars represent standard deviation. Together, more than 500 dendritic sections were analysed for this study. Scale bars: 2 µm.

As a test for this new method I analysed synaptogenesis in dissociated hippocampal cultures at different stages of development (7-21 DIV, Fig. 20 A+B). Dendrites of 7-day-old cultures were characterised by a relatively low number of presynaptic terminals. Accordingly, we found hardly any synapse at this stage. However, these cells exhibited a relative high number of postsynaptic sites which was three times higher compared to presynaptic terminals. After 14 days in culture approximately equal numbers of pre- and postsynaptic elements were found, of which about 50% being involved in synapses. A small increase of the total number of synaptic elements between DIV 14 and DIV 17 was followed by a large increase between DIV 17 and DIV 21. Finally, more than 65% of the pre- and postsynaptic structures were involved in synapses at DIV 21 (Fig. 20 D). Each time point included data from more than 100 dendritic segments which were imaged from 6 individual coverslips each. Representative images of dendrites used for this quantification are shown in Fig 20 A+B.

3.4.2 Involvement of transmembrane agrin in TGF-β1 signalling

Extracellular signals are an essential factor that regulates the assembly of pre- and postsynaptic elements during synaptogenesis. Members of the transforming growth factor-beta (TGF-β) superfamily, which are well known for its key roles in embryogenesis, immune response or cell cycle control, were also found to be involved in synaptogenesis of the neuromuscular junction of *Drosophila* (Marques, 2005) and modulation of synaptic signalling in *Aplysia* (Zhang *et al.*, 1997). A recent study demonstrated that agrin is capable of binding four members of the TGF-β superfamily by its N-terminal located follistatin domains (Banyai *et al.*, 2010). In the CNS agrin appears predominantly in its transmembrane splice variant and is localised in close proximity to synapses (Stephan *et al.*, 2008). We hypothesised that an agrin-mediated accumulation of cytokines at the plasma membrane may have consequences for the generation of new synaptic contacts or maintenance of existing synapses.

For this experiment I generated hippocampal neuronal cultures from E18 agrin knock-out mice, as well as its wild-type (wt) litter mates. After 10 days *in vitro*, 2 ng/ml TGF-β1 protein were applied to individual cultures. The cytokine was incubated for 48h, before cells were immunohistochemically stained and quantified for synaptic elements. The result in Table 4 represent the mean values observed for a single coverslip and show relatively low differences between the experimental conditions. A statistically significant difference could be found, for the mean of all coverslips, between the wt control vs. wt TGF-β1 group when comparing presynaptic elements. Interestingly, the number of postsynapses was significantly decreased for all conditions when compared to the control group. Synaptic contacts were significantly decreased for wild-type and agrin knock-out neurons treated with TGF-β1 compared to control conditions. However, it has to be mentioned that the observed differences are smaller than the deviation between single coverslips of the same experimental conditions. Statistical significance could be

reached because of the high number of analysed dendrites, but these results do not allow for a clear conclusion on the basis of the raw data.

Table 4. Involvement of transmembrane agrin in TGF-β1 signalling

Experimental conditions	Presynapses		Postsynapses		Synapses		Analysed dendrites (n)
wild-type control I	8.1	(± 2.6)	7.8	(± 2.1)	4.6	(± 1.5)	29.0
wild-type control II	9.9	(± 2.6)	9.5	(± 1.7)	5.9	(± 1.4)	25.0
wild-type control III	11.5	(± 3.2)	11.4	(± 2.7)	6.7	(± 2.0)	29.0
wild-type control IV	8.9	(± 2.5)	10.1	(± 2.4)	5.6	(± 1.8)	30.0
wild-type control V	8.2	(± 2.6)	8.8	(± 1.8)	5.0	(± 1.5)	29.0
wild-type control VI	7.5	(± 1.9)	7.4	(± 1.4)	4.9	(± 1.2)	23.0
wt control mean	**9.0**	(± 2.9)	**9.2**	(± 2.5)	**5.5**	(± 1.7)	**165.0**
wt TGF-β1 I	10.1	(± 2.7)	11.2	(±2.6)	6.3	(± 1.7)	22.0
wt TGF-β1 II	7.5	(± 2.2)	8.3	(± 1.8)	4.4	(± 1.2)	28.0
wt TGF-β1 III	8.3	(± 3.0)	8.2	(± 2.0)	4.9	(± 1.6)	26.0
wt TGF-β1 IV	7.1	(±1.8)	7.0	(± 1.5)	4.3	(± 1.0)	28.0
wt TGF-β1 V	7.5	(±2.0)	7.0	(± 1.0)	4.5	(± 0.9)	27.0
wt TGF-β1 VI	8.1	(± 2.0)	7.8	(± 1.9)	4.6	(± 1.3)	28.0
wt TGF-β1 mean	**8.0 ***	(± 2.4)	**8.1 ***	(± 2.2)	**4.8 ***	(±1.4)	**159.0**
knock-out control I	5.8	(± 1.8)	6.9	(± 1.6)	3.4	(± 1.0)	28.0
knock-out control II	7.4	(± 2.0)	7.8	(± 1.5)	4.2	(± 1.2)	29.0
knock-out control III	7.5	(± 1.7)	7.3	(± 1.4)	4.3	(± 1.1)	28.0
knock-out control IV	12.2	(± 0.9)	6.2	(± 3.3)	6.9	(± 3.8)	29.0
knock-out control V	9.6	(± 3.6)	12.1	(± 3.2)	6.2	(± 2.4)	28.0
knock-out control VI	9.2	(± 3.2)	9.2	(± 2.2)	4.9	(±1.7)	28.0
ko control mean	**8.6**	(± 3.1)	**8.2 ***	(± 3.0)	**5.0**	(± 2.4)	**170.0**
ko TGF-β1 I	10.6	(± 2.3)	8.0	(± 1.8)	5.4	(± 1.6)	27.0
ko TGF-β1 II	7.9	(± 2.1)	8.1	(± 1.4)	4.7	(± 1.1)	28.0
ko TGF-β1 III	7.2	(± 2.2)	7.4	(± 2.0)	3.9	(± 1.1)	28.0
ko TGF-β1 IV	7.2	(± 2.8)	7.8	(± 2.0)	4.4	(± 1.2)	27.0
ko TGF-β1 V	10.2	(± 3.5)	9.1	(± 2.3)	5.6	(± 1.7)	28.0
ko TGF-β1 VI	6.9	(± 1.7)	7.6	(± 1.4)	4.2	(± 1.2)	27.0
ko TGF-β1 mean	**8.4**	(± 2.9)	**8.0 ***	(± 1.9)	**4.7 ***	(± 1.2)	**165.0**

* $P < 0.05$ compared to wt control (ANOVA withTamhane post-hoc test) ± STDEV , I-VI represent independent coverslips

3.4.3 Influence of TGF-β family members on synaptic density

I additionally screened other TGF-β family members: TGF-β2 and BMP-2. In this experiment hippocampal neuron cultures were generated from E18 NMRI mice. Proteins were applied at following concentrations: 2 ng/ml TGF-β1, 2 ng/ml TGF-β2 and 10 ng/ml BMP-2 and incubated for 48 h. The results were again characterised by a relatively high deviation between different coverslips of the same experiment. For that reason, the data

of each condition is presented separately for all analysed coverslips (Table 5). Application of TGF-β1 did not significantly change the amount of synaptic elements or synapses compared to control conditions. Similar to the previous experiment TGF-β1 also decreased the total amount of presynapses and synapses, however the number of postsynapses was slightly increased. BMP-2 significantly increased the number of presynapses while the number of postsynapses and synapses was slightly increased but not significantly changed. Interestingly, application of TGF-β2 induced a strong increase in both synaptic elements and synapses. With an increase of about 30% these results represented the most prominent change in the study and were highly significant.

Table 5. Influence of TGF-β family members on synaptogenesis

Experimental conditions	Presynapses	Postsynapses	Synapses	Analysed dendrites (n)
control I	14.4 (± 3.3)	11.4 (± 2.7)	9.5 (± 2.6)	49
control II	8.5 (± 2.7)	9.1 (± 2.5)	5.9 (± 2.0)	54
control III	7.4 (± 2.3)	7.7 (± 1.5)	5.4 (± 1.6)	26
control IV	5.3 (± 1.0)	8.1 (± 1.5)	4.4 (± 1.1)	26
control mean	**9.6** (±4.3)	**9.4** (± 2.7)	**6.7** (± 2.8)	**155**
TGF-β1 I	11.0 (± 4.8)	14.2 (± 3.4)	8.4 (± 3.5)	48
TGF-β1 II	9.5 (± 2.8)	8.3 (± 2.3)	5.9 (± 2.0)	52
TGF-β1 III	6.1 (± 2.7)	10.6 (± 3.9)	4.8 (± 2.3)	26
TGF-β1 IV	8.8 (± 3.4)	7.0 (± 1.9)	4.8 (± 2.0)	25
TGF- β1 mean	**9.3** (± 4.0)	**10.3** (± 4.1)	**6.3** (± 3.0)	**151**
BMP-2 I	12.6 (± 4.0)	11.3 (± 2.9)	8.1 (± 2.8)	45
BMP-2 II	13.3 (± 5.2)	9.8 (± 3.5)	7.3 (± 2.9)	47
BMP-2 III	8.1 (± 2.2)	9.2 (± 2.0)	5.4 (± 1.2)	26
BMP-2 IV	11.0 (± 3.0)	8.4 (± 2.1)	6.1 (± 1.7)	26
BMP-2 mean	**11.7*** (± 4.4)	**9.9** (± 3.0)	**7.0** (± 2.6)	**144**
TGF-β2 I	14.7 (± 5.0)	14.8 (± 4.2)	10.0 (± 4.0)	48
TGF-β2 II	15.4 (± 2.6)	13.3 (± 3.0)	10.2 (± 2.3)	53
TGF-β2 III	6.9 (± 2.1)	7.7 (± 2.5)	4.1 (± 1.2)	25
TGF-β2 IV	9.9 (± 2.7)	10.9 (± 2.4)	6.8 (± 1.9)	26
TGF-β2 mean	**12.8*** (± 4.7)	**12.5*** (± 4.1)	**8.6*** (±3.6)	**153**

* $P < 0.05$ compared to wt control (ANOVA withTamhane post-hoc test) ± STDEV, I-IV represent single coverslips

Although this project covered a very interesting question we decided to stop it at this stage for several reasons. The automated synapse quantification proved to be a very useful tool for analysing large datasets. However, image acquisition and sample preparation alone were still extremely time-consuming and exceeded the available resources for this project. In addition, preparation of agrin knock-out cultures was a very tedious procedure that resulted in only low yield of agrin-deficient cultures (25%)

because preselection was impossible due to the perinatal death of the animals. The high variance indicated further that some other factors may have an uneven higher impact than the analysed cytokines, which strongly impede the interpretation of the findings.

At this stage we could conclude that TGF-β2 had the highest potential to influence synapses in dissociated neuron cultures. New experiments on agrin knock-out cultures would be required to confirm that this effect is dependent on cytokines binding to agrin. Next, it would be interesting to reveal if the increment in synaptic number is based on the strengthening of synaptogenesis or mediated by a synapse stabilising effect of TGF-β2.

3.5 Muscarinic receptor activation induces spine head filopodia

3.5.1 Activation of muscarinic receptor alters spine head morphology in pyramidal neurons

Pharmacological studies on humans indicate that acetylcholine (ACh) plays an important role in the encoding of new memories (Hasselmo, 2006). Cholinergic stimulation mediates its effects via nicotinic (nAChR) and muscarinic (mAChR) receptors. Muscarinic receptors activate a G-protein coupled signalling cascade and exist in five subtypes (M1-M5), which are widely expressed across the CNS. Synaptic plasticity is considered as one of the basic mechanism of learning and memory. In the following project, Dr. José María Mateos, Biochemistry Institute, Uni. Zurich and I focused on structural plasticity of dendritic spines induced by muscarinic receptor activation.

Experiments were performed on organotypic slice cultures (Gahwiler, 1981) that were prepared from mice expressing membrane targeted eGFP in a subpopulation of CA1 pyramidal cells (De Paola *et al.*, 2003) (Fig. 21 A+B). Dendritic spines were observed by time-lapse confocal laser scanning microscopy at short intervals. Under control conditions dendritic spines showed small variations in volume and underwent rapid changes in shape, as previously reported (Fischer *et al.*, 2000). Activation of muscarinic receptors by a short application of the specific muscarinic receptor agonist, methacholine chloride (MCh; 100 μM; 5 minutes) induced a pronounced morphological response in dendritic spines (Fig. 21 C-E). The classical round shape of dendritic spine heads was altered to a complex structure characterized by the emergence of one to several thin filopodia. The effect was rapidly reversible and spines returned to their original shape when the drug was washed out again.

Quantification of the formation of spine head filopodia (SHF) over different time points (Fig. 23 A-A') showed that strong stimulation of muscarinic receptors induced the emergence of one or more filopodia in almost half (48.02 ± 6.51%) of all analysed spines (n = 8 cultures; n = 19 dendrites; n = 550 spines; $P < 0.001$). In control conditions SHF were rare (2.87 ± 2.09 %), and after wash out of the drug (5 to 10 minutes) these

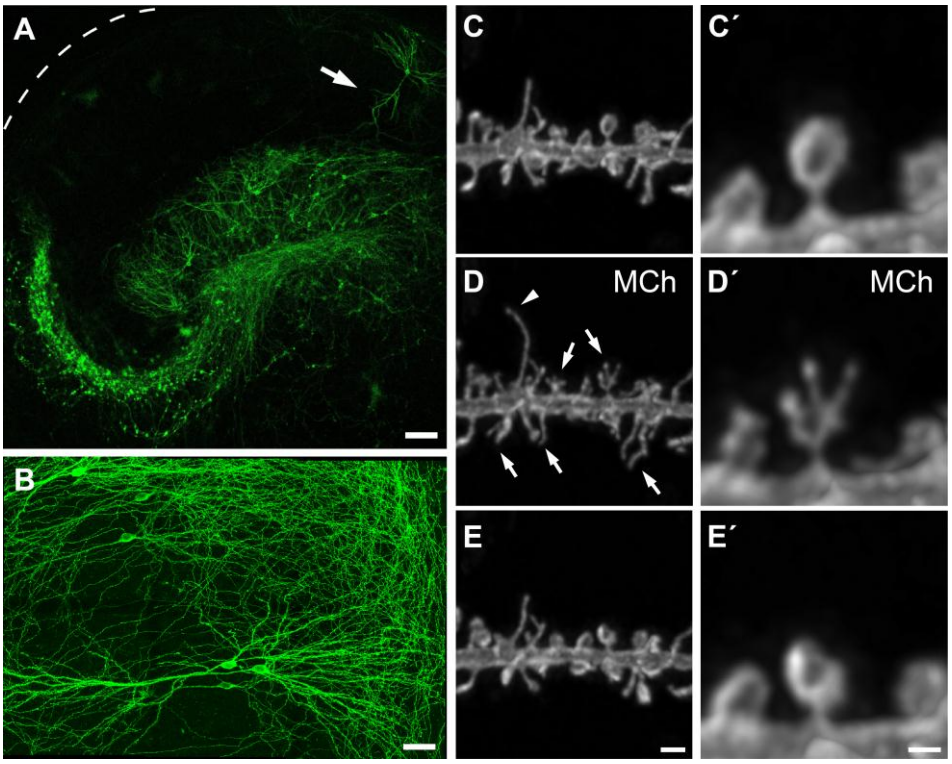

Figure 21. Muscarinic receptor activation leads to reversible formation of SHF in mouse hippocampus

(A) Organotypic hippocampal slice culture prepared from a L15 mouse and imaged at low magnification. Arrow points on the basal dendrite of a CA1 pyramidal cell. (B) Higher magnification of the CA1 region with a higher density of eGFP positive cells. (C-E) Time-frames of a dendrite from an eGFP positive CA1 pyramidal cell. (C) Dendritic spines were imaged under control conditions. (C') High magnification of (C) showing a classical round spine head shape. (D) Application to the superfusate of 100 µM MCh for 5 minutes induces rapid and prominent changes in the morphology of spine heads. The sphere-like shape of many of the mushroom spines becomes distorted and small filopodia appear from the heads of all classes of spines (arrows point to representative SHF). In a few cases, filopodia also showed extensions (arrowhead) (D') During MCh application this spine head exhibits an irregular shape with three emerging thin filopodia. (E-E') This effect is transient as spine heads return to their original shape soon after MCh is washed-out (6 min). Scale bars: A: 100 µm B: 50 µm E: 2 µm and E' 1 µm.

.parameters returned to control levels (n = 6 cultures; n = 9 dendrites; n = 192 spines, 3.36 ± 2.17 %; $P < 0.001$). All spine types were affected: mushroom, thin and stubby spines. The effect was most prominent and best visible in mushroom spines. Thin spines usually changed their morphology by extending one small filopodium from the tip of the spine head.

Imaging at high temporal resolution (30 sec intervals) revealed that changes occur within minutes after MCh stimulation, recover quickly during washout and can be formed again in response to subsequent MCh applications. We analysed these changes in three dimensions (3D) and over time by calculating the sphericity index of isolated spines heads. The formation of SHF following muscarinic receptor activation clearly decreased the spine head sphericity (15.67 ± 3.79 %; Figure 22 C). The transitory nature of the MCh response was well illustrated by recovery of the sphericity value during washout of

the drug. These changes show the ability of the spine head to accomplish extensive changes in morphology in response to activation of muscarinic receptors.

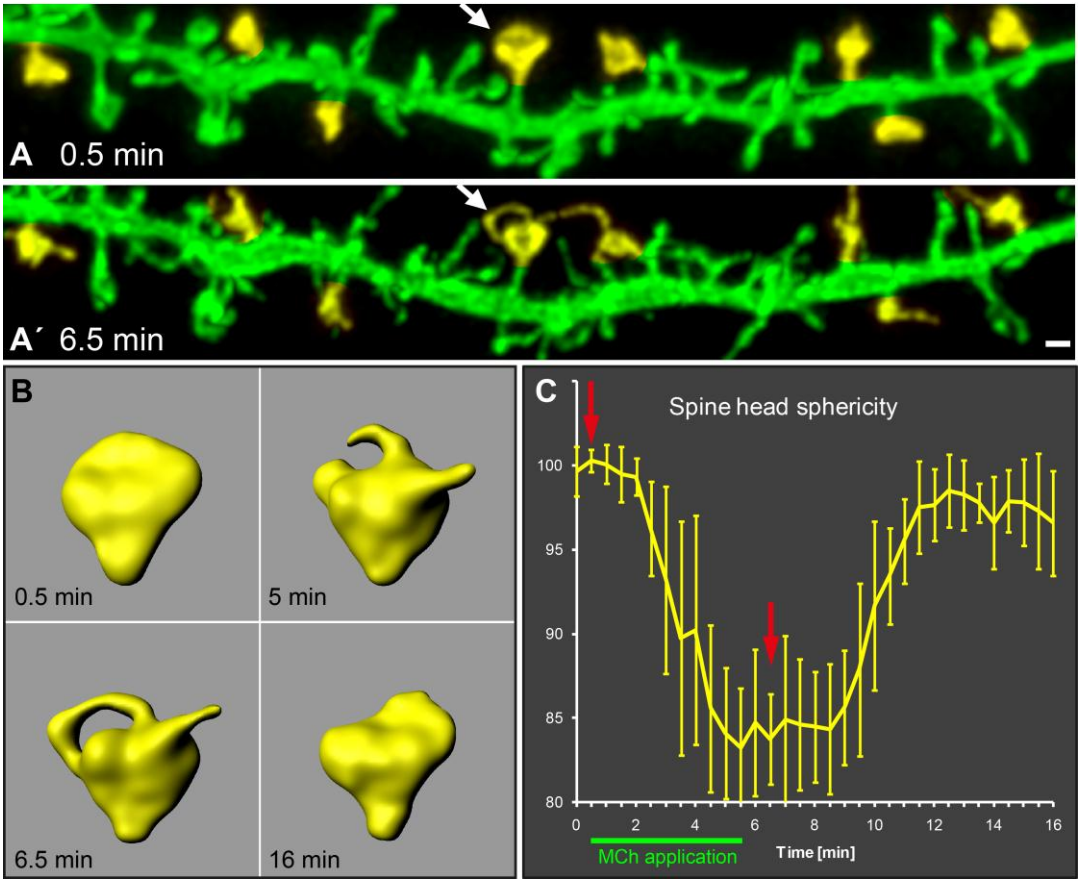

Figure 22. 3D reconstruction and analysis of spine head changes

Two time points taken by live imaging of a dendritic segment before (A) and during stimulation with 100 µM methacholine (A´). Fluorescent signals of individual spine heads were isolated (yellow) for quantification with Imaris software. (B) 3D reconstructions of a spine head based on its fluorescence signals. First image was under control conditions, 5 - 6.5 min during MCh stimulation and 16 min after wash out of the drug. MCh application induces several protrusions emerging from the head of the spine. (C) Quantification of the MCh-induced change in spine head sphericity, of eight individual spines (yellow labelled in (A)), plotted over time. Scale: 1 µm.

Morphological changes at dendritic spines are believed to reflect rather long-term than short-term plasticity. In contrast to this paradigm, we demonstrated that the MCh-mediated modulation of spine morphology was very short-lived, strongly correlating with the time course of cholinergic stimulation. To rule out potential long-term effects of the MCh treatment, we analysed dendrites over a longer period of time. For this experiment slice cultures were imaged before and during MCh stimulation and then returned back to the incubator. The same dendritic segments were subsequently analysed after 24h and 48h, respectively. Stimulated cultures and a control group were analysed for effects such as changes in the turnover of spines, spine class type transformation, or variations in filopodia generation. However, we did not observe significant differences in these parameters.

3.5.2 Formation of spine head filopodia requires activation of muscarinic receptors and mobilisation of calcium from internal stores

We confirmed the specificity of the activation of muscarinic receptors by using a specific muscarinic receptor antagonist, atropine (1 µM) before and during the application of MCh. The response to MCh is clearly mediated by muscarinic receptors as the effect on spines was abolished in the presence of atropine (control: 8.5 ± 3.6 %; atropine + MCh: 6.3 ± 3.6 %; n = 3 cultures; n = 9 dendrites; n = 275 spines; Fig. 23 B). Atropine alone in the same experiments had no effect on spine head morphology (4.8 ± 3.0 %; Fig. 23 B). This finding is in agreement with the results from a morphological demonstration of muscarinic receptors in dendritic spines of CA1 pyramidal cells (Yamasaki *et al.*, 2010).

Muscarinic receptor subtypes M1, M3 and M5 are coupled to $G_{q/11}$ proteins which can lead to calcium mobilisation from internal stores (Power & Sah, 2002). To test whether the response we observed is dependent on this pathway, we analysed the effect of MCh on spines in neurons pretreated with cyclopiazonic acid (CPA) to deplete internal calcium stores (Goeger *et al.*, 1988). In presence of CPA (20 µM) induction of SHF by MCh still occurred (control: 2.7 ± 2.7 %; CPA + TTX + MCh: 23.3 ± 8.5 %; n = 3 cultures; n = 9 dendrites; n = 234 spines; Fig. 23 C) but was significantly reduced compared with MCh alone (MCh: 48.02 ± 6.51 %; CPA + TTX + MCh: 23.3 ± 8.5 %; $P < 0.001$). CPA alone in the same experiments had no effect on spine head morphology (2.7 ± 3.6 %; Fig. 23 C).

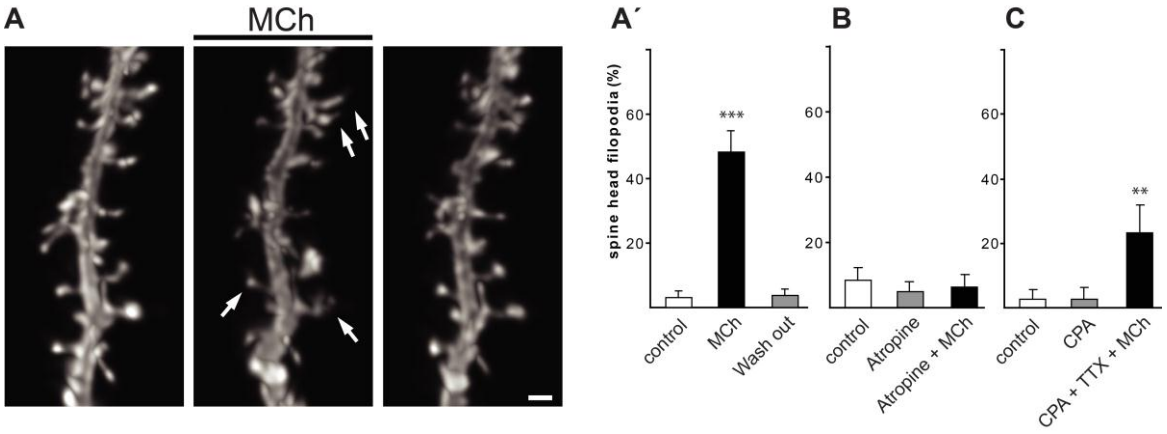

Figure 23. Quantification of spine head filopodia

(A - A') Comparison of control conditions versus a 5 minute application of MCh (100 µM) reveals a strong increase in the proportion of spines expressing filopodia (arrows). After washout of MCh spine heads revert to their original morphology. (B) Spine head modifications induced by MCh are mediated by muscarinic receptors. Blockade of muscarinic receptors by application of atropine 1 µM abolishes spine head changes induced by MCh application. (C) Intracellular calcium stores are involved in the induction of spine head changes. After treatment with CPA, to deplete calcium stores, MCh induction of SHF is reduced. ** $P < 0.01$, *** $P < 0.001$, scale bar: 1 µm.

3.5.3 Epileptiform activity is not sufficient to form SHF

At this point electrophysiological recordings were required to elucidate further details. We collaborated with the laboratory of Prof. Urs Gerber, Brain Research Institute, Uni. Zurich. All following electrophysiological experiments were performed and analysed by Dr. Jeanne Ster.

Changes in the synaptic activity pattern are a major factor that drives structural plasticity at the synapse. For example, persistent induction of epileptiform activity by long-term exposure to $GABA_A$ receptor blockers (24 hours) produces changes in spine density (Muller *et al.*, 1993) and also creates filopodia-like dendritic structures (Zha *et al.*, 2005). We hypothesised that MCh may induce SHF indirectly by inducing epileptiform activity. First, we therefore examined the effects of MCh (100 µM, bath-applied for 5 min) on the activity of CA1 pyramidal cells voltage-clamped at -70 mV. We observed a marked increase in neuronal excitability characterized by numerous epileptiform events (EE). The epileptiform activity was no longer present 15 minutes after washout and was never observed in the absence of MCh (EE amplitude: -1769 ± 772 pA; EE frequency: 0.033 ± 0.015 Hz; EE duration: 14.1 ± 2.35 sec; Fig. 24). Then we tested whether epileptiform discharge *per se* influences the morphology of spine heads by blocking $GABA_A$ receptors with picrotoxin (100 µM; 10 min), which induced robust epileptiform bursting in voltage-clamped CA1 pyramidal cells (EE amplitude: -4028 ± 321 pA; EE frequency: 0.008 ± 0.002 Hz; EE duration: 12.3 ± 4.7 sec; Fig. 24). Application of picrotoxin did not, however, alter spine head morphology (control 3.31 ± 4.57 %; Pic: 4.78 ± 4.15 %; Fig. 24 D´). Interestingly, a subsequent co-application of picrotoxin and MCh induced a strong change in spine heads (control 3.31 ± 4.57 %; Pic + MCh: 59.33 ± 10.58 %; $P < 0.001$; n cultures: 4; n dendrites: 8; n spines: 210; Fig. 24 D´).

Further evidence against a role for epileptiform activity in the induction of SHF came from experiments in which network activity was prevented by blocking voltage-dependent sodium channels with tetrodotoxin (TTX; 1µM). In a previous study, application of TTX alone for more than one hour led to the formation of spine head protrusions (Richards *et al.*, 2005). In our current experiments, we used a shorter application of TTX (10 min) which did not induce significant changes in spine heads (control: 6.38 ± 4.99 %; TTX: 4.8 ± 4.0 %). Interestingly, TTX failed to block SHF induced by MCh (control 6.38 ± 4.99 %; TTX + MCh: 37.9 ± 11.3 %; $P < 0.001$; n = 5 cultures; n = 16 dendrites; n = 543 spines; Fig. 25 A-A'). To determine whether this MCh response, in the presence of TTX, was mediated by an increase in action potential independent release of glutamate we examined the effect of additionally blocking AMPA/kainate and NMDA receptors with CNQX (25 µM) and D-AP5 (40 µM), respectively. Under these conditions, however, MCh still induced the formation of SHF (control: 9.0 ± 12.4 %; all blockers + MCh: 51.1 ± 10.1 %; $P < 0.001$; n = 4 cultures; n = 7 dendrite; n = 161 spines; Fig. 25 B), indicating that SHF mediated by muscarinic receptors does not depend on activation of ionotropic glutamate receptors. These blockers applied without MCh in the same experiments had no effect on spine head morphology (all blockers: 9.8 ± 8.7 %; Fig. 25 B).

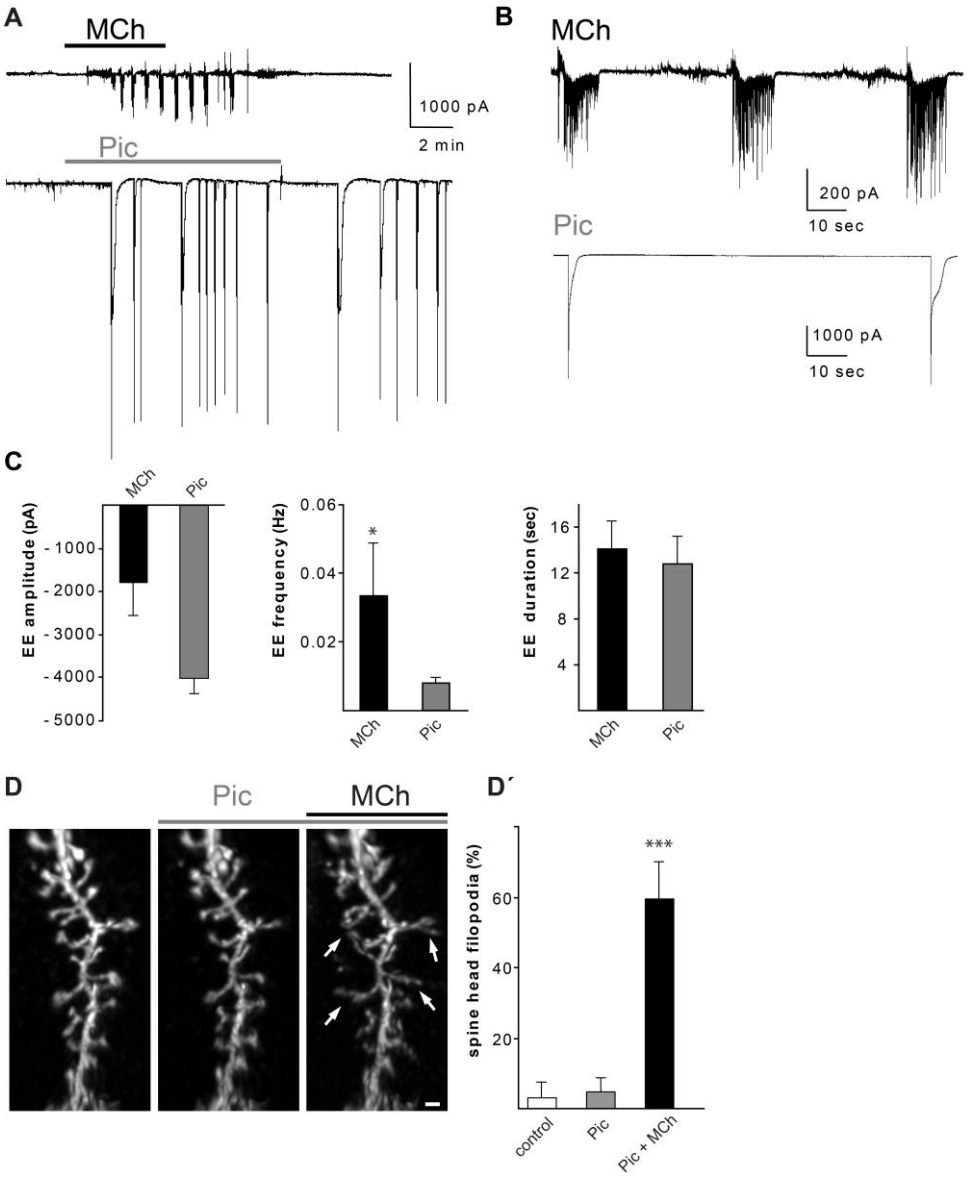

Figure 24. Epileptiform activity induced by picrotoxin (Pic) or MCh

(A) Sample traces recorded in a CA1 pyramidal cell reveal epileptiform events (EEs) after application of MCh (100 µM) or Pic (100 µM). The horizontal bars indicate the duration of drug application. (B) Expanded traces of EEs in presence of MCh or Pic. (C) Summary histograms of the amplitude, frequency and duration of EEs record in presence of MCh (n = 5) or Pic (n = 5). * $P < 0.05$ (Mann-Whitney test). Error bars represent SEM (Electrophysiological experiments performed by Dr. Jeanne Ster). (D - D´) Blockade of inhibitory transmission does not affect the induction of spine head changes induced by MCh. A 10 minute application of Pic at 100 µM does not alter spine head morphology. However, SHF appeared (arrows) when MCh was applied in the presence of Pic. *** $P < 0.001$, scale: 1 µm.

3.5.4 Activation of metabotropic glutamate receptors induces similar effects as found for muscarinic receptor activation

Combining picrotoxin and MCh increased spine head transformations compared to muscarinic stimulation alone. Even though, we could show that ionotropic glutamate receptors are not required for the induction of spine head changes, this data suggested that glutamatergic activity might contribute to the effect. Interestingly, stimulation of group

I metabotropic glutamate receptors (mGluR) was reported to increase the length of spines in granule cells and this effect was not inhibited by AMPA and NMDA receptor blockage (Vanderklish & Edelman, 2002). Group I mGluR and muscarinic receptors overlap in their signal transduction cascades. For instance, they both initiate IP_3-mediated Ca^{2+} release from internal stores (Barbara, 2002). Based on the analogy of the signalling cascade we hypothesised that strong stimulation of group I mGluR may also induce short-term morphological changes. Stimulation with DHPG (500 μM, 10 min) induced spine head changes (control: 2.7± 3.5%; DHPG: 32.5 ± 12.2%; $P < 0.001$; n = 6 cultures; n = 12 dendrite; n = 372 spines; Fig. 25 A') to a similar extend as found for muscarinic receptor activation. This indicates that muscarinic and glutamatergic metabotropic receptors can both mediate morphological modification of spine head shapes. Further, it suggests that the increased spine head transformation, after combined application of picrotoxin and MCh, is triggered by metabotropic glutamate receptors. However, strong synaptic release of glutamate caused by epileptiform activity does not reach sufficient concentration to induce spine head modifications via mGluR. We therefore concluded that glutamergic activity rather modulates than initiates the morphological spine head plasticity.

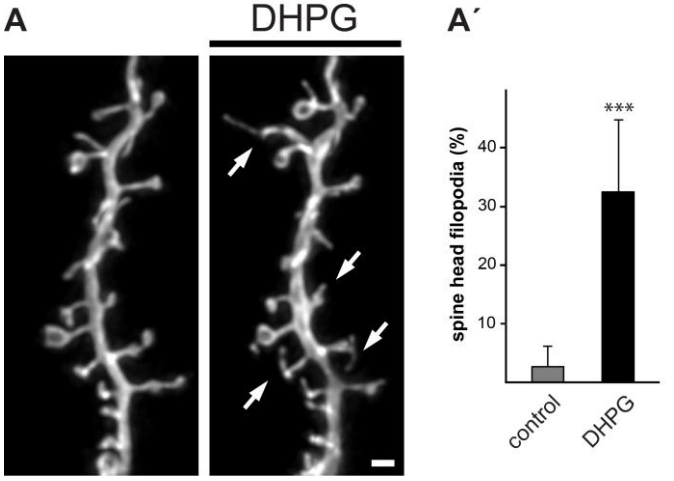

Figure 25. Activation of metabotropic glutamate receptors induces spine head modifications

(A – A´) Application of DHPG (500 μM) induces a strong increase in the proportion of spines that extending filopodia (arrows). The appearance of spine head changes is comparable to the muscarinic induced changes. *** $P < 0.001$, scale bar: 1 μm.

3.5.5 Activation of muscarinic receptors potentiates currents mediated by AMPA receptors

Next, we tested whether the structural alterations induced by MCh could lead to changes in synaptic function. To prevent epileptiform bursting during MCh application we recorded in the presence of TTX. Synaptic activity was mimicked by brief pressure application (200 - 300 msec) of AMPA (40 μM), via a micropipette positioned close to the soma. We recorded currents in CA1 pyramidal cells voltage-clamped at -70 mV. AMPA currents were pharmacologically isolated by adding D-AP5, picrotoxin, and TTX to the superfusing solution. After establishing a steady baseline of AMPA responses MCh was applied (100 μM, 5 min), which increased the amplitude of AMPA currents by 11.5 ± 1.5 % (n = 5; $P < 0.01$; Figure 26 C-D). Bath application of atropine (1 μM, n = 5, Figure 26 E-E') prevented the MCh-induced increase in AMPA currents (MCh + atropine: 5 ± 2 %,

P > 0.05 vs. baseline and *P* < 0.05 vs. MCh alone). This data included first evidence that our structural spine head changes may be accompanied by functional changes at the synapse.

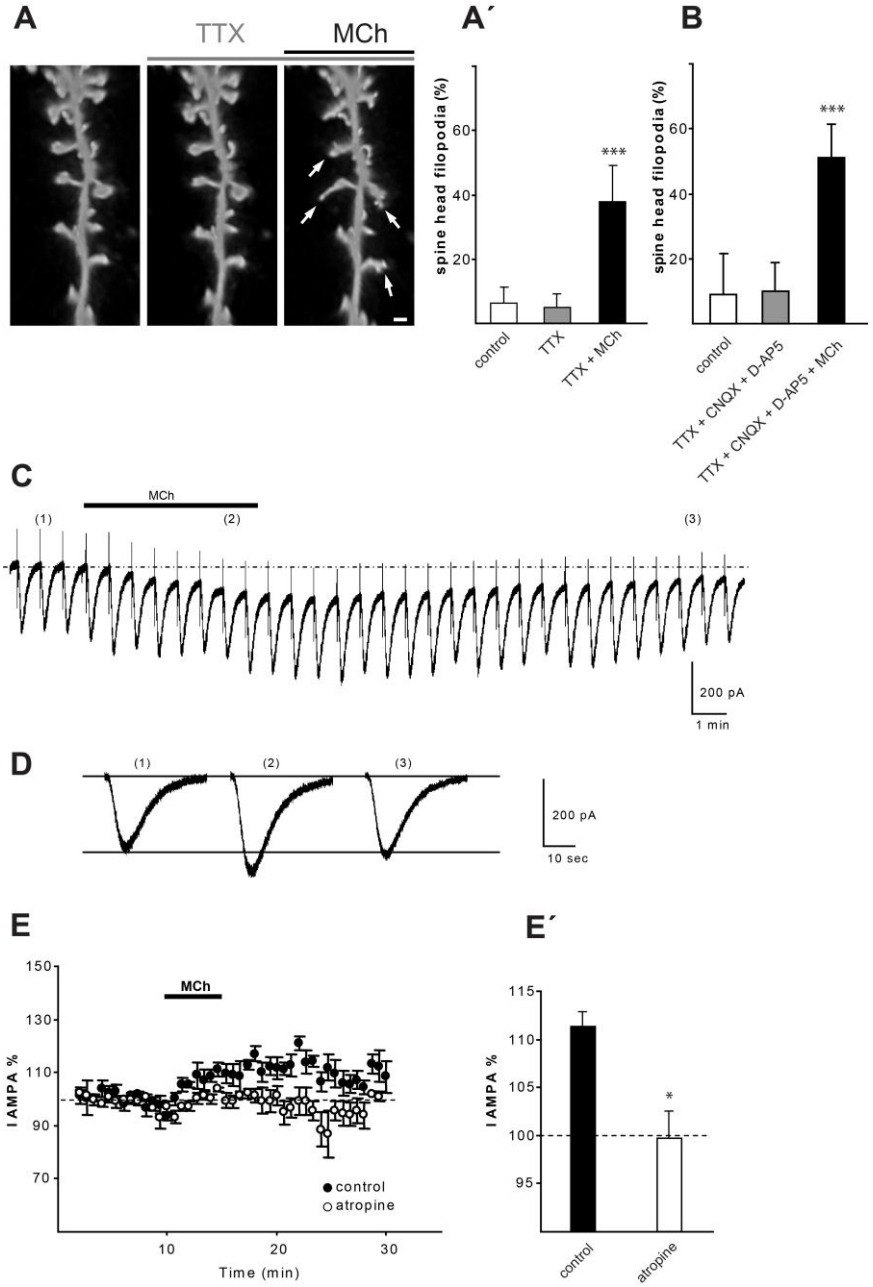

Figure 26. Synaptic activity is not required for generation of spine head filopodia

(A - A') Blockade of action potentials does not affect the induction of SHF by MCh. A 10 minute application of tetrodotoxin (TTX) alone at 1 µM does not alter spine head morphology. However, the application of TTX does not prevent MCh from inducing SHF (arrows). (B) Additional blockade of glutamatergic transmission does not impede the action of MCh on spine head morphology. When applied alone, a 10 minute application of TTX 1 µM, CNQX 25 µM and D-AP5 40 µM did not alter spine head morphology. When co-applied with MCh, however, this cocktail of blockers failed to stop the formation of SHF. (C) Activation of muscarinic receptors potentiates currents mediated by AMPA receptors in CA1 pyramidal cells. AMPA currents induced by pressure application of AMPA (50 µM for 200 msec) every 40 sec in presence of TTX are potentiated by bath application of MCh (100 µM for 5 min). (D) Representative AMPA current traces shown at an expanded time scale before (1) during (2)

and after (3) washout of MCh. (E) Atropine blocks the MCh-induced potentiation of AMPA current. (E), Average time course of the MCh-induced potentiation in presence (n = 4) or absence (n = 5) of atropine (1 µM). Atropine alone does not alter AMPA currents (n = 4). (E') Pooled data comparing responses after MCh alone and MCh in the presence of atropine; dashed lines indicate baseline or control responses. (Electrophysiological experiments performed by Dr. Jeanne Ster) * $P < 0.05$, *** $P < 0.001$, scale: 1 µm.

3.5.6 Induction of spine head filopodia is primarily dependent on microtubules

Filamentous actin (f-actin) is the primary cytoskeletal element in dendritic spines. It undergoes dynamic assembly and disassembly and allows the assumption that both the structure and function of spines is dictated by actin dynamics (Dent *et al.*, 2011). To determine the cytoskeletal component involved in the generation of SHF we applied blockers that interfere with cytoskeletal dynamics. SHF induced by MCh stimulation were not affected by the actin inhibitor cytochalasin D (10 µM; cytochalasin D: 5.2 ± 5.1 %; cytochalasin D + MCh: 29.8 ± 12.1 %; $P < 0.05$; n = 6 cultures; n = 7 dendrite; n = 134 spines; Figure 27 A). This was surprising given the known prominent role of actin-dependent spine remodelling (Fischer *et al.*, 1998). However, emerging evidences point to a role for microtubules in spine plasticity (Gu *et al.*, 2008; Hu *et al.*, 2008). Interestingly, we observed a significant reduction in SHF following treatment with 500 nM nocodazole (one hour preincubation), which prevents microtubule polymerisation (nocodazole: 5.2 ± 3.9 %; nocodazole + MCh: 8.1 ± 10.7 % $P > 0.05$; n = 6 cultures; n = 6 dendrites; n = 156 spines; $P < 0.05$; Figure 27 A). The finding that microtubule dynamics are involved in the generation of SHF, and can be induced by muscarinic receptor stimulation, cleared the field for a completely new interpretation of the potential role of this effect.

3.5.7 Formation of SHF affects mEPSC decay times

Electrophysiological experiments were performed to investigate possible functional consequences of these SHF. Whole-cell patch-clamp recordings were obtained from CA1 pyramidal cells, in the presence of TTX, before and after application of MCh. A global analysis of mEPSCs revealed an increase of the decay times (mean: 3.6 ± 0.3 ms in control and 4.7 ± 0.4 ms after MCh, $P < 0.05$, Student's t-test), also observed as a right shift in the cumulative distribution of the decay times of mEPSCs (Fig. 27 C). Application of MCh also affected mEPSP amplitude (control: -16.2 ± 1.8 pA, after MCh: -18.7 ± 1.6 pA, n = 5, Fig. 27 D). The rise time of mEPSCs was 2.8 ± 1.1 ms and did not change significantly after MCh application (data not shown). Next, we looked at whether cytoskeletal components were involved in the modification of decay times. Nocodazole (preincubation for 1h and maintained application during recordings) prevented the increase in tau decay times after application of MCh (n = 5, mean: 2.6 ± 0.2 ms in control and 2.7 ± 0.3 ms after MCh, $P > 0.05$, Student's test, Fig. 27 D) and also the increase in mEPSC amplitude (n = 5, mean: -12.9 ± 0.6 ms in control and -14.7 ± 0.7 ms after MCh, $P > 0.05$, student test, Fig. 27 D). Together, these results suggest that activation of

muscarinic receptors changes spine structure such that diffusion or reuptake of glutamate from the synaptic cleft is decreased thereby enhancing synaptic transmission.

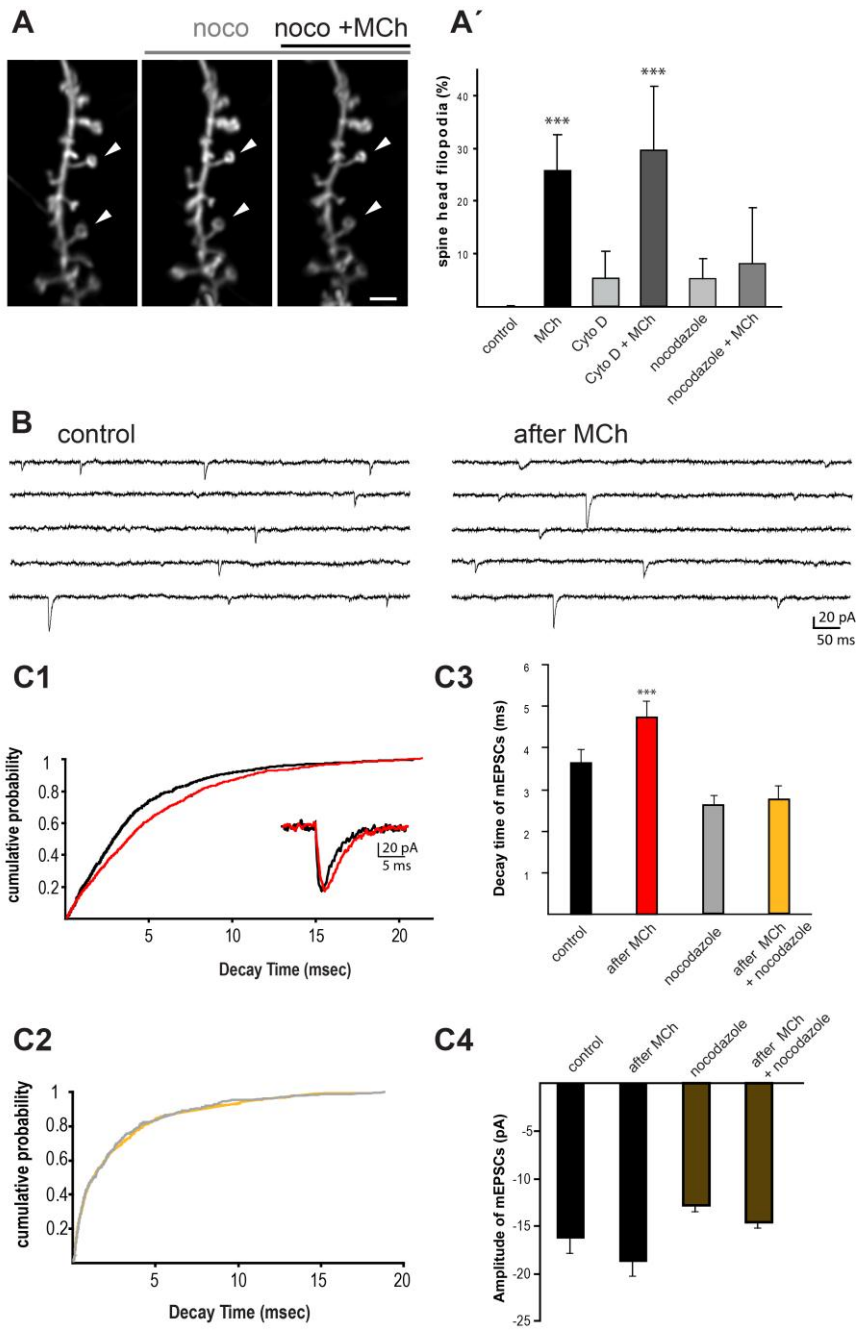

Figure 27. Spine head filopodia depend on microtubule dynamics

(A) Nocodazole, a microtubule polymerisation blocker, reduces the formation of SHF. Representative images of dendritic spines during treatment with nocodazole and MCh. Arrowheads point to representative spines. (A´) The actin polymerisation blocker, cytochalasin D, does not affect formation of SHF. (B) Traces show miniature synaptic excitatory currents (mEPSCs, TTX, D-AP5, and picrotoxin) in control conditions (left) and after application of MCh (100 µM; right). (C) Pooled data are represented as cumulative distributions of decay times in control conditions (n = 5, 400 events before and 527 events after MCh, $P < 0.0001$, Fig C1) or in the presence of nocodazole (n = 5, 361 events before and 478 events after MCh, $P > 0.05$. Fig C2). Quantification of decay time (C3) and amplitude (C4) of mEPSCs in control conditions, after MCh, in presence of nocodazole and after MCh + nocodazole. Scale bar: 2 µm.

3.5.8 SHF extend along the presynaptic membrane

To visualise the spatial relationship of SHF with respect to other synaptic components, we performed single and serial section electron microscopy (SSEM). The electron microscopy work was performed by Dr. José María Mateos. Hippocampal cultures were imaged with confocal microscopy to confirm the morphological alterations induced by MCh. Cultures were then immediately fixed and further processed for SSEM. Single section imaging revealed many cup-synapses (Roelandse *et al.*, 2003) as well as thin membrane extensions emerging from postsynaptic densities (Fig. 28 A and B). This finding was even more evident in serial sections, which allowed the reconstruction of longer structures (Fig. 28 C). In all 3D synapses studied (cultures n = 4; synapses in single sections n = 51; synapses in 3D n = 11) SHF extruded from the tip of the spine and extended along the presynaptic membrane.

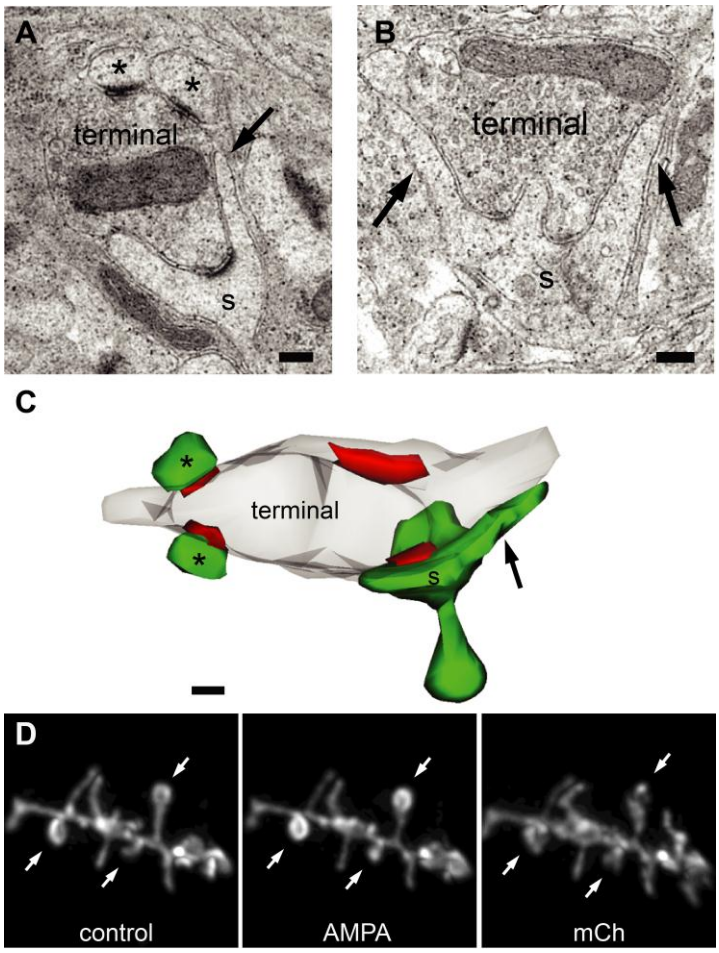

Figure 28. Spine head filopodia extend along the presynaptic terminal

Single (A and B) and serial sections (C), from slice cultures stimulated with MCh, show long protrusions (arrows) emanating from spine heads (s) and advancing along the presynaptic membrane (terminal). Some multisynaptic boutons (terminals in A and C) make contacts with round spines (asterisks) and with spines from which filopodia emerge (arrows in A and C). (D) Spine morphology becomes more regular after AMPA application (1 µM for 5 min) and, in the same dendrite, spines form SHF after MCh application (5 min). (EM experiments performed by Dr. José María Mateos) Scale bars: 0.2 µm.

Activation of AMPA receptors reduces spine head motility and caused spine heads to round up (Fischer *et al.*, 2000). Stimulation of muscarinic receptors creates the opposite effect and increases spine surface by the extension of SHF. We demonstrated both effects in our cultures by applying the two substances subsequently (Fig. 28 D). Inspired by the two forms of spine head modifications we created a functional model that interprets the structural modification as a potential approach to regulate transmitter diffusion from the synaptic cleft (Fig. 29).

4. Discussion

4.1 Functions of N-terminal agrin in the neurotrypsin-agrin system

Agrin cleavage by neurotrypsin releases a C-terminal fragment of 22 kD (agrin-22), which promotes the growth of dendritic filopodia (Matsumoto-Miyai *et al.*, 2009) and, thus, is an important regulator of structural plasticity in the CNS. The functional role of the N-terminal region of agrin, however, has not yet been extensively characterized.

In my thesis, I present evidence that N-terminal agrin mediates binding of neurotrypsin. Previous attempts to demonstrate this interaction by ELISA or Biacore based surface plasmon resonance did not result in significant readouts because of technical problems (see PhD thesis of D. Lüscher, 2008). For that reason, I used cell culture-based neurotrypsin binding assays and immunoprecipitations, which identified the glycosaminoglycan (GAG) chains and the agrin y4-splice insert as the responsible structures for agrin's ability to bind neurotrypsin. Currently, the mode of interaction between neurotrypsin and the GAG chains is not clarified yet. Kringle domains and SRCR repeats were reported to be involved in protein-protein interactions (Patthy *et al.*, 1984; Xu & Su, 2005). However, NMR-based structural analysis of the kringle domain of neurotrypsin showed only low affinity for heparin (Ozhogina *et al.*, 2008). Experimental evidence from our laboratory indicates that the protease domain alone is sufficient to bind to agrin, which could be mediated by a cluster of basic amino acids (D. Lüscher, PhD thesis). Surprisingly, the LG2 domain containing the heparin-binding site was at least twice as efficient in binding neurotrypsin compared to the GAG chains possessing constructs. The binding capacities of the LG2 domain is most likely mediated by the interaction with secreted glycoproteins.

The potential functions of the neurotrypsin-GAG binding are diverse: enhancement of agrin cleavage, neurotrypsin activation, spatial and/or temporal restriction of neurotrypsin activity. *In vitro* digestions of purified agrin variants showed that agrin cleavage by neurotrypsin is up to 4 times decreased when GAG chains are removed from the protein (D. Lüscher, PhD thesis). This indicates that GAGs have a significant impact on the proteolytic process, possibly by concentrating and guiding neurotrypsin to the cleavage sites. The latter hypothesis assumes that binding of neurotrypsin to GAGs possess a high dissociation constant. The fast association and dissociation rates measured in the Biacore experiment provide preliminary evidence for such an interaction (D. Lüscher,

PhD thesis). Neurotrypsin interaction with GAG may also have a function in the protease activation process. Recently, our laboratory demonstrated that synaptically released neurotrypsin requires coincident postsynaptic activation for the efficient cleavage of synaptic agrin (Matsumoto-Miyai *et al.*, 2009). We assume that neurotrypsin is released from the presynaptic terminal in a catalytically inactive stage and requires proteolytic cleavage for its activation. Our current model of this activation process involves a postsynaptic secretory proprotein convertase that is released upon postsynaptic activation. The binding of neurotrypsin to the GAG chains of agrin suggests that also the activation of neurotrypsin may take place while neurotrypsin is bound to agrin's GAG. Accordingly, two proprotein convertases, PC5A and PACE4, were reported to bind to heparin sulphate proteoglycans (Nour *et al.*, 2005; Mayer *et al.*, 2008). It is therefore likely that the responsible convertase for neurotrypsin activation binds to the GAG chains of agrin and that this interaction enhances the activation process. Preliminary data from our laboratory provide evidence for this hypothesis because we find decreased activation of neurotrypsin when agrin GAG chains lacking (unpublished results C. Gisler).

The neurotrypsin-agrin system promotes the formation of dendritic filopodia in an activity-dependent manner, by release of the agrin-22 cleavage product (Matsumoto-Miyai *et al.*, 2009). Dendritic filopodia are believed to form synaptic contacts when they get in contact with an appropriate presynaptic terminal (Knott *et al.*, 2006; Toni *et al.*, 2007). Agrin-22 is sufficient for the induction of filopodia and therefore, it may act as a signalling molecule that induces synaptic reorganisation. A prerequisite for such a signalling function are spatial and/or temporal regulation of the formation of agrin-22. Both could be mediated by the binding of neurotrypsin to agrin. Agrin is an abundant protein in the CNS expressed by neurons and astrocytes (Bezakova & Ruegg, 2003). The generation of agrin-22 strictly depends on the presence of activated neurotrypsin. Binding to agrin restricts the radius of operation of neurotrypsin to the place of release by limiting its diffusion. Thus, generation of agrin-22 is spatially restricted to synapses and its concentration gradient may provide positional information. It was planned to demonstrate this spatial restriction of neurotrypsin by live imaging of agrin cleavage in organotypic slice cultures. Unfortunately, I could not achieve sufficient expression of fluorescently labelled agrin to demonstrate this effect.

The association of neurotrypsin with the N-terminal region of agrin may further indicate a potential mechanism of neurotrypsin inactivation. Endocytosis of cleaved N-terminal agrin followed by endosomal degradation would terminate the activity of neurotrypsin. A basic requirement for this model is the demonstration of N-terminal agrin internalisation. I addressed this by performing immunocytochemistry and Western blotting experiments. However, these experiments did not reveal a clear indication for the endocytosis of agrin in hippocampal neuron cultures. A major problem was the low endogenous expression of agrin that required the use of viral overexpression. Ectopic protein expression, however, may interfere in the trafficking processes and overload the cellular system. There is evidence that agrin is unevenly distributed along the neuronal surface and accumulates in lipid rafts (Ramseger *et al.*, 2009). This suggests that also the internalisation of agrin

could occur at distinct subcellular locations. On dendritic spines agrin is found in perisynaptic and extrasynaptic locations (Stephan *et al.*, 2008). These regions contain specialised endocytic zones, which were postulated to regulate the composition of proteins in the PSD (Blanpied *et al.*, 2002; Racz *et al.*, 2004). Possibly, these structures also facilitate a quick internalisation of agrin after cleavage. For technical limitations I was not able to analyse endocytosis of agrin at spines. Instead, I analysed somatic internalisation of agrin by confocal microscopy and total uptake of N-terminal agrin by Western blotting. This approach could not detect the relatively small amounts of internalised agrin from spines when already the complete pool of axonal and dendritic agrin resulted in weak Western blot signals. Therefore, my results indicate that a general cellular mechanism for the endocytosis of cleaved N-terminal agrin is absent, while the internalisation of agrin at specialised subcellular locations cannot be ruled out.

Another well-documented feature of the N-terminal region of transmembrane agrin is the promotion of filopodia-like structures. Agrin overexpression (McCroskery *et al.*, 2006), as well as cell surface clustering of endogenous agrin by antibodies (Annies *et al.*, 2006), can induce the formation of these protrusions in both neurons and non-neural cells. A recent paper identified the GAG chains of agrin as an essential structure in mediating this effect (Lin *et al.*, 2010). Also other heparan sulphate proteoglycans are known to promote the formation of protrusions. Overexpression of syndecan-2 generates cellular protrusions that identically resemble the reported morphological changes induced by transmembrane agrin (Granes *et al.*, 1999). Unpublished data from our lab demonstrate that the filopodia-inducing properties of agrin are strongly reduced when the protein is co-expressed with neurotrypsin (PhD thesis A. Stephan). Interestingly, this effect is independent of the protease activity because also a proteolytic inactive variant of neurotrypsin reduced the formation of filopodia. Therefore, my results suggest that the reduction of the filopodia-promoting effect of agrin is caused by the interaction of neurotrypsin with agrin's GAG chains. This may also provide a hint on the mechanism of filopodia induction by agrin. Many growth factors, like fibroblast growth factor-2 or EGF-like growth factor, are known to bind to the GAG chains of heparan sulphate proteoglycans (Forsten-Williams *et al.*, 2008). A possible explanation for the neurotrypsin -mediated reduction in promoting filopodia structures may be the blockage of interaction sites for these heparin-binding growth factors on the GAG chains. Evidence for such a theory comes from the observation that application of heparin to the cell culture medium reduces formation of protrusions in syndecan-2 expressing cells (Granes *et al.*, 1999). It is therefore likely that the filopodia-inducing property of the N-terminal segment of agrin is mediated by the GAG chains. The binding of growth factors by agrin would strongly enlarge the functional spectrum of the molecule and could explain its suggested role in the formation of new synapses (McCroskery *et al.*, 2009).

Recently, it was reported that the N-terminally located follistatin domains of agrin are capable of binding several members of the TGF-β superfamily (Banyai *et al.*, 2010). This function points in a similar direction as above, that agrin may facilitate the signalling function of growth factors by their accumulation on the cell surface. Proteins of the TGF-

β superfamily are secreted cytokines which are involved in a multitude of developmental processes (Wu & Hill, 2009). Studies in *Drosophila* showed that TGF-β proteins provide retrograde signalling and thereby regulate synaptogenesis at the neuromuscular junction (Marques *et al.*, 2003; McCabe *et al.*, 2003). In the CNS, agrin expression peaks in the first postnatal week, which is the time of massive synaptogenesis. I hypothesised that binding of TGF-β proteins to agrin may modulate the formation of synapses during this phase. Synapse quantification in dissociated neuron cultures supplemented with TGF-β1 or BMP-2 resulted only in weak changes of synaptogenesis compared to control cultures. In contrast, application of TGF-β2 clearly increased (~30%) the formation of both pre- and postsynaptic elements. However, this result is in conflict with a study on TGF-β2-deficient mice that show a reduction of synaptic elements (Heupel *et al.*, 2008). A general weakness of my approach was the undetermined endogenous expression of TGF-β proteins by neurons and astrocytes. It is possible that an additional effect on synaptogenesis could not be observed because the system was already saturated by the baseline expression of TGF-β proteins. In principle, this could have been prevented by using TGF-β-deficient mice but this was beyond the scope of this project. The critical experiment for my hypothesis was the analysis of neuron cultures deficient for agrin. The deletion of agrin expression in neurons should abolish or at least reduce the effect of TGF-β on synaptogenesis to provide evidence for the validity of this model. However, the obtained results were not conclusive for pre- and postsynapses. The major problem in the quantifications was the strong variations within experiments. Dissociated neuron cultures, as other *in vitro* systems, are strongly reliant on extrinsic factors. The most important factor influencing synaptogenesis in this system is cell density (Fletcher *et al.*, 1994; Cullen *et al.*, 2010; Ivenshitz & Segal, 2010). The overall number of cells on the coverslip can be controlled during cell plating but the arrangement of cells is random and results in local differences of cell densities. This general problem of dissociated neuron cultures was circumvented by analysing an appropriately high number of samples. Therefore, I developed an automated image analysis system that facilitates quantification of large datasets with a minimum of user interaction (Schaetzle et al. 2011, J. Neuroscience Methods, manuscript submitted). The validity of this synapse quantification method was successful demonstrated on developing neurons at different developmental stages.

4.2 Metabotropic receptor activation induces spine head plasticity

This part of the discussion addresses structural changes in dendritic spine heads induced by activation of metabotropic receptors. Pyramidal CA1 neurons respond to methacholine stimulation with a pronounced morphological alteration, characterised by the emergence of thin membrane extensions from the spine heads. Time-lapse imaging showed the transient nature of these spine head filopodia, which rapidly and reversibly modify the shape of dendritic spines. These morphological changes were accompanied

by an increase in the decay time of excitatory synaptic responses (Schaetzle *et al.*, 2011). Apart from muscarinic stimulation, also activation of metabotropic glutamate receptors induces comparable spine head modifications (results in this thesis and Vanderklish & Edelman, 2002). SHF depend on microtubule dynamics and appear very rapidly (within a few minutes) suggesting that they do not form synaptic contacts. These results point to a new form of structural plasticity induced by metabotropic receptor activation occuring at the subspine level and which might modulate synaptic transmission.

Filopodia-like extensions have been reported to emerge from spine heads in hippocampal neurons. They are postulated to compete for axonal boutons during the development of neuronal networks (Konur & Yuste, 2004). Spine head filopodia in mature hippocampal neurons have also been reported after a 48 hour treatment with the GABAA receptor antagonist gabazine, which causes epileptiform activity. This chronic hyperexcitability promoted the formation of long-lived filopodia that emerged mainly from PSD-positive structures (Zha *et al.*, 2005). In contrast, application of MCh or DHPG, which can also induce epileptiform activity, resulted in a much faster formation of SHF and affected all imaged neurons. Moreover, methacholine-induced SHF were not altered when epileptiform activity was prevented by addition of TTX and antagonists of AMPA/kainate and NMDA receptors. The induction of SHF by MCh was, however, blocked by atropine, a muscarinic acetylcholine receptor antagonist. Group I metabotropic glutamate receptors and muscarinic receptors in the hippocampus are expressed in dendrites and extrasynaptic regions of spines in hippocampal pyramidal cells (Lopez-Bendito *et al.*, 2002; Yamasaki *et al.*, 2010). Therefore, formation of SHF can be rapidly induced by activation of metabotropic receptors located on spine heads.

The appearance of filopodia-like extension is believed to indicate synaptic reorganisation at the dendrite (Zuo *et al.*, 2005; Toni *et al.*, 2007). High turnover of spines and spine remodelling are prominent during the early postnatal development and are necessary for establishing functional synaptic circuits. Spine plasticity is also observed in mature neurons of adult animals and include changes of spine type (Matsuzaki *et al.*, 2004) and spine turnover (Holtmaat *et al.*, 2005; De Roo *et al.*, 2008), although to a lesser extent than during development. The metabotropic receptor-dependent SHF identified in our experiments are unlikely to contribute to new postsynaptic contacts for two reasons: First, all SHF identified by EM were devoid of a PSD specialisation. Second, SHF were very transient and its maintenance depend on the sustained activation of the receptors. Under physiological conditions SHF were short-lived and rarely found, indicating that the required concentrations of acetylcholine and glutamate are relatively unusual. The establishment of synapses requires minutes to hours to form which is much longer than the observed average live times of these SHF (Nagerl *et al.*, 2007; Zito *et al.*, 2009). Nevertheless, the appearance of SHF might indicate the induction of plastic changes that emerge over a longer time scale. To address this, we analysed spine morphology, following MCh stimulation, over two days. However, we did not observe significant changes in spine turnover or spine type changes between MCh-stimulated and non-

stimulated control cultures. This result is in conflict with data from De Roo and colleagues who reported an increased protrusion turnover after stimulation with the cholinergic agonist carbachol (De Roo *et al.*, 2008). Beside the use of MCh instead of carbachol, we applied a considerably shorter drug incubation time (5 min vs. 20-60 min) that is likely to account for the found discrepancy. In general, one could question if bath application, and thus global activation of the culture, is a good approach to induce long-term plasticity on the level of single spines.

Plasticity induced by metabotropic receptors massively alters spine head morphology in a short time frame and this effect is reversible and re-inducible. In organotypic slice cultures, almost half of the spines on CA1 pyramidal cells were affected, indicating that mature spines maintain the capacity to respond as a population to sudden stimulation of metabotropic receptors. Confocal time-lapse imaging in combination with electron microscopy showed that spine heads maintain a high degree of plasticity (Dunaevsky *et al.*, 1999; Roelandse *et al.*, 2003). Half of all spines presented a cup form with continuous changes in shape involving actin-rich extensions (Roelandse *et al.*, 2003). Further, several studies reported small movements of spine heads in mature neurons, which are dependent on actin polymerisation (Fischer *et al.*, 1998; Dunaevsky *et al.*, 1999; Fischer *et al.*, 2000; Ackermann & Matus, 2003; Roelandse *et al.*, 2003). The actin motilities are inhibited by activation of AMPA receptors that results in a conversion from irregular shaped spines into round spines with stable heads (Fischer *et al.*, 2000; and our data Fig 28 D). This effect is reversible, affects a large population of spines, and shows a time course similar to our present results. Interestingly, the metabotropic effect we observed is just the opposite, in that activation of muscarinic receptors converts round spines into spines with SHF. Our EM data of MCh stimulated spines demonstrate that SHF extend along the presynaptic terminals. The structural appearance in the three-dimensional reconstructions suggested that extension of SHF may insulate the synaptic cleft from the extracellular space and may prevent transmitter diffusion and spillover. Neurotransmitter spillover is controlled by glutamate transporters located at astrocytic processes (Diamond & Jahr, 1997; Oliet *et al.*, 2001), which thereby regulate synaptic activity (Panatier *et al.*, 2006). Astrocytes rapidly extend and retract processes in close proximity to dendritic spines (Haber *et al.*, 2006). 3D electron microscopy studies have determined that glial processes tend to be associated with dendritic spines rather than with presynaptic terminals (Lehre & Rusakov, 2002). Furthermore, glial coverage of synaptic elements is highly sensitive to levels of neuronal activity (Genoud *et al.*, 2006; Lushnikova *et al.*, 2009) and exhibits kinetics which suggest that this process could compete in time and space with SHF (Hirrlinger *et al.*, 2004). Our electron microscopic data indicate that emerging SHF are aimed towards presynaptic elements and we recorded longer decay times of miniature EPSCs suggesting that by reducing the access of astrocytes to the synaptic cleft, SHF may promote the exposure of dendritic spines to synaptically released neurotransmitter. Based on these observations we created a model that suggests modification of the spine shape as a regulatory element on synaptic transmission (Fig 29). Here, activation of AMPA receptors is followed by a rounding of

spines, which facilitate transmitter diffusion and spillover. In contrast, extension of SHF reduces the contact with the extrasynaptic space and prolongs activity of the neurotransmitter.

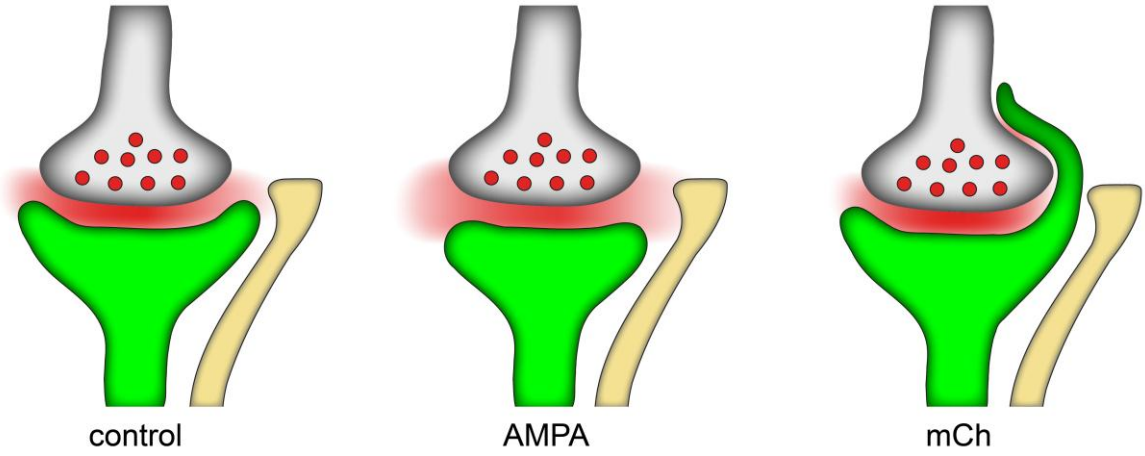

Figure 29. Model of structural spine head plasticity

Activation of AMPA receptors causes spine heads to become more round. The opening to the extrasynaptic space is widened and glutamate diffusion/astrocytic uptake improve. In contrast, MCh application induces the extension of long SHF along the terminals reducing the capacity of glutamate to diffuse out of the synaptic cleft.

Filamentous actin (F-actin) is the major cytoskeleton component within spines (Hotulainen & Hoogenraad, 2010). Structural modifications in dendritic spines are, therefore, believed to depend primarily on changes of actin filaments. Surprisingly, we could not observe a reduction in SHF when we blocked actin dynamics by cytochalasin D, indicating that the driving force of SHF induction is actin-independent. Recent evidence supports an involvement of microtubules in altering spine head shape (Hoogenraad & Akhmanova, 2010; Dent *et al.*, 2011). Microtubule invasion of dendritic spines is enhanced by synaptic activity and is a transient process that affects a relatively small proportion of spines. Indeed, we could show that the MCh-induced formation of SHF is strongly reduced when microtubule dynamics were inhibited by nocodazole.

Interestingly, in few cases, the presence of microtubules in spine heads was reported to be associated with the extension of transient spine head protrusions (Hu *et al.*, 2008). The dynamics of this process was investigated by time-lapse recordings of the microtubule-binding protein EB3. The initial extension of the spine head protrusion was triggered by invasion of a microtubule, visualised by the EB3-eGFP signal at the tip of this protrusion. Subsequently, the first protrusion was followed by a more dramatic spine head alteration that depends on actin polymerisation and exhibit several short protrusions and lamellipodia formation (Fig. 6 d in Hu *et al.*, 2008). This suggests that the presence of microtubules in dendritic spine may produce sustained influence on actin dynamics. Indeed EB3 was reported to bind to p140Cap, which is localised in the postsynaptic density (Jaworski *et al.*, 2009). The protein regulates Src tyrosine kinase activity (Di Stefano *et al.*, 2007) and is likely to induce a signalling cascade that leads to

Arp2/3 complex activation (Hotulainen & Hoogenraad, 2010). This is consistent with our finding that MCh activation mostly induces only single protrusions in thin spines (resulting only from the microtubule extension), while actin rich mushroom spines mostly generate a more complex appearance (based on microtubule and actin dynamics). However, this raises the question why we did not observe a difference in spine head morphology after blockage of actin dynamics by cytochalasin D. It is likely that we missed these delicate changes because the quantification method for this assay was optimised to detect spine head changes rather quantitatively than qualitatively. The initial morphological change induced by the invasion of the microtubule was, therefore, sufficient to count the spine as a responder to MCh.

Another striking feature is the promoting effect of synaptic activity on microtubule invasion (Hu *et al.*, 2008; Mitsuyama *et al.*, 2008). We have demonstrated that beside cholinergic also glutamergic stimulation can induce spine head modifications by activation of metabotropic glutamate receptors. Ionotropic glutamate receptors are probably not critically involved because their blockage did not prevent the morphological spine head changes. Increased levels of glutamate induced by neuronal depolarisation further extend the time microtubules remain inside of spine heads (Hu *et al.*, 2008). This is remarkable considering the otherwise transient character (mean of about 3 min) of the spine invasion (Dent *et al.*, 2011). Similarly, our data demonstrate that the appearance of spine head filopodia closely correlates with the presence of the drug and wash-out leads to quick recovery of spine heads within minutes.

Currently, the mechanism that regulates microtubules entry into spines is unclear. The overall high microtubule dynamics, but only low absolute number (~1%) of microtubule positive spines at a given time-point, indicates the involvement of a restrictive component. Live imaging data showed that microtubules exclusively depart from the dendritic shaft and enter the spine through the spine neck (Hu *et al.*, 2008; Jaworski *et al.*, 2009). Both, the localisation of muscarinic and metabotropic glutamate receptors at spines, as well as the enhancing effect of synaptic activity, suggest that the regulation could emerge from inside the spine. A recent study using platinum replica electron microscopy, present high resolution images of the cytoskeletal arrangement within spines (Korobova & Svitkina, 2010). Spine necks of thin and mushroom spines are composed of a dense arrangement of linear and branched actin filaments. Additionally, they are enriched with nonmuscle myosin II motor protein, which can induce contractile forces and tension by association with actin filaments (Korobova & Svitkina, 2010; Parsons *et al.*, 2010). Given the relatively big diameter of microtubules, it might be possible that the actin-myosin II network is capable of providing a structural barrier against spine invasion. The activity of myosin II can be regulated by phosphorylation (Vicente-Manzanares *et al.*, 2009), which would provide a mechanism to control spine neck passability. The groups of muscarinic and metabotropic glutamate receptors coupling to the $G_{i/o}$-type pathway activate PKC that was shown to phosphorylate myosin II (Vicente-Manzanares *et al.*, 2009). During blockage of actin by cytochalasin D we observed a slightly stronger MCh effect compared to only MCh stimulation. In the model

above the disruption of the actin cytoskeleton would provide an additive effect in reducing the barrier for microtubule entry into the spine neck. Therefore, this result might be interpreted as an argument in favour of this hypothesis. In this context, it is very interesting that functional inhibition of myosin IIB (the predominant isoform in spines) induces the formation of spine head filopodia in dissociated neuronal cultures (Ryu *et al.*, 2006; Rubio *et al.*, 2011). However, it remains to be elucidated if these protrusions result from spine invasion by microtubules or altered actin dynamics.

What could be the functional role of transient microtubule invasion into dendritic spines? Incubation in nocodazole decreases the number of mushroom spines and increases the number of filopodia, without affecting the total number of protrusions (Jaworski *et al.*, 2009). The same study also shows that RNAi-mediated EB3 knock-down results in an increased number of thin filopodia-like spines, while overexpression of EB3 increases the number of mushroom spines (Jaworski *et al.*, 2009). Further, microtubules target mushroom-shaped spines more frequently than thin spines or filopodia-like protrusions (Hu *et al.*, 2008; Hoogenraad & Akhmanova, 2010). Together, these studies suggest that microtubule invasion in dendritic spines promotes maturation and maintenance of mushroom spines.

Microtubules are the major long-distance transport machinery in neurons. Dendritic microtubules have mixed orientations (Baas *et al.*, 1988), while in contrast all microtubules that enter spines grow with their plus-end towards the spine head and manifest a uniform directionality (Hoogenraad & Bradke, 2009). This facilitates a specific kinesin-mediated delivery and/or dynein-mediated removal of vesicular synaptic cargo. The potential spine cargo is manifold, including neurotransmitter receptors, ion channels, signalling complexes, and mRNAs. Dendritic delivery of polyribosomes, organelles and smooth endoplasmic reticulum also depends on microtubule-associated transport and might be directly guided into spines (Ostroff *et al.*, 2002; Zinsmaier *et al.*, 2009; Ramirez & Couve, 2011). The speed of kinesin and dynein driven transport is much faster than microtubule polymerisation/depolymerisation and thus enables the transport of substantial amounts of cargo even during the relatively short time of spine invasion (Dent *et al.*, 2011). Microtubule invasion in spines could therefore play a role in modifying not only structural, but also functional properties of spines and our data suggest that this process is controlled by the activation of metabotropic receptors.

Brain disorders can be associated with genetic alterations that make it possible to draw conclusion about the functional role of the affected proteins. Dysfunctions of microtubule associated proteins have been linked to several brain disorders (Gu & Zheng, 2009). Williams syndrome is a mild mental retardation that is caused by mutations on chromosome 7 and involves among others the gene encoding for CLIP-115. The microtubule plus-end binding protein CLIP-115 interacts with EB1 and EB3 and regulates microtubule dynamics (Komarova *et al.*, 2005). Mice deficient for CLIP-115 show changes in LTP and an altered fear response, indicating a defect in hippocampus-dependent learning (Hoogenraad *et al.*, 2004). Mutations in the gene DISC1 strongly

increase the risk for schizophrenia and bipolar disorder. The protein is involved in dendritic development and spine formation in adult newborn neurons (Duan *et al.*, 2007). Analysis of the subcellular location shows enrichment at the PSD of spines and association with microtubules, probably mediated by interaction with microtubule associated protein 1A (Morris *et al.*, 2003; Kirkpatrick *et al.*, 2006). Recently, it has been demonstrated that DISC1 regulates Rac1 activity in response to NMDA receptors, thereby controlling spine morphology (Hayashi-Takagi *et al.*, 2010). This finding may explain the decreased densities of dendritic spines found on pyramidal cells of schizophrenia patients (Garey *et al.*, 1998). The fragile X syndrome is the most common form of inherited mental retardation. Fragile X mental retardation protein (FMRP) regulates translation of the microtubule associated protein 1B (MAP1B) and thereby indirectly controls the stability of microtubule networks (Lu *et al.*, 2004; Menon *et al.*, 2008). Adult FMRP-deficient mice show a loss of mushroom shaped spines and an increase of immature spines like thin spines and filopodia (Galvez & Greenough, 2005). Interestingly, this phenotype is similar to the report of EB3 knock-down that is also described as a shift to more filopodia-like spines at the cost of mushroom spines (Jaworski *et al.*, 2009). It would be interesting to investigate whether these mouse models of brain diseases also comprise alterations of microtubule invasion into spine.

Given the prominent function of acetylcholine in learning and memory (Hasselmo & McGaughy, 2004; Hasselmo, 2006), it is tempting to speculate about a potential involvement of microtubule-mediated spine modifications in this process. High levels of acetylcholine are implicated with enhancement in attention and the encoding of information in memory. Recent studies indicate that the encoding of behavioural task directly affects the structural configuration of dendritic spines (Xu *et al.*, 2009; Yang *et al.*, 2009). Our data provide a link between cholinergic activation and structural modification of spines. Several studies report that spine invasion by microtubules promotes stabilisation of mushroom spines and may also be involved in the maturation of thin to mushroom spines (Hu *et al.*, 2008; Jaworski *et al.*, 2009; Hoogenraad & Akhmanova, 2010). Our data suggests that both muscarinic and metabotropic glutamate receptors may mediate microtubule entry in spines, which indicates that this process is controlled by at least two independent pathways. Additionally, our electrophysiological data suggests that the structural modifications might also affect synaptic transmission. It remains to be elucidated if the muscarinic driven spine plasticity can be regarded as the cellular equivalence of enhanced attention and improved encoding of memory.

5. References

Abraham WC and Williams JM. (2008). LTP maintenance and its protein synthesis-dependence. *Neurobiol Learn Mem* **89,** 260-268.

Ackermann M and Matus A. (2003). Activity-induced targeting of profilin and stabilization of dendritic spine morphology. *Nat Neurosci* **6,** 1194-1200.

Ahmed T and Frey JU. (2005). Plasticity-specific phosphorylation of CaMKII, MAP-kinases and CREB during late-LTP in rat hippocampal slices in vitro. *Neuropharmacology* **49,** 477-492.

Aimes RT, Zijlstra A, Hooper JD, Ogbourne SM, Sit ML, Fuchs S, Gotley DC, Quigley JP and Antalis TM. (2003). Endothelial cell serine proteases expressed during vascular morphogenesis and angiogenesis. *Thromb Haemost* **89,** 561-572.

Almonte AG and Sweatt JD. (2011). Serine proteases, serine protease inhibitors, and protease-activated receptors: Roles in synaptic function and behavior. *Brain Res*.

Andersen P. (2007). *The hippocampus book*. Oxford University Press, Oxford ; New York.

Andersen P, Blackstad TW and Lomo T. (1966). Location and identification of excitatory synapses on hippocampal pyramidal cells. *Exp Brain Res* **1,** 236-248.

Annies M, Bittcher G, Ramseger R, Loschinger J, Woll S, Porten E, Abraham C, Ruegg MA and Kroger S. (2006). Clustering transmembrane-agrin induces filopodia-like processes on axons and dendrites. *Mol Cell Neurosci* **31,** 515-524.

Aoyagi A, Nishikawa K, Saito H and Abe K. (1994). Characterization of basic fibroblast growth factor-mediated acceleration of axonal branching in cultured rat hippocampal neurons. *Brain Res* **661,** 117-126.

Araya R, Jiang J, Eisenthal KB and Yuste R. (2006). The spine neck filters membrane potentials. *Proc Natl Acad Sci U S A* **103,** 17961-17966.

Arellano JI, Benavides-Piccione R, Defelipe J and Yuste R. (2007). Ultrastructure of dendritic spines: correlation between synaptic and spine morphologies. *Front Neurosci* **1,** 131-143.

Baas PW, Deitch JS, Black MM and Banker GA. (1988). Polarity orientation of microtubules in hippocampal neurons: uniformity in the axon and nonuniformity in the dendrite. *Proc Natl Acad Sci U S A* **85,** 8335-8339.

Bahr BA. (1995). Long-term hippocampal slices: a model system for investigating synaptic mechanisms and pathologic processes. *J Neurosci Res* **42,** 294-305.

Banker G and Goslin K. (1998). *Culturing nerve cells*. MIT Press, Cambridge, Mass.

Banker GA and Cowan WM. (1979). Further observations on hippocampal neurons in dispersed cell culture. *J Comp Neurol* **187,** 469-493.

Banyai L, Sonderegger P and Patthy L. (2010). Agrin binds BMP2, BMP4 and TGFbeta1. *PLoS One* **5,** e10758.

Barbara JG. (2002). IP3-dependent calcium-induced calcium release mediates bidirectional calcium waves in neurones: functional implications for synaptic plasticity. *Biochim Biophys Acta* **1600,** 12-18.

Barnes SJ and Finnerty GT. (2010). Sensory experience and cortical rewiring. *Neuroscientist* **16,** 186-198.

Barria A, Muller D, Derkach V, Griffith LC and Soderling TR. (1997). Regulatory phosphorylation of AMPA-type glutamate receptors by CaM-KII during long-term potentiation. *Science* **276,** 2042-2045.

Bayer SA. (1980). Development of the hippocampal region in the rat. II. Morphogenesis during embryonic and early postnatal life. *J Comp Neurol* **190,** 115-134.

Bayer SA and Altman J. (1974). Hippocampal development in the rat: cytogenesis and morphogenesis examined with autoradiography and low-level X-irradiation. *J Comp Neurol* **158,** 55-79.

Bear MF, Connors BW and Paradiso MA. (2007). *Neuroscience : exploring the brain*. Lippincott Williams & Wilkins, Philadelphia, PA.

Beaulieu C and Colonnier M. (1987). Effect of the richness of the environment on the cat visual cortex. *J Comp Neurol* **266,** 478-494.

Becker N, Wierenga CJ, Fonseca R, Bonhoeffer T and Nagerl UV. (2008). LTD induction causes morphological changes of presynaptic boutons and reduces their contacts with spines. *Neuron* **60,** 590-597.

Bergstrom RA, Sinjoanu RC and Ferreira A. (2007). Agrin induced morphological and structural changes in growth cones of cultured hippocampal neurons. *Neuroscience* **149,** 527-536.

Bezakova G and Ruegg MA. (2003). New insights into the roles of agrin. *Nat Rev Mol Cell Biol* **4,** 295-308.

Bhatt DH, Zhang S and Gan WB. (2009). Dendritic spine dynamics. *Annu Rev Physiol* **71,** 261-282.

Blanpied TA, Scott DB and Ehlers MD. (2002). Dynamics and regulation of clathrin coats at specialized endocytic zones of dendrites and spines. *Neuron* **36,** 435-449.

Bloodgood BL and Sabatini BL. (2005). Neuronal activity regulates diffusion across the neck of dendritic spines. *Science* **310,** 866-869.

Bolliger MF, Zurlinden A, Luscher D, Butikofer L, Shakhova O, Francolini M, Kozlov SV, Cinelli P, Stephan A, Kistler AD, Rulicke T, Pelczar P, Ledermann B, Fumagalli G, Gloor SM, Kunz B and Sonderegger P. (2010). Specific proteolytic cleavage of agrin regulates maturation of the neuromuscular junction. *J Cell Sci* **123,** 3944-3955.

Bonhoeffer T and Yuste R. (2002). Spine motility. Phenomenology, mechanisms, and function. *Neuron* **35,** 1019-1027.

Bose CM, Qiu D, Bergamaschi A, Gravante B, Bossi M, Villa A, Rupp F and Malgaroli A. (2000). Agrin controls synaptic differentiation in hippocampal neurons. *J Neurosci* **20,** 9086-9095.

Bourne J and Harris KM. (2007). Do thin spines learn to be mushroom spines that remember? *Curr Opin Neurobiol* **17,** 381-386.

Bourne JN and Harris KM. (2008). Balancing Structure and Function at Hippocampal Dendritic Spines. *Annu Rev Neurosci*.

Bourne JN and Harris KM. (2011). Coordination of size and number of excitatory and inhibitory synapses results in a balanced structural plasticity along mature hippocampal CA1 dendrites during LTP. *Hippocampus* **21,** 354-373.

Bozdagi O, Nagy V, Kwei KT and Huntley GW. (2007). In vivo roles for matrix metalloproteinase-9 in mature hippocampal synaptic physiology and plasticity. *J Neurophysiol* **98,** 334-344.

Bredt DS and Nicoll RA. (2003). AMPA receptor trafficking at excitatory synapses. *Neuron* **40,** 361-379.

Bulow HE and Hobert O. (2006). The molecular diversity of glycosaminoglycans shapes animal development. *Annu Rev Cell Dev Biol* **22,** 375-407.

Burgess RW, Dickman DK, Nunez L, Glass DJ and Sanes JR. (2002). Mapping sites responsible for interactions of agrin with neurons. *J Neurochem* **83,** 271-284.

Burgess RW, Nguyen QT, Son YJ, Lichtman JW and Sanes JR. (1999). Alternatively spliced isoforms of nerve- and muscle-derived agrin: their roles at the neuromuscular junction. *Neuron* **23,** 33-44.

Burnashev N, Khodorova A, Jonas P, Helm PJ, Wisden W, Monyer H, Seeburg PH and Sakmann B. (1992). Calcium-permeable AMPA-kainate receptors in fusiform cerebellar glial cells. *Science* **256,** 1566-1570.

Cajigas IJ, Will T and Schuman EM. (2010). Protein homeostasis and synaptic plasticity. *EMBO J* **29,** 2746-2752.

Calabrese B, Wilson MS and Halpain S. (2006). Development and regulation of dendritic spine synapses. *Physiology (Bethesda)* **21,** 38-47.

Chan CS, Weeber EJ, Kurup S, Sweatt JD and Davis RL. (2003). Integrin requirement for hippocampal synaptic plasticity and spatial memory. *J Neurosci* **23,** 7107-7116.

Chklovskii DB, Mel BW and Svoboda K. (2004). Cortical rewiring and information storage. *Nature* **431,** 782-788.

Christopherson KS, Ullian EM, Stokes CC, Mullowney CE, Hell JW, Agah A, Lawler J, Mosher DF, Bornstein P and Barres BA. (2005). Thrombospondins are astrocyte-secreted proteins that promote CNS synaptogenesis. *Cell* **120,** 421-433.

Citri A and Malenka RC. (2008). Synaptic plasticity: multiple forms, functions, and mechanisms. *Neuropsychopharmacology* **33,** 18-41.

Cohen NA, Kaufmann WE, Worley PF and Rupp F. (1997). Expression of agrin in the developing and adult rat brain. *Neuroscience* **76,** 581-596.

Cotman SL, Halfter W and Cole GJ. (1999). Identification of extracellular matrix ligands for the heparan sulfate proteoglycan agrin. *Exp Cell Res* **249,** 54-64.

Cullen DK, Gilroy ME, Irons HR and Laplaca MC. (2010). Synapse-to-neuron ratio is inversely related to neuronal density in mature neuronal cultures. *Brain Res* **1359,** 44-55.

Dailey ME and Smith SJ. (1996). The dynamics of dendritic structure in developing hippocampal slices. *J Neurosci* **16,** 2983-2994.

De Paola V, Arber S and Caroni P. (2003). AMPA receptors regulate dynamic equilibrium of presynaptic terminals in mature hippocampal networks. *Nat Neurosci* **6,** 491-500.

De Paola V, Holtmaat A, Knott G, Song S, Wilbrecht L, Caroni P and Svoboda K. (2006). Cell type-specific structural plasticity of axonal branches and boutons in the adult neocortex. *Neuron* **49,** 861-875.

De Roo M, Klauser P and Muller D. (2008). LTP promotes a selective long-term stabilization and clustering of dendritic spines. *PLoS Biol* **6,** e219.

De Simoni A, Griesinger CB and Edwards FA. (2003). Development of rat CA1 neurones in acute versus organotypic slices: role of experience in synaptic morphology and activity. *J Physiol* **550,** 135-147.

Dent EW, Merriam EB and Hu X. (2011). The dynamic cytoskeleton: backbone of dendritic spine plasticity. *Curr Opin Neurobiol* **21,** 175-181.

Dent EW, Tang F and Kalil K. (2003). Axon guidance by growth cones and branches: common cytoskeletal and signaling mechanisms. *Neuroscientist* **9,** 343-353.

Denzer AJ, Brandenberger R, Gesemann M, Chiquet M and Ruegg MA. (1997). Agrin binds to the nerve-muscle basal lamina via laminin. *J Cell Biol* **137,** 671-683.

Descarries L, Gisiger V and Steriade M. (1997). Diffuse transmission by acetylcholine in the CNS. *Prog Neurobiol* **53,** 603-625.

Di Stefano P, Damiano L, Cabodi S, Aramu S, Tordella L, Praduroux A, Piva R, Cavallo F, Forni G, Silengo L, Tarone G, Turco E and Defilippi P. (2007). p140Cap protein suppresses tumour cell properties, regulating Csk and Src kinase activity. *EMBO J* **26,** 2843-2855.

Diamond JS and Jahr CE. (1997). Transporters buffer synaptically released glutamate on a submillisecond time scale. *J Neurosci* **17,** 4672-4687.

Diekelmann S and Born J. (2010). The memory function of sleep. *Nat Rev Neurosci* **11,** 114-126.

Dino MR, Harroch S, Hockfield S and Matthews RT. (2006). Monoclonal antibody Cat-315 detects a glycoform of receptor protein tyrosine phosphatase beta/phosphacan early in CNS development that localizes to extrasynaptic sites prior to synapse formation. *Neuroscience* **142,** 1055-1069.

Dityatev A and Schachner M. (2003). Extracellular matrix molecules and synaptic plasticity. *Nat Rev Neurosci* **4,** 456-468.

Dityatev A, Schachner M and Sonderegger P. (2010). The dual role of the extracellular matrix in synaptic plasticity and homeostasis. *Nat Rev Neurosci* **11,** 735-746.

Dotti CG, Sullivan CA and Banker GA. (1988). The establishment of polarity by hippocampal neurons in culture. *J Neurosci* **8,** 1454-1468.

Duan X, Chang JH, Ge S, Faulkner RL, Kim JY, Kitabatake Y, Liu XB, Yang CH, Jordan JD, Ma DK, Liu CY, Ganesan S, Cheng HJ, Ming GL, Lu B and Song H. (2007). Disrupted-In-Schizophrenia 1 regulates integration of newly generated neurons in the adult brain. *Cell* **130,** 1146-1158.

Dunaevsky A, Tashiro A, Majewska A, Mason C and Yuste R. (1999). Developmental regulation of spine motility in the mammalian central nervous system. *Proc Natl Acad Sci U S A* **96,** 13438-13443.

Ehlers MD. (2003). Activity level controls postsynaptic composition and signaling via the ubiquitin-proteasome system. *Nat Neurosci* **6,** 231-242.

Engert F and Bonhoeffer T. (1999). Dendritic spine changes associated with hippocampal long-term synaptic plasticity. *Nature* **399,** 66-70.

Ethell IM and Pasquale EB. (2005). Molecular mechanisms of dendritic spine development and remodeling. *Prog Neurobiol* **75,** 161-205.

Evers MR, Salmen B, Bukalo O, Rollenhagen A, Bosl MR, Morellini F, Bartsch U, Dityatev A and Schachner M. (2002). Impairment of L-type Ca2+ channel-dependent forms of hippocampal synaptic plasticity in mice deficient in the extracellular matrix glycoprotein tenascin-C. *J Neurosci* **22,** 7177-7194.

Faissner A, Pyka M, Geissler M, Sobik T, Frischknecht R, Gundelfinger ED and Seidenbecher C. (2010). Contributions of astrocytes to synapse formation and maturation - Potential functions of the perisynaptic extracellular matrix. *Brain Res Rev* **63,** 26-38.

Ferreira A. (1999). Abnormal synapse formation in agrin-depleted hippocampal neurons. *J Cell Sci* **112 (Pt 24),** 4729-4738.

Fiala JC, Spacek J and Harris KM. (2002). Dendritic spine pathology: cause or consequence of neurological disorders? *Brain Res Brain Res Rev* **39,** 29-54.

Fischer M, Kaech S, Knutti D and Matus A. (1998). Rapid actin-based plasticity in dendritic spines. *Neuron* **20,** 847-854.

Fischer M, Kaech S, Wagner U, Brinkhaus H and Matus A. (2000). Glutamate receptors regulate actin-based plasticity in dendritic spines. *Nat Neurosci* **3,** 887-894.

Fletcher TL, De Camilli P and Banker G. (1994). Synaptogenesis in hippocampal cultures: evidence indicating that axons and dendrites become competent to form synapses at different stages of neuronal development. *J Neurosci* **14,** 6695-6706.

Forsten-Williams K, Chu CL, Fannon M, Buczek-Thomas JA and Nugent MA. (2008). Control of growth factor networks by heparan sulfate proteoglycans. *Ann Biomed Eng* **36,** 2134-2148.

Fortin DA, Srivastava T and Soderling TR. (2011). Structural Modulation of Dendritic Spines during Synaptic Plasticity. *Neuroscientist*.

Frey U, Krug M, Reymann KG and Matthies H. (1988). Anisomycin, an inhibitor of protein synthesis, blocks late phases of LTP phenomena in the hippocampal CA1 region in vitro. *Brain Res* **452,** 57-65.

Friedman HV, Bresler T, Garner CC and Ziv NE. (2000). Assembly of new individual excitatory synapses: time course and temporal order of synaptic molecule recruitment. *Neuron* **27,** 57-69.

Frischknecht R, Fejtova A, Viesti M, Stephan A and Sonderegger P. (2008). Activity-induced synaptic capture and exocytosis of the neuronal serine protease neurotrypsin. *J Neurosci* **28,** 1568-1579.

Frischknecht R, Heine M, Perrais D, Seidenbecher CI, Choquet D and Gundelfinger ED. (2009). Brain extracellular matrix affects AMPA receptor lateral mobility and short-term synaptic plasticity. *Nat Neurosci* **12,** 897-904.

Gahwiler BH. (1981). Organotypic monolayer cultures of nervous tissue. *J Neurosci Methods* **4,** 329-342.

Gahwiler BH, Capogna M, Debanne D, McKinney RA and Thompson SM. (1997). Organotypic slice cultures: a technique has come of age. *Trends Neurosci* **20,** 471-477.

Galtrey CM and Fawcett JW. (2007). The role of chondroitin sulfate proteoglycans in regeneration and plasticity in the central nervous system. *Brain Res Rev* **54,** 1-18.

Galvez R and Greenough WT. (2005). Sequence of abnormal dendritic spine development in primary somatosensory cortex of a mouse model of the fragile X mental retardation syndrome. *Am J Med Genet A* **135,** 155-160.

Garcia-Lopez P, Garcia-Marin V and Freire M. (2007). The discovery of dendritic spines by Cajal in 1888 and its relevance in the present neuroscience. *Prog Neurobiol* **83,** 110-130.

Garey LJ, Ong WY, Patel TS, Kanani M, Davis A, Mortimer AM, Barnes TR and Hirsch SR. (1998). Reduced dendritic spine density on cerebral cortical pyramidal neurons in schizophrenia. *J Neurol Neurosurg Psychiatry* **65,** 446-453.

Gautam M, DeChiara TM, Glass DJ, Yancopoulos GD and Sanes JR. (1999). Distinct phenotypes of mutant mice lacking agrin, MuSK, or rapsyn. *Brain Res Dev Brain Res* **114,** 171-178.

Gautam M, Noakes PG, Moscoso L, Rupp F, Scheller RH, Merlie JP and Sanes JR. (1996). Defective neuromuscular synaptogenesis in agrin-deficient mutant mice. *Cell* **85,** 525-535.

Genoud C, Quairiaux C, Steiner P, Hirling H, Welker E and Knott GW. (2006). Plasticity of astrocytic coverage and glutamate transporter expression in adult mouse cortex. *PLoS Biol* **4,** e343.

Gerber U, Gee CE and Benquet P. (2007). Metabotropic glutamate receptors: intracellular signaling pathways. *Curr Opin Pharmacol* **7,** 56-61.

Gerfin-Moser A and Monyer H. (2002). In situ hybridization on organotypic slice cultures. *Int Rev Neurobiol* **47,** 125-134.

Gesemann M, Cavalli V, Denzer AJ, Brancaccio A, Schumacher B and Ruegg MA. (1996). Alternative splicing of agrin alters its binding to heparin, dystroglycan, and the putative agrin receptor. *Neuron* **16,** 755-767.

Giovannini MG, Rakovska A, Benton RS, Pazzagli M, Bianchi L and Pepeu G. (2001). Effects of novelty and habituation on acetylcholine, GABA, and glutamate release from the frontal cortex and hippocampus of freely moving rats. *Neuroscience* **106,** 43-53.

Glynn MW and McAllister AK. (2006). Immunocytochemistry and quantification of protein colocalization in cultured neurons. *Nat Protoc* **1,** 1287-1296.

Goeger DE, Riley RT, Dorner JW and Cole RJ. (1988). Cyclopiazonic acid inhibition of the Ca2+-transport ATPase in rat skeletal muscle sarcoplasmic reticulum vesicles. *Biochem Pharmacol* **37,** 978-981.

Gogolla N, Caroni P, Luthi A and Herry C. (2009). Perineuronal nets protect fear memories from erasure. *Science* **325,** 1258-1261.

Grabrucker A, Vaida B, Bockmann J and Boeckers TM. (2009). Synaptogenesis of hippocampal neurons in primary cell culture. *Cell Tissue Res* **338,** 333-341.

Granes F, Garcia R, Casaroli-Marano RP, Castel S, Rocamora N, Reina M, Urena JM and Vilaro S. (1999). Syndecan-2 induces filopodia by active cdc42Hs. *Exp Cell Res* **248,** 439-456.

Greenough WT, Hwang HM and Gorman C. (1985). Evidence for active synapse formation or altered postsynaptic metabolism in visual cortex of rats reared in complex environments. *Proc Natl Acad Sci U S A* **82,** 4549-4552.

Grunditz A, Holbro N, Tian L, Zuo Y and Oertner TG. (2008). Spine neck plasticity controls postsynaptic calcium signals through electrical compartmentalization. *J Neurosci* **28,** 13457-13466.

Grutzendler J, Kasthuri N and Gan WB. (2002). Long-term dendritic spine stability in the adult cortex. *Nature* **420,** 812-816.

Gschwend TP, Krueger SR, Kozlov SV, Wolfer DP and Sonderegger P. (1997). Neurotrypsin, a novel multidomain serine protease expressed in the nervous system. *Mol Cell Neurosci* **9,** 207-219.

Gu J, Firestein BL and Zheng JQ. (2008). Microtubules in dendritic spine development. *J Neurosci* **28,** 12120-12124.

Gu J and Zheng JQ. (2009). Microtubules in Dendritic Spine Development and Plasticity. *Open Neurosci J* **3,** 128-133.

Haber M, Zhou L and Murai KK. (2006). Cooperative astrocyte and dendritic spine dynamics at hippocampal excitatory synapses. *J Neurosci* **26,** 8881-8891.

Haeckel A, Ahuja R, Gundelfinger ED, Qualmann B and Kessels MM. (2008). The actin-binding protein Abp1 controls dendritic spine morphology and is important for spine head and synapse formation. *J Neurosci* **28,** 10031-10044.

Harris KM. (1999). Structure, development, and plasticity of dendritic spines. *Curr Opin Neurobiol* **9,** 343-348.

Harris KM, Jensen FE and Tsao B. (1992). Three-dimensional structure of dendritic spines and synapses in rat hippocampus (CA1) at postnatal day 15 and adult ages: implications for the maturation of synaptic physiology and long-term potentiation. *J Neurosci* **12,** 2685-2705.

Harris KM and Kater SB. (1994). Dendritic spines: cellular specializations imparting both stability and flexibility to synaptic function. *Annu Rev Neurosci* **17,** 341-371.

Harris KM and Stevens JK. (1989). Dendritic spines of CA 1 pyramidal cells in the rat hippocampus: serial electron microscopy with reference to their biophysical characteristics. *J Neurosci* **9,** 2982-2997.

Harvey CD and Svoboda K. (2007). Locally dynamic synaptic learning rules in pyramidal neuron dendrites. *Nature* **450,** 1195-1200.

Hasselmo ME. (2006). The role of acetylcholine in learning and memory. *Curr Opin Neurobiol* **16,** 710-715.

Hasselmo ME and McGaughy J. (2004). High acetylcholine levels set circuit dynamics for attention and encoding and low acetylcholine levels set dynamics for consolidation. *Prog Brain Res* **145,** 207-231.

Hayashi-Takagi A, Takaki M, Graziane N, Seshadri S, Murdoch H, Dunlop AJ, Makino Y, Seshadri AJ, Ishizuka K, Srivastava DP, Xie Z, Baraban JM, Houslay MD, Tomoda T, Brandon NJ, Kamiya A, Yan Z, Penzes P and Sawa A. (2010). Disrupted-in-Schizophrenia 1 (DISC1) regulates spines of the glutamate synapse via Rac1. *Nat Neurosci* **13,** 327-332.

Hebb DO. (1949). *The Organization of Behavior*. Wiley, New York.

Heiman MG and Shaham S. (2010). Twigs into branches: how a filopodium becomes a dendrite. *Curr Opin Neurobiol* **20,** 86-91.

Hering H and Sheng M. (2001). Dendritic spines: structure, dynamics and regulation. *Nat Rev Neurosci* **2,** 880-888.

Herz J and Chen Y. (2006). Reelin, lipoprotein receptors and synaptic plasticity. *Nat Rev Neurosci* **7,** 850-859.

Heupel K, Sargsyan V, Plomp JJ, Rickmann M, Varoqueaux F, Zhang W and Krieglstein K. (2008). Loss of transforming growth factor-beta 2 leads to impairment of central synapse function. *Neural Dev* **3,** 25.

Higley MJ and Sabatini BL. (2008). Calcium signaling in dendrites and spines: practical and functional considerations. *Neuron* **59,** 902-913.

Hilgenberg LG and Smith MA. (2004). Agrin signaling in cortical neurons is mediated by a tyrosine kinase-dependent increase in intracellular Ca2+ that engages both CaMKII and MAPK signal pathways. *J Neurobiol* **61,** 289-300.

Hilgenberg LG, Su H, Gu H, O'Dowd DK and Smith MA. (2006). Alpha3Na+/K+-ATPase is a neuronal receptor for agrin. *Cell* **125,** 359-369.

Hirrlinger J, Hulsmann S and Kirchhoff F. (2004). Astroglial processes show spontaneous motility at active synaptic terminals in situ. *Eur J Neurosci* **20,** 2235-2239.

Holahan MR, Rekart JL, Sandoval J and Routtenberg A. (2006). Spatial learning induces presynaptic structural remodeling in the hippocampal mossy fiber system of two rat strains. *Hippocampus* **16,** 560-570.

Holtmaat A, De Paola V, Wilbrecht L and Knott GW. (2008). Imaging of experience-dependent structural plasticity in the mouse neocortex in vivo. *Behav Brain Res* **192,** 20-25.

Holtmaat A and Svoboda K. (2009). Experience-dependent structural synaptic plasticity in the mammalian brain. *Nat Rev Neurosci* **10,** 647-658.

Holtmaat A, Wilbrecht L, Knott GW, Welker E and Svoboda K. (2006). Experience-dependent and cell-type-specific spine growth in the neocortex. *Nature* **441,** 979-983.

Holtmaat AJ, Trachtenberg JT, Wilbrecht L, Shepherd GM, Zhang X, Knott GW and Svoboda K. (2005). Transient and persistent dendritic spines in the neocortex in vivo. *Neuron* **45,** 279-291.

Honkura N, Matsuzaki M, Noguchi J, Ellis-Davies GC and Kasai H. (2008). The subspine organization of actin fibers regulates the structure and plasticity of dendritic spines. *Neuron* **57,** 719-729.

Hoogenraad CC and Akhmanova A. (2010). Dendritic spine plasticity: new regulatory roles of dynamic microtubules. *Neuroscientist* **16,** 650-661.

Hoogenraad CC, Akhmanova A, Galjart N and De Zeeuw CI. (2004). LIMK1 and CLIP-115: linking cytoskeletal defects to Williams syndrome. *Bioessays* **26,** 141-150.

Hoogenraad CC and Bradke F. (2009). Control of neuronal polarity and plasticity--a renaissance for microtubules? *Trends Cell Biol* **19,** 669-676.

Hoover CL, Hilgenberg LG and Smith MA. (2003). The COOH-terminal domain of agrin signals via a synaptic receptor in central nervous system neurons. *J Cell Biol* **161,** 923-932.

Hotulainen P and Hoogenraad CC. (2010). Actin in dendritic spines: connecting dynamics to function. *J Cell Biol* **189,** 619-629.

Hotulainen P, Llano O, Smirnov S, Tanhuanpaa K, Faix J, Rivera C and Lappalainen P. (2009). Defining mechanisms of actin polymerization and depolymerization during dendritic spine morphogenesis. *J Cell Biol* **185,** 323-339.

Hu X, Viesselmann C, Nam S, Merriam E and Dent EW. (2008). Activity-dependent dynamic microtubule invasion of dendritic spines. *J Neurosci* **28,** 13094-13105.

Humeau Y, Herry C, Kemp N, Shaban H, Fourcaudot E, Bissiere S and Luthi A. (2005). Dendritic spine heterogeneity determines afferent-specific Hebbian plasticity in the amygdala. *Neuron* **45,** 119-131.

Hutchins BI and Kalil K. (2008). Differential outgrowth of axons and their branches is regulated by localized calcium transients. *J Neurosci* **28,** 143-153.

Inokuchi K. (2011). Adult neurogenesis and modulation of neural circuit function. *Curr Opin Neurobiol* **21,** 360-364.

Ivenshitz M and Segal M. (2010). Neuronal density determines network connectivity and spontaneous activity in cultured hippocampus. *J Neurophysiol* **104,** 1052-1060.

Jarrard LE. (1993). On the role of the hippocampus in learning and memory in the rat. *Behav Neural Biol* **60,** 9-26.

Jaworski J, Kapitein LC, Gouveia SM, Dortland BR, Wulf PS, Grigoriev I, Camera P, Spangler SA, Di Stefano P, Demmers J, Krugers H, Defilippi P, Akhmanova A and Hoogenraad CC. (2009). Dynamic microtubules regulate dendritic spine morphology and synaptic plasticity. *Neuron* **61,** 85-100.

Kaech S and Banker G. (2006). Culturing hippocampal neurons. *Nat Protoc* **1,** 2406-2415.

Kaech S, Brinkhaus H and Matus A. (1999). Volatile anesthetics block actin-based motility in dendritic spines. *Proc Natl Acad Sci U S A* **96,** 10433-10437.

Kamiya H and Zucker RS. (1994). Residual Ca2+ and short-term synaptic plasticity. *Nature* **371,** 603-606.

Kantor DB, Chivatakarn O, Peer KL, Oster SF, Inatani M, Hansen MJ, Flanagan JG, Yamaguchi Y, Sretavan DW, Giger RJ and Kolodkin AL. (2004). Semaphorin 5A is a bifunctional axon guidance cue regulated by heparan and chondroitin sulfate proteoglycans. *Neuron* **44,** 961-975.

Karetko M and Skangiel-Kramska J. (2009). Diverse functions of perineuronal nets. *Acta Neurobiol Exp (Wars)* **69,** 564-577.

Kasai H, Fukuda M, Watanabe S, Hayashi-Takagi A and Noguchi J. (2010). Structural dynamics of dendritic spines in memory and cognition. *Trends Neurosci* **33,** 121-129.

Kim N, Stiegler AL, Cameron TO, Hallock PT, Gomez AM, Huang JH, Hubbard SR, Dustin ML and Burden SJ. (2008). Lrp4 is a receptor for Agrin and forms a complex with MuSK. *Cell* **135,** 334-342.

Kirkpatrick B, Xu L, Cascella N, Ozeki Y, Sawa A and Roberts RC. (2006). DISC1 immunoreactivity at the light and ultrastructural level in the human neocortex. *J Comp Neurol* **497,** 436-450.

Kirov SA and Harris KM. (1999). Dendrites are more spiny on mature hippocampal neurons when synapses are inactivated. *Nat Neurosci* **2,** 878-883.

Knott GW, Holtmaat A, Wilbrecht L, Welker E and Svoboda K. (2006). Spine growth precedes synapse formation in the adult neocortex in vivo. *Nat Neurosci* **9,** 1117-1124.

Koch C and Zador A. (1993). The function of dendritic spines: devices subserving biochemical rather than electrical compartmentalization. *J Neurosci* **13,** 413-422.

Kochlamazashvili G, Henneberger C, Bukalo O, Dvoretskova E, Senkov O, Lievens PM, Westenbroek R, Engel AK, Catterall WA, Rusakov DA, Schachner M and Dityatev A. (2010). The extracellular matrix molecule hyaluronic acid regulates hippocampal synaptic plasticity by modulating postsynaptic L-type Ca(2+) channels. *Neuron* **67,** 116-128.

Komarova Y, Lansbergen G, Galjart N, Grosveld F, Borisy GG and Akhmanova A. (2005). EB1 and EB3 control CLIP dissociation from the ends of growing microtubules. *Mol Biol Cell* **16,** 5334-5345.

Konur S and Yuste R. (2004). Imaging the motility of dendritic protrusions and axon terminals: roles in axon sampling and synaptic competition. *Mol Cell Neurosci* **27,** 427-440.

Kopec CD, Li B, Wei W, Boehm J and Malinow R. (2006). Glutamate receptor exocytosis and spine enlargement during chemically induced long-term potentiation. *J Neurosci* **26,** 2000-2009.

Korobova F and Svitkina T. (2010). Molecular architecture of synaptic actin cytoskeleton in hippocampal neurons reveals a mechanism of dendritic spine morphogenesis. *Mol Biol Cell* **21,** 165-176.

Kramar EA, Lin B, Rex CS, Gall CM and Lynch G. (2006). Integrin-driven actin polymerization consolidates long-term potentiation. *Proc Natl Acad Sci U S A* **103,** 5579-5584.

Kroger S and Schroder JE. (2002). Agrin in the developing CNS: new roles for a synapse organizer. *News Physiol Sci* **17,** 207-212.

Ksiazek I, Burkhardt C, Lin S, Seddik R, Maj M, Bezakova G, Jucker M, Arber S, Caroni P, Sanes JR, Bettler B and Ruegg MA. (2007). Synapse loss in cortex of agrin-deficient mice after genetic rescue of perinatal death. *J Neurosci* **27,** 7183-7195.

Kullmann DM, Asztely F and Walker MC. (2000). The role of mammalian ionotropic receptors in synaptic plasticity: LTP, LTD and epilepsy. *Cell Mol Life Sci* **57,** 1551-1561.

Lamprecht R and LeDoux J. (2004). Structural plasticity and memory. *Nat Rev Neurosci* **5,** 45-54.

Lang C, Barco A, Zablow L, Kandel ER, Siegelbaum SA and Zakharenko SS. (2004). Transient expansion of synaptically connected dendritic spines upon induction of hippocampal long-term potentiation. *Proc Natl Acad Sci U S A* **101,** 16665-16670.

Lehre KP and Rusakov DA. (2002). Asymmetry of glia near central synapses favors presynaptically directed glutamate escape. *Biophys J* **83,** 125-134.

Lendvai B, Stern EA, Chen B and Svoboda K. (2000). Experience-dependent plasticity of dendritic spines in the developing rat barrel cortex in vivo. *Nature* **404,** 876-881.

Lewis PR and Shute CC. (1967). The cholinergic limbic system: projections to hippocampal formation, medial cortex, nuclei of the ascending cholinergic reticular system, and the subfornical organ and supra-optic crest. *Brain* **90,** 521-540.

Li Z, Hilgenberg LG, O'Dowd DK and Smith MA. (1999). Formation of functional synaptic connections between cultured cortical neurons from agrin-deficient mice. *J Neurobiol* **39,** 547-557.

Li Z, Massengill JL, O'Dowd DK and Smith MA. (1997). Agrin gene expression in mouse somatosensory cortical neurons during development in vivo and in cell culture. *Neuroscience* **79,** 191-201.

Lin B, Kramar EA, Bi X, Brucher FA, Gall CM and Lynch G. (2005). Theta stimulation polymerizes actin in dendritic spines of hippocampus. *J Neurosci* **25,** 2062-2069.

Lin L, McCroskery S, Ross JM, Chak Y, Neuhuber B and Daniels MP. (2010). Induction of filopodia-like protrusions by transmembrane agrin: role of agrin glycosaminoglycan chains and Rho-family GTPases. *Exp Cell Res* **316,** 2260-2277.

Lin W, Burgess RW, Dominguez B, Pfaff SL, Sanes JR and Lee KF. (2001). Distinct roles of nerve and muscle in postsynaptic differentiation of the neuromuscular synapse. *Nature* **410,** 1057-1064.

Lohmann C and Bonhoeffer T. (2008). A role for local calcium signaling in rapid synaptic partner selection by dendritic filopodia. *Neuron* **59,** 253-260.

Lohmann C, Finski A and Bonhoeffer T. (2005). Local calcium transients regulate the spontaneous motility of dendritic filopodia. *Nat Neurosci* **8,** 305-312.

Lopez-Bendito G, Shigemoto R, Fairen A and Lujan R. (2002). Differential distribution of group I metabotropic glutamate receptors during rat cortical development. *Cereb Cortex* **12,** 625-638.

Lowndes M and Stewart MG. (1994). Dendritic spine density in the lobus parolfactorius of the domestic chick is increased 24 h after one-trial passive avoidance training. *Brain Res* **654,** 129-136.

Lu R, Wang H, Liang Z, Ku L, O'Donnell W T, Li W, Warren ST and Feng Y. (2004). The fragile X protein controls microtubule-associated protein 1B translation and microtubule stability in brain neuron development. *Proc Natl Acad Sci U S A* **101,** 15201-15206.

Luscher C, Xia H, Beattie EC, Carroll RC, von Zastrow M, Malenka RC and Nicoll RA. (1999). Role of AMPA receptor cycling in synaptic transmission and plasticity. *Neuron* **24,** 649-658.

Lushnikova I, Skibo G, Muller D and Nikonenko I. (2009). Synaptic potentiation induces increased glial coverage of excitatory synapses in CA1 hippocampus. *Hippocampus* **19,** 753-762.

Majewska A and Sur M. (2003). Motility of dendritic spines in visual cortex in vivo: changes during the critical period and effects of visual deprivation. *Proc Natl Acad Sci U S A* **100,** 16024-16029.

Majewska AK, Newton JR and Sur M. (2006). Remodeling of synaptic structure in sensory cortical areas in vivo. *J Neurosci* **26,** 3021-3029.

Malenka RC and Bear MF. (2004). LTP and LTD: an embarrassment of riches. *Neuron* **44,** 5-21.

Maletic-Savatic M, Malinow R and Svoboda K. (1999). Rapid dendritic morphogenesis in CA1 hippocampal dendrites induced by synaptic activity. *Science* **283,** 1923-1927.

Man HY, Lin JW, Ju WH, Ahmadian G, Liu L, Becker LE, Sheng M and Wang YT. (2000). Regulation of AMPA receptor-mediated synaptic transmission by clathrin-dependent receptor internalization. *Neuron* **25,** 649-662.

Mantych KB and Ferreira A. (2001). Agrin differentially regulates the rates of axonal and dendritic elongation in cultured hippocampal neurons. *J Neurosci* **21,** 6802-6809.

Margolis RU and Margolis RK. (1997). Chondroitin sulfate proteoglycans as mediators of axon growth and pathfinding. *Cell Tissue Res* **290,** 343-348.

Marino MJ, Rouse ST, Levey AI, Potter LT and Conn PJ. (1998). Activation of the genetically defined m1 muscarinic receptor potentiates N-methyl-D-aspartate (NMDA) receptor currents in hippocampal pyramidal cells. *Proc Natl Acad Sci U S A* **95,** 11465-11470.

Marques G. (2005). Morphogens and synaptogenesis in Drosophila. *J Neurobiol* **64,** 417-434.

Marques G, Haerry TE, Crotty ML, Xue M, Zhang B and O'Connor MB. (2003). Retrograde Gbb signaling through the Bmp type 2 receptor wishful thinking regulates systemic FMRFa expression in Drosophila. *Development* **130,** 5457-5470.

Matsumoto-Miyai K, Sokolowska E, Zurlinden A, Gee CE, Luscher D, Hettwer S, Wolfel J, Ladner AP, Ster J, Gerber U, Rulicke T, Kunz B and Sonderegger P. (2009). Coincident pre- and postsynaptic activation induces dendritic filopodia via neurotrypsin-dependent agrin cleavage. *Cell* **136,** 1161-1171.

Matsuzaki M, Ellis-Davies GC, Nemoto T, Miyashita Y, Iino M and Kasai H. (2001). Dendritic spine geometry is critical for AMPA receptor expression in hippocampal CA1 pyramidal neurons. *Nat Neurosci* **4,** 1086-1092.

Matsuzaki M, Honkura N, Ellis-Davies GC and Kasai H. (2004). Structural basis of long-term potentiation in single dendritic spines. *Nature* **429,** 761-766.

Mayer G, Hamelin J, Asselin MC, Pasquato A, Marcinkiewicz E, Tang M, Tabibzadeh S and Seidah NG. (2008). The regulated cell surface zymogen activation of the proprotein convertase PC5A directs the processing of its secretory substrates. *J Biol Chem* **283,** 2373-2384.

McCabe BD, Marques G, Haghighi AP, Fetter RD, Crotty ML, Haerry TE, Goodman CS and O'Connor MB. (2003). The BMP homolog Gbb provides a retrograde signal that regulates synaptic growth at the Drosophila neuromuscular junction. *Neuron* **39,** 241-254.

McCroskery S, Bailey A, Lin L and Daniels MP. (2009). Transmembrane agrin regulates dendritic filopodia and synapse formation in mature hippocampal neuron cultures. *Neuroscience* **163,** 168-179.

McCroskery S, Chaudhry A, Lin L and Daniels MP. (2006). Transmembrane agrin regulates filopodia in rat hippocampal neurons in culture. *Mol Cell Neurosci* **33,** 15-28.

Menon L, Mader SA and Mihailescu MR. (2008). Fragile X mental retardation protein interactions with the microtubule associated protein 1B RNA. *RNA* **14,** 1644-1655.

Mesulam MM, Mufson EJ, Wainer BH and Levey AI. (1983). Central cholinergic pathways in the rat: an overview based on an alternative nomenclature (Ch1-Ch6). *Neuroscience* **10,** 1185-1201.

Mielke JG, Comas T, Woulfe J, Monette R, Chakravarthy B and Mealing GA. (2005). Cytoskeletal, synaptic, and nuclear protein changes associated with rat interface organotypic hippocampal slice culture development. *Brain Res Dev Brain Res* **160,** 275-286.

Mitsuyama F, Niimi G, Kato K, Hirosawa K, Mikoshiba K, Okuya M, Karagiozov K, Kato Y, Kanno T, Sanoe H and Koide T. (2008). Redistribution of microtubules in dendrites of hippocampal CA1 neurons after tetanic stimulation during long-term potentiation. *Ital J Anat Embryol* **113,** 17-27.

Miyata S, Nishimura Y and Nakashima T. (2007). Perineuronal nets protect against amyloid beta-protein neurotoxicity in cultured cortical neurons. *Brain Res* **1150,** 200-206.

Mohanty S, Spinas GA, Maedler K, Zuellig RA, Lehmann R, Donath MY, Trub T and Niessen M. (2005). Overexpression of IRS2 in isolated pancreatic islets causes proliferation and protects human beta-cells from hyperglycemia-induced apoptosis. *Exp Cell Res* **303,** 68-78.

Molinari F, Meskanaite V, Munnich A, Sonderegger P and Colleaux L. (2003). Extracellular proteases and their inhibitors in genetic diseases of the central nervous system. *Hum Mol Genet* **12 Spec No 2,** R195-200.

Molinari F, Rio M, Meskenaite V, Encha-Razavi F, Auge J, Bacq D, Briault S, Vekemans M, Munnich A, Attie-Bitach T, Sonderegger P and Colleaux L. (2002). Truncating neurotrypsin mutation in autosomal recessive nonsyndromic mental retardation. *Science* **298,** 1779-1781.

Morin FO, Takamura Y and Tamiya E. (2005). Investigating neuronal activity with planar microelectrode arrays: achievements and new perspectives. *J Biosci Bioeng* **100,** 131-143.

Morris JA, Kandpal G, Ma L and Austin CP. (2003). DISC1 (Disrupted-In-Schizophrenia 1) is a centrosome-associated protein that interacts with MAP1A, MIPT3, ATF4/5 and NUDEL: regulation and loss of interaction with mutation. *Hum Mol Genet* **12,** 1591-1608.

Moser MB, Trommald M and Andersen P. (1994). An increase in dendritic spine density on hippocampal CA1 pyramidal cells following spatial learning in adult rats suggests the formation of new synapses. *Proc Natl Acad Sci U S A* **91,** 12673-12675.

Muller D, Wang C, Skibo G, Toni N, Cremer H, Calaora V, Rougon G and Kiss JZ. (1996). PSA-NCAM is required for activity-induced synaptic plasticity. *Neuron* **17,** 413-422.

Muller M, Gahwiler BH, Rietschin L and Thompson SM. (1993). Reversible loss of dendritic spines and altered excitability after chronic epilepsy in hippocampal slice cultures. *Proc Natl Acad Sci U S A* **90,** 257-261.

Murakoshi H, Wang H and Yasuda R. (2011). Local, persistent activation of Rho GTPases during plasticity of single dendritic spines. *Nature* **472,** 100-104.

Nagerl UV, Eberhorn N, Cambridge SB and Bonhoeffer T. (2004). Bidirectional activity-dependent morphological plasticity in hippocampal neurons. *Neuron* **44,** 759-767.

Nagerl UV, Kostinger G, Anderson JC, Martin KA and Bonhoeffer T. (2007). Protracted synaptogenesis after activity-dependent spinogenesis in hippocampal neurons. *J Neurosci* **27,** 8149-8156.

Nagy V, Bozdagi O, Matynia A, Balcerzyk M, Okulski P, Dzwonek J, Costa RM, Silva AJ, Kaczmarek L and Huntley GW. (2006). Matrix metalloproteinase-9 is required for hippocampal late-phase long-term potentiation and memory. *J Neurosci* **26,** 1923-1934.

Nakamura Y, Wood CL, Patton AP, Jaafari N, Henley JM, Mellor JR and Hanley JG. (2011). PICK1 inhibition of the Arp2/3 complex controls dendritic spine size and synaptic plasticity. *EMBO J* **30,** 719-730.

Neumann FR, Bittcher G, Annies M, Schumacher B, Kroger S and Ruegg MA. (2001). An alternative amino-terminus expressed in the central nervous system converts agrin to a type II transmembrane protein. *Mol Cell Neurosci* **17,** 208-225.

Neves G, Cooke SF and Bliss TV. (2008). Synaptic plasticity, memory and the hippocampus: a neural network approach to causality. *Nat Rev Neurosci* **9,** 65-75.

Newey SE, Velamoor V, Govek EE and Van Aelst L. (2005). Rho GTPases, dendritic structure, and mental retardation. *J Neurobiol* **64,** 58-74.

Newpher TM and Ehlers MD. (2008). Glutamate receptor dynamics in dendritic microdomains. *Neuron* **58,** 472-497.

Nimchinsky EA, Yasuda R, Oertner TG and Svoboda K. (2004). The number of glutamate receptors opened by synaptic stimulation in single hippocampal spines. *J Neurosci* **24,** 2054-2064.

Niswender CM and Conn PJ. (2010). Metabotropic glutamate receptors: physiology, pharmacology, and disease. *Annu Rev Pharmacol Toxicol* **50,** 295-322.

Nitkin RM, Smith MA, Magill C, Fallon JR, Yao YM, Wallace BG and McMahan UJ. (1987). Identification of agrin, a synaptic organizing protein from Torpedo electric organ. *J Cell Biol* **105,** 2471-2478.

Noguchi J, Nagaoka A, Watanabe S, Ellis-Davies GC, Kitamura K, Kano M, Matsuzaki M and Kasai H. (2011). In vivo two-photon uncaging of glutamate revealing the structure-function relationships of dendritic spines in the neocortex of adult mice. *J Physiol* **589,** 2447-2457.

Nour N, Mayer G, Mort JS, Salvas A, Mbikay M, Morrison CJ, Overall CM and Seidah NG. (2005). The cysteine-rich domain of the secreted proprotein convertases PC5A and PACE4 functions as a cell surface anchor and interacts with tissue inhibitors of metalloproteinases. *Mol Biol Cell* **16,** 5215-5226.

Nowak L, Bregestovski P, Ascher P, Herbet A and Prochiantz A. (1984). Magnesium gates glutamate-activated channels in mouse central neurones. *Nature* **307,** 462-465.

O'Connor LT, Lauterborn JC, Gall CM and Smith MA. (1994). Localization and alternative splicing of agrin mRNA in adult rat brain: transcripts encoding isoforms that aggregate acetylcholine receptors are not restricted to cholinergic regions. *J Neurosci* **14,** 1141-1152.

O'Malley A, O'Connell C, Murphy KJ and Regan CM. (2000). Transient spine density increases in the mid-molecular layer of hippocampal dentate gyrus accompany consolidation of a spatial learning task in the rodent. *Neuroscience* **99,** 229-232.

O'Toole JJ, Deyst KA, Bowe MA, Nastuk MA, McKechnie BA and Fallon JR. (1996). Alternative splicing of agrin regulates its binding to heparin alpha-dystroglycan, and the cell surface. *Proc Natl Acad Sci U S A* **93,** 7369-7374.

Oertner TG and Matus A. (2005). Calcium regulation of actin dynamics in dendritic spines. *Cell Calcium* **37,** 477-482.

Okabe S, Miwa A and Okado H. (2001). Spine formation and correlated assembly of presynaptic and postsynaptic molecules. *J Neurosci* **21,** 6105-6114.

Okamoto K, Nagai T, Miyawaki A and Hayashi Y. (2004). Rapid and persistent modulation of actin dynamics regulates postsynaptic reorganization underlying bidirectional plasticity. *Nat Neurosci* **7,** 1104-1112.

Oliet SH, Piet R and Poulain DA. (2001). Control of glutamate clearance and synaptic efficacy by glial coverage of neurons. *Science* **292,** 923-926.

Opazo P and Choquet D. (2011). A three-step model for the synaptic recruitment of AMPA receptors. *Mol Cell Neurosci* **46,** 1-8.

Ostroff LE, Fiala JC, Allwardt B and Harris KM. (2002). Polyribosomes redistribute from dendritic shafts into spines with enlarged synapses during LTP in developing rat hippocampal slices. *Neuron* **35,** 535-545.

Ozhogina OA, Grishaev A, Bominaar EL, Patthy L, Trexler M and Llinas M. (2008). NMR solution structure of the neurotrypsin Kringle domain. *Biochemistry* **47,** 12290-12298.

Panatier A, Theodosis DT, Mothet JP, Touquet B, Pollegioni L, Poulain DA and Oliet SH. (2006). Glia-derived D-serine controls NMDA receptor activity and synaptic memory. *Cell* **125,** 775-784.

Paoletti P and Neyton J. (2007). NMDA receptor subunits: function and pharmacology. *Curr Opin Pharmacol* **7,** 39-47.

Park M, Salgado JM, Ostroff L, Helton TD, Robinson CG, Harris KM and Ehlers MD. (2006). Plasticity-induced growth of dendritic spines by exocytic trafficking from recycling endosomes. *Neuron* **52,** 817-830.

Parsons JT, Horwitz AR and Schwartz MA. (2010). Cell adhesion: integrating cytoskeletal dynamics and cellular tension. *Nat Rev Mol Cell Biol* **11,** 633-643.

Patthy L, Trexler M, Vali Z, Banyai L and Varadi A. (1984). Kringles: modules specialized for protein binding. Homology of the gelatin-binding region of fibronectin with the kringle structures of proteases. *FEBS Lett* **171,** 131-136.

Pena F. (2010). Organotypic cultures as tool to test long-term effects of chemicals on the nervous system. *Curr Med Chem* **17,** 987-1001.

Petrak LJ, Harris KM and Kirov SA. (2005). Synaptogenesis on mature hippocampal dendrites occurs via filopodia and immature spines during blocked synaptic transmission. *J Comp Neurol* **484,** 183-190.

Pizzorusso T, Medini P, Berardi N, Chierzi S, Fawcett JW and Maffei L. (2002). Reactivation of ocular dominance plasticity in the adult visual cortex. *Science* **298,** 1248-1251.

Porten E, Seliger B, Schneider VA, Woll S, Stangel D, Ramseger R and Kroger S. (2010). The process-inducing activity of transmembrane agrin requires follistatin-like domains. *J Biol Chem* **285,** 3114-3125.

Portera-Cailliau C, Pan DT and Yuste R. (2003). Activity-regulated dynamic behavior of early dendritic protrusions: evidence for different types of dendritic filopodia. *J Neurosci* **23,** 7129-7142.

Portera-Cailliau C, Weimer RM, De Paola V, Caroni P and Svoboda K. (2005). Diverse modes of axon elaboration in the developing neocortex. *PLoS Biol* **3,** e272.

Power JM and Sah P. (2002). Nuclear calcium signaling evoked by cholinergic stimulation in hippocampal CA1 pyramidal neurons. *J Neurosci* **22,** 3454-3462.

Pozo K and Goda Y. (2010). Unraveling mechanisms of homeostatic synaptic plasticity. *Neuron* **66,** 337-351.

Racz B, Blanpied TA, Ehlers MD and Weinberg RJ. (2004). Lateral organization of endocytic machinery in dendritic spines. *Nat Neurosci* **7,** 917-918.

Ramirez OA and Couve A. (2011). The endoplasmic reticulum and protein trafficking in dendrites and axons. *Trends Cell Biol* **21,** 219-227.

Ramseger R, White R and Kroger S. (2009). Transmembrane form agrin-induced process formation requires lipid rafts and the activation of Fyn and MAPK. *J Biol Chem* **284,** 7697-7705.

Rauch U. (2004). Extracellular matrix components associated with remodeling processes in brain. *Cell Mol Life Sci* **61,** 2031-2045.

Rebola N, Srikumar BN and Mulle C. (2010). Activity-dependent synaptic plasticity of NMDA receptors. *J Physiol* **588,** 93-99.

Reif R, Sales S, Dreier B, Luscher D, Wolfel J, Gisler C, Baici A, Kunz B and Sonderegger P. (2008). Purification and enzymological characterization of murine neurotrypsin. *Protein Expr Purif* **61,** 13-21.

Reif R, Sales S, Hettwer S, Dreier B, Gisler C, Wolfel J, Luscher D, Zurlinden A, Stephan A, Ahmed S, Baici A, Ledermann B, Kunz B and Sonderegger P. (2007). Specific cleavage of agrin by neurotrypsin, a synaptic protease linked to mental retardation. *Faseb J*.

Reimers S, Hartlage-Rubsamen M, Bruckner G and Rossner S. (2007). Formation of perineuronal nets in organotypic mouse brain slice cultures is independent of neuronal glutamatergic activity. *Eur J Neurosci* **25,** 2640-2648.

Richards DA, Mateos JM, Hugel S, de Paola V, Caroni P, Gahwiler BH and McKinney RA. (2005). Glutamate induces the rapid formation of spine head protrusions in hippocampal slice cultures. *Proc Natl Acad Sci U S A* **102,** 6166-6171.

Roelandse M, Welman A, Wagner U, Hagmann J and Matus A. (2003). Focal motility determines the geometry of dendritic spines. *Neuroscience* **121,** 39-49.

Rubio MD, Johnson R, Miller CA, Huganir RL and Rumbaugh G. (2011). Regulation of synapse structure and function by distinct myosin II motors. *J Neurosci* **31,** 1448-1460.

Ruegg MA and Bixby JL. (1998). Agrin orchestrates synaptic differentiation at the vertebrate neuromuscular junction. *Trends Neurosci* **21,** 22-27.

Ryu J, Liu L, Wong TP, Wu DC, Burette A, Weinberg R, Wang YT and Sheng M. (2006). A critical role for myosin IIb in dendritic spine morphology and synaptic function. *Neuron* **49,** 175-182.

Sala C, Cambianica I and Rossi F. (2008). Molecular mechanisms of dendritic spine development and maintenance. *Acta Neurobiol Exp (Wars)* **68,** 289-304.

Sambrook J and Russell DW. (2001). *MOLECULAR CLONING A Laboratory Manual Cold Spring Harbor Laboratory*.

Sarter M, Parikh V and Howe WM. (2009). Phasic acetylcholine release and the volume transmission hypothesis: time to move on. *Nat Rev Neurosci* **10,** 383-390.

Scanziani M, Salin PA, Vogt KE, Malenka RC and Nicoll RA. (1997). Use-dependent increases in glutamate concentration activate presynaptic metabotropic glutamate receptors. *Nature* **385,** 630-634.

Schaetzle P, Ster J, Verbich D, McKinney RA, Gerber U, Sonderegger P and Mateos JM. (2011). Rapid and reversible formation of spine head filopodia in response to muscarinic receptor activation in CA1 pyramidal cells. *J Physiol*.

Schmolck H, Kensinger EA, Corkin S and Squire LR. (2002). Semantic knowledge in patient H.M. and other patients with bilateral medial and lateral temporal lobe lesions. *Hippocampus* **12,** 520-533.

Scoville WB and Milner B. (1957). Loss of recent memory after bilateral hippocampal lesions. *J Neurol Neurosurg Psychiatry* **20,** 11-21.

Seeger T, Fedorova I, Zheng F, Miyakawa T, Koustova E, Gomeza J, Basile AS, Alzheimer C and Wess J. (2004). M2 muscarinic acetylcholine receptor knock-out mice show deficits in behavioral flexibility, working memory, and hippocampal plasticity. *J Neurosci* **24,** 10117-10127.

Segal M. (2010). Dendritic spines, synaptic plasticity and neuronal survival: activity shapes dendritic spines to enhance neuronal viability. *Eur J Neurosci* **31,** 2178-2184.

Segal M and Murphy DD. (1998). CREB activation mediates plasticity in cultured hippocampal neurons. *Neural Plast* **6,** 1-7.

Serpinskaya AS, Feng G, Sanes JR and Craig AM. (1999). Synapse formation by hippocampal neurons from agrin-deficient mice. *Dev Biol* **205,** 65-78.

Sheng M. (2001). Molecular organization of the postsynaptic specialization. *Proc Natl Acad Sci U S A* **98,** 7058-7061.

Shepherd GM and Harris KM. (1998). Three-dimensional structure and composition of CA3-->CA1 axons in rat hippocampal slices: implications for presynaptic connectivity and compartmentalization. *J Neurosci* **18,** 8300-8310.

Shinoe T, Matsui M, Taketo MM and Manabe T. (2005). Modulation of synaptic plasticity by physiological activation of M1 muscarinic acetylcholine receptors in the mouse hippocampus. *J Neurosci* **25,** 11194-11200.

Shiosaka S. (2004). Serine proteases regulating synaptic plasticity. *Anat Sci Int* **79,** 137-144.

Siebler M, Koller H, Stichel CC, Muller HW and Freund HJ. (1993). Spontaneous activity and recurrent inhibition in cultured hippocampal networks. *Synapse* **14,** 206-213.

Skrede KK and Westgaard RH. (1971). The transverse hippocampal slice: a well-defined cortical structure maintained in vitro. *Brain Res* **35,** 589-593.

Sorra KE and Harris KM. (2000). Overview on the structure, composition, function, development, and plasticity of hippocampal dendritic spines. *Hippocampus* **10,** 501-511.

Squire LR. (2009). *Encyclopedia of neuroscience*. Elsevier, Boston, MA.

Stepanyants A, Hof PR and Chklovskii DB. (2002). Geometry and structural plasticity of synaptic connectivity. *Neuron* **34,** 275-288.

Stephan A, Mateos JM, Kozlov SV, Cinelli P, Kistler AD, Hettwer S, Rulicke T, Streit P, Kunz B and Sonderegger P. (2008). Neurotrypsin cleaves agrin locally at the synapse. *FASEB J*.

Stoppini L, Buchs PA and Muller D. (1991). A simple method for organotypic cultures of nervous tissue. *J Neurosci Methods* **37,** 173-182.

Svoboda K, Tank DW and Denk W. (1996). Direct measurement of coupling between dendritic spines and shafts. *Science* **272,** 716-719.

Thomson AM. (2000). Facilitation, augmentation and potentiation at central synapses. *Trends Neurosci* **23,** 305-312.

Toni N, Buchs PA, Nikonenko I, Povilaitite P, Parisi L and Muller D. (2001). Remodeling of synaptic membranes after induction of long-term potentiation. *J Neurosci* **21,** 6245-6251.

Toni N, Teng EM, Bushong EA, Aimone JB, Zhao C, Consiglio A, van Praag H, Martone ME, Ellisman MH and Gage FH. (2007). Synapse formation on neurons born in the adult hippocampus. *Nat Neurosci* **10,** 727-734.

Trachtenberg JT, Chen BE, Knott GW, Feng G, Sanes JR, Welker E and Svoboda K. (2002). Long-term in vivo imaging of experience-dependent synaptic plasticity in adult cortex. *Nature* **420,** 788-794.

Tsen G, Halfter W, Kroger S and Cole GJ. (1995). Agrin is a heparan sulfate proteoglycan. *J Biol Chem* **270,** 3392-3399.

Van Vactor D, Wall DP and Johnson KG. (2006). Heparan sulfate proteoglycans and the emergence of neuronal connectivity. *Curr Opin Neurobiol* **16,** 40-51.

Vanderklish PW and Edelman GM. (2002). Dendritic spines elongate after stimulation of group 1 metabotropic glutamate receptors in cultured hippocampal neurons. *Proc Natl Acad Sci U S A* **99,** 1639-1644.

Ventura R and Harris KM. (1999). Three-dimensional relationships between hippocampal synapses and astrocytes. *J Neurosci* **19,** 6897-6906.

Vicente-Manzanares M, Ma X, Adelstein RS and Horwitz AR. (2009). Non-muscle myosin II takes centre stage in cell adhesion and migration. *Nat Rev Mol Cell Biol* **10,** 778-790.

Volpicelli LA and Levey AI. (2004). Muscarinic acetylcholine receptor subtypes in cerebral cortex and hippocampus. *Prog Brain Res* **145,** 59-66.

von Bohlen und Halbach O. (2009). Structure and function of dendritic spines within the hippocampus. *Ann Anat* **191,** 518-531.

Wang XB, Bozdagi O, Nikitczuk JS, Zhai ZW, Zhou Q and Huntley GW. (2008). Extracellular proteolysis by matrix metalloproteinase-9 drives dendritic spine enlargement and long-term potentiation coordinately. *Proc Natl Acad Sci U S A* **105,** 19520-19525.

Webb DJ, Zhang H, Majumdar D and Horwitz AF. (2007). alpha5 integrin signaling regulates the formation of spines and synapses in hippocampal neurons. *J Biol Chem* **282,** 6929-6935.

Wess J, Eglen RM and Gautam D. (2007). Muscarinic acetylcholine receptors: mutant mice provide new insights for drug development. *Nat Rev Drug Discov* **6,** 721-733.

Wessel D and Flugge UI. (1984). A method for the quantitative recovery of protein in dilute solution in the presence of detergents and lipids. *Anal Biochem* **138,** 141-143.

Winzen U, Cole GJ and Halfter W. (2003). Agrin is a chimeric proteoglycan with the attachment sites for heparan sulfate/chondroitin sulfate located in two multiple serine-glycine clusters. *J Biol Chem* **278,** 30106-30114.

Witter MP, Wouterlood FG, Naber PA and Van Haeften T. (2000). Anatomical organization of the parahippocampal-hippocampal network. *Ann N Y Acad Sci* **911,** 1-24.

Wlodarczyk J, Mukhina I, Kaczmarek L and Dityatev A. (2011). Extracellular matrix molecules, their receptors and secreted proteases in synaptic plasticity. *Dev Neurobiol*.

Wolfer DP, Lang R, Cinelli P, Madani R and Sonderegger P. (2001). Multiple roles of neurotrypsin in tissue morphogenesis and nervous system development suggested by the mRNA expression pattern. *Mol Cell Neurosci* **18,** 407-433.

Wong WT and Wong RO. (2001). Changing specificity of neurotransmitter regulation of rapid dendritic remodeling during synaptogenesis. *Nat Neurosci* **4,** 351-352.

Wu MY and Hill CS. (2009). Tgf-beta superfamily signaling in embryonic development and homeostasis. *Dev Cell* **16,** 329-343.

Xu HL and Su B. (2005). Genetic evidence of a strong functional constraint of neurotrypsin during primate evolution. *Cytogenet Genome Res* **108,** 303-309.

Xu T, Yu X, Perlik AJ, Tobin WF, Zweig JA, Tennant K, Jones T and Zuo Y. (2009). Rapid formation and selective stabilization of synapses for enduring motor memories. *Nature* **462,** 915-919.

Yamasaki M, Matsui M and Watanabe M. (2010). Preferential localization of muscarinic M1 receptor on dendritic shaft and spine of cortical pyramidal cells and its anatomical evidence for volume transmission. *J Neurosci* **30,** 4408-4418.

Yang G, Pan F and Gan WB. (2009). Stably maintained dendritic spines are associated with lifelong memories. *Nature* **462,** 920-924.

Yang Y, Wang XB, Frerking M and Zhou Q. (2008). Spine expansion and stabilization associated with long-term potentiation. *J Neurosci* **28,** 5740-5751.

Yang Y and Zhou Q. (2009). Spine modifications associated with long-term potentiation. *Neuroscientist* **15,** 464-476.

Yasumatsu N, Matsuzaki M, Miyazaki T, Noguchi J and Kasai H. (2008). Principles of long-term dynamics of dendritic spines. *J Neurosci* **28,** 13592-13608.

Zha XM, Green SH and Dailey ME. (2005). Regulation of hippocampal synapse remodeling by epileptiform activity. *Mol Cell Neurosci* **29,** 494-506.

Zhang B, Luo S, Wang Q, Suzuki T, Xiong WC and Mei L. (2008). LRP4 serves as a coreceptor of agrin. *Neuron* **60,** 285-297.

Zhang F, Endo S, Cleary LJ, Eskin A and Byrne JH. (1997). Role of transforming growth factor-beta in long-term synaptic facilitation in Aplysia. *Science* **275,** 1318-1320.

Zhang W, Basile AS, Gomeza J, Volpicelli LA, Levey AI and Wess J. (2002). Characterization of central inhibitory muscarinic autoreceptors by the use of muscarinic acetylcholine receptor knock-out mice. *J Neurosci* **22,** 1709-1717.

Zhou Q, Homma KJ and Poo MM. (2004). Shrinkage of dendritic spines associated with long-term depression of hippocampal synapses. *Neuron* **44,** 749-757.

Zinsmaier KE, Babic M and Russo GJ. (2009). Mitochondrial transport dynamics in axons and dendrites. *Results Probl Cell Differ* **48,** 107-139.

Zito K, Scheuss V, Knott G, Hill T and Svoboda K. (2009). Rapid functional maturation of nascent dendritic spines. *Neuron* **61,** 247-258.

Ziv NE and Ahissar E. (2009). Neuroscience: New tricks and old spines. *Nature* **462,** 859-861.

Ziv NE and Smith SJ. (1996). Evidence for a role of dendritic filopodia in synaptogenesis and spine formation. *Neuron* **17,** 91-102.

Zucker RS and Regehr WG. (2002). Short-term synaptic plasticity. *Annu Rev Physiol* **64,** 355-405.

Zuo Y, Lin A, Chang P and Gan WB. (2005). Development of long-term dendritic spine stability in diverse regions of cerebral cortex. *Neuron* **46,** 181-189.

Acknowledgment

First of all, I gratefully thank my supervisor Peter Sonderegger for offering me the opportunity to work in his laboratory and for patiently guiding me through each step of my PhD project. It was great to work in an atmosphere of freedom and personal responsibility, but never having the feeling of being completely on my own. For your support, academic and otherwise, I thank you.

Thanks to my committee members Fritjof Helmchen and Urs Gerber who followed this thesis throughout and gave valuable advice.

Particularly, I would like to thank José María Mateos for being my unoffical co-supervisor. I appreciate all his contributions of time, ideas, and advice to make my PhD a productive and stimulating experience. I learned a lot from you Txema!

Thanks to Jeanne Ster and Urs Gerber for their collaboration on the field of electrophysiology and the discussions and suggestions to this project.

I wish to express my appreciation to Urs Ziegler, and his team in the ZMB, for the initial training in microscopy and especially for his contribution to the synapse quantification project. Also many thanks to René Wuttke for writing the program code to simulate the synapse quantification.

I am also thankful to Beat Kunz for lab management and running of our animal facility. Furthermore, I want to thank Dubravka Göckeritz-Dujmovic for continuously preparing slice cultures for us.

Moreover, I acknowledge all past and present members of the Sonderegger group with special thanks to Alexander Stephan and Alexander Ludwig for guiding me during the first months of my PhD. Thanks to my bench neighbours Tu-My Diep and Claudio Gisler for our daily lunch meetings and the great lab atmosphere.

Finally, I want to thank my family and especially Silvia, who supported and encouraged me the whole time.

Curriculum Vitae

Philipp Schätzle, born in Göttingen, Germany on 04th of October, 1979

Education

09/2007 - 09/2011	PhD student at the Department of Biochemistry, University of Zürich, Dissertation: “Functional Analysis of the N-terminal Segment of Agrin & Characterisation of the Response of Dendritic Spines to Cholinergic Stimulation” supervised by Prof. Peter Sonderegger
02/2007	Diploma degree in Biology from the University of Mainz, Germany Subjects: Zoology, Genetics, Botanic and Business Administration
05/2006 - 02/2007	Diploma thesis: “The role of the NG2-interacting partner Syntenin in migration of glial precursor cells”, supervised by Prof. Jacqueline Trotter
10/2000 - 12/2003	Undergraduate studies in Biology and Business Administration, University of Mainz
07/1999 - 03/2000	Military Service
08/1990 - 06/1999	Immanuel-Kant-Gymnasium, Rüsselsheim

Publications

Schätzle P, Ster J, Verbich D, McKinney RA, Gerber U, Sonderegger P, Mateos JM. **Rapid and reversible formation of spine head filopodia in response to muscarinic receptor activation in CA1 pyramidal cells.** J Physiol. 2011 Jul 18. [Epub ahead of print]

Steuble M, Gerrits B, Ludwig A, Mateos JM, Diep TM, Tagaya M, Stephan A, Schätzle P, Kunz B, Streit P, Sonderegger P. **Molecular characterization of a trafficking organelle: dissecting the axonal paths of calsyntenin-1 transport vesicles.** Proteomics. 2010 Nov;10(21):3775-88.

Chatterjee N, Stegmüller J, Schätzle P, Karram K, Koroll M, Werner HB, Nave KA, Trotter J. **Interaction of syntenin-1 and the NG2 proteoglycan in migratory oligodendrocyte precursor cells.** J Biol Chem. 2008 Mar 28;283(13):8310-7. Epub 2008 Jan 24.